

ANALYSIS AND EVALUATION OF PHYSICAL AND HYDROLOGICAL CHARACTERISTICS OF DIFFERENT MATERIALS RELATED TO THE USE IN CONSTRUCTED WETLANDS

**Diplomarbeit
zur Erlangung des akademischen Grades
Diplomingenieur**

eingereicht von:
MÜLLER, HEINER

Betreuer: Haberl, Raimund, Univ. Prof. Dipl.-Ing. Dr. nat. techn.

Mitbetreuer: Langergraber, Günter, Dipl.-Ing. Dr.

Preface

This diploma thesis was carried out at the Institute of Sanitary Engineering and Water Pollution Control of the University of Natural Resources and Applied Life Sciences, Vienna.

I want to thank to Univ.-Prof. Dipl.-Ing. Dr. Raimund Haberl, Dipl.-Ing. Dr. Günter Langergraber, and Dr. Eilif Asuman Korkusuz for mentoring. Moreover, I want to thank to all employees of the Institute who advised me in all difficulties and problems.

Thank you, to all my friends who supported me.

Special thank appertains my companion in live Vera for her exceptional support during the whole duration of study.

This diploma thesis is dedicated to my parents.

Kurzfassung

Die vorliegende Diplomarbeit wurde im Rahmen des Forschungsprojektes „ONUREM“ (Optimization of Nutrient Removal) durchgeführt und am Institut für Siedlungswasserbau, Industriewasserwirtschaft und Gewässerschutz am Department für Wasser, Atmosphäre und Umwelt der Universität für Bodenkultur Wien verfasst. Dieses Forschungsprojekt wurde von der Europäischen Union durch ein „Marie-Curie-Stipendium“ finanziert. Ziel dieses Projektes war es, die Leistungsfähigkeit von vertikal durchströmten, bepflanzten Bodenfiltern in Hinblick auf die Nährstoffelimination zu verbessern und damit ihren zurzeit hohen Flächenbedarf zu verringern. Zu diesem Zweck wurde der Gebrauch verschiedener natürlicher und künstlicher Materialien, die in der Türkei und in Österreich kommerziell erhältlich sind, untersucht. Die untersuchten Materialien waren Schlacke, Perlit, Bims, Zeolith und Sand aus der Türkei, Sand, Zeolith (in zwei unterschiedlichen Korngrößenverteilungen), Betonbruch und Ferro-Sorp© aus Österreich. Darüber hinaus wurde eine Mischung zu gleichen Teilen bestehend aus den genannten Materialien und eine Mischung zu gleichen Teilen bestehend aus Ferro-Sorp© und türkischem Zeolith untersucht.

Im Rahmen dieser Diplomarbeit wurden die physikalischen und hydrologischen Eigenschaften der oben genannten Materialien untersucht und beurteilt. Zu diesem Zweck wurde mittels Siebanalyse die Kornverteilung, mittels Pyknometerversuch die Raumdichte, Korndichte und der Porenanteil und mittels k-Wert Messung die Durchlässigkeit untersucht. In einem Säulenversuch wurden die hydraulische Aufenthaltszeit und die Abflussganglinie untersucht.

Bezüglich der angewandten Messmethoden und durchgeführten Versuche hat sich gezeigt, daß bei den Messungen der k-Werte hohe Standardabweichungen auftraten und die gemessenen Werte durchwegs um ein Vielfaches höher waren als die, wie in der DWA A 262 (2006) empfohlen, auf Basis des effektiven Korndurchmessers berechneten Werte. Es erscheint daher durchaus sinnvoll die k-Wert Messung durch diese Berechnung zu ersetzen. Im Rahmen der Pyknometerversuche zeigte sich, daß die Standardabweichungen der Porenanteile primär von den Standardabweichungen der Messungen der Korndichten herrühren. Das ist auf mangelnde Belüftung der Poren und der daraus resultierenden mangelnden Wassersättigung des Filtermaterials im Pyknometer zurückzuführen. Im Säulenversuch war es schwierig, stationäre Versuchsbedingungen aufrechtzuerhalten, da die Beschickungsschläuche verstopften und daher eine manuelle Reinigung nötig war. Das lag einerseits an der unzureichenden Entfernung der im kommunalen Abwasser enthaltenen partikulären Stoffe, andererseits schuf das hohe Nährstoffangebot im kommunalen Abwasser in Verbindung mit der Lichtdurchlässigkeit der Beschickungsschläuche sehr gute Lebensbedingungen für Mikroorganismen. Wodurch die Verstopfung zusätzlich verstärkt wurde.

Es zeigte sich, daß trotz der Tatsache, daß alle Materialien, außer türkischem Zeolith, die Anforderungen der einschlägigen Normen und Regelwerke bezüglich der physikalischen Eigenschaften erfüllten, sich einige Materialien in den Säulenversuchen als ungeeignet für die Verwendung als Hauptschicht in vertikal durchströmten, bepflanzten Bodenfiltern erwiesen. So entwickelten sich in den Säulen mit türkischem Zeolith, mit österreichischem Zeolith und in der Säule mit der Mischung aus allen Materialien und einer Filterhöhe von 30 cm Kurzschlussströme. Der türkische Zeolith erfüllte die Anforderungen bezüglich des effektiven Korndurchmesser nicht. Das stimmt mit der Entwicklung von Kurzschlussströmen überein. Im Gegensatz dazu traten in den Säulen mit Ferro-Sorp©, mit der Mischung aus allen Materialien und einer Filterhöhe von 50 cm und 75 cm und in der Säule mit Betonbruch zum Teil starke Kolmationserscheinungen auf. Der Einsatz dieser Materialien ist aus diesem Grund nicht zu empfehlen. Zusätzlich ist in Zusammenhang mit Betonbruch zu bedenken, daß Stoffe wie z.B. Chromat, Arsen, Blei, Kupfer, Nickel, Zink, Cadmium, Quecksilber und PAK im unversehrten Bauteil in der Betonmatrix gebunden sind durch das Zerkleinern einer Auswaschung zugänglich gemacht werden. Daher sind Betonbruch und Mischungen die Betonbruch enthalten als Filtermaterial grundsätzlich nicht geeignet.

Abstract

This diploma thesis was carried out within the framework of the research project ONUREM (Optimization of Nutrient Removal) and written at the Institute of Sanitary Engineering and Water Pollution Control of the University of Natural Resources and Life Sciences, Vienna. The European Commission funded this research project by a “Marie Curie Intra European Individual Fellowship”. The aim of this project was the enhancement of the capability of Vertical Subsurface Flow Constructed Wetlands in terms of nutrient removal therewith the reduction of currently high surface demand. For this purpose, the use of several natural and artificial materials, commercially available in Turkey and Austria, was investigated. The materials investigated were slag, pumice, perlite, zeolite and sand from Turkey, sand, zeolite (in two different grain size distributions), crushed concrete, and Ferro-Sorp® from Austria. Moreover a mixture of all materials in equal parts and of Ferro-Sorp® and Turkish zeolite, respectively, in equal parts were composed.

In this thesis the physical and the hydrological characteristics of the materials mentioned above were analysed and evaluated. For this purpose, sieving analysis for determination of particle size distribution, pycnometer experiments for determination of bulk density, particle density and porosity, k-value measurements for determination of permeability, and lab scale column experiments for determination of hydraulic retention times and for measurements of hydrographs were conducted.

Concerning applied methods of measurement and conducted experiments it became evident that at k-value measurements high standard deviations occurred. Additionally, each measured k-value was a multiple of the calculated ones. Calculation was based on effective grain diameter, as recommended by DWA A 262 (2006). Thus, a substitution of the k-value measurement by calculation based on effective grain diameter seems to be reasonable. At pycnometer experiments, it became evident that the standard deviations of the results of porosities mainly originate from the standard deviations of particle density measurements. This is caused by unsaturated conditions within the filter material due to insufficient deaeration of the pores of the filter material within the pycnometers. Due to the occurrence of clogging within the silicon pipes, used for feeding of columns, it was difficult to provide stable test conditions at the column experiment. The reason for clogging was on the one hand the insufficient removal of particles by sedimentation and sieving on the other hand provided the diaphanous silicon pipes in combination with an high nutrient amount good living conditions for micro organisms so that the clogging effect was intensified.

Although, all materials, except Turkish zeolite, fulfilled the requirements and recommendations of the relevant standards concerning physical characteristics, the column experiments revealed that some materials are inappropriate for the use as filter material for the main layer of VF CWs. At the columns filled with Turkish zeolite, Austrian zeolite and the mixture of materials (30 cm filter height) short circuit flows developed. Turkish zeolite did not meet the requirements concerning effective grain diameter, which corresponds to the development of short circuit flow. In contrast, at the columns of Ferro-Sorp®, mixtures with a height of filter of 50 cm and 75 cm, and crushed concrete clogging occurred. Thus, for the use in constructed wetlands, these materials cannot be recommended. Additionally, concerning crushed concrete, it has to be considered that substances like chromate, arsenic, lead, copper, nickel, zinc, cadmium, mercury and PAH are bonded within the matrix of concrete. Crushing processes make these substances accessible to elution. Thus, crushed concrete and mixtures, including crushed concrete, are not applicable as filter material.

Table of contents

1	Introduction	1
1.1	General	1
1.2	The project ONUREM	2
1.3	Goals of the diploma thesis	3
2	Fundamentals	4
2.1	Phosphorus removal	4
2.1.1	Filtration	4
2.1.2	Precipitation	5
2.1.3	Adsorption.....	5
2.2	Nitrogen removal.....	6
2.2.1	Nitrification	6
2.2.2	Denitrification	6
3	Materials and methods.....	7
3.1	Filter materials	7
3.1.1	Turkish filter materials	7
3.1.1.1	Slag (SL)	7
3.1.1.2	Perlit (PE).....	8
3.1.1.3	Pumice (PU).....	9
3.1.1.4	Turkish sand (TS)	10
3.1.1.5	Turkish zeolite (TZ)	11
3.1.2	Austrian filter materials.....	12
3.1.2.1	Crushed concrete (BE)	12
3.1.2.2	Ferro-Sorp© (FE)	13
3.1.2.3	Austrian zeolite 1 (AZ1)	14
3.1.2.4	Austrian zeolite 2 (AZ2)	14
3.1.2.5	Austrian sand (AS)	15
3.1.3	Mixed materials.....	15
3.1.3.1	Ferro-Sorp© + Turkish zeolite (FE+TZ)	15
3.1.3.2	Mixture (MX).....	16
3.2	Experimental set-up	17
3.2.1	Design of the column experiment	17
3.2.2	Operation of the column experiment.....	19
3.3	Measurements	22
3.3.1	Sieve analysis	23

3.3.1.1	Grading curve.....	24
3.3.2	Pycnometer experiments.....	27
3.3.2.1	Particle density	28
3.3.2.2	Bulk density	29
3.3.3	Determination of permeability.....	30
3.3.3.1	Measurement of k-value	32
3.3.3.2	k-value calculation based on effective grain diameter.....	34
3.3.4	Water flow at column experiments	35
3.3.4.1	Hydraulic load rate	35
3.3.4.2	Hydrographs and cumulative effluent	36
3.3.5	Tracer studies	38
3.3.5.1	Method	40
3.3.5.2	Data processing	44
3.3.6	HRT calculation.....	47
4	Results	49
4.1	Sieve analysis	49
4.1.1	Slag.....	49
4.1.2	Perlit.....	51
4.1.3	Pumice.....	53
4.1.4	Turkish Sand.....	55
4.1.5	Turkish Zeolite	57
4.1.6	Crushed concrete.....	59
4.1.7	Ferro-Sorp©.....	61
4.1.8	Austrian Zeolite 1	62
4.1.9	Austrian Zeolite 2	62
4.1.10	Austrian Sand	63
4.1.11	Ferro-Sorp© + Turkish Zeolite.....	64
4.1.12	Mixtures	64
4.1.13	Summary.....	65
4.2	Pycnometer Experiments	66
4.2.1	General	66
4.2.2	Particle density.....	67
4.2.3	Bulk density.....	69
4.2.4	Porosity	71
4.3	Permeability	73
4.4	Hydrographs and cumulative effluent	75

4.4.1	General	75
4.4.2	Slag.....	76
4.4.3	Perlit.....	77
4.4.4	Pumice	78
4.4.5	Turkish Sand.....	79
4.4.6	Turkish Zeolite	80
4.4.7	Crushed Concrete	81
4.4.8	Ferro-Sorp©.....	82
4.4.9	Austrian Zeolite 1	83
4.4.10	Austrian Zeolite 2	84
4.4.11	Austrian Sand	85
4.4.12	Ferro-Sorp© + Turkish Zeolite	86
4.4.13	Mixture 30	87
4.4.14	Mixture 50	88
4.4.15	Mixture 75	89
4.5	Tracer studies	90
4.5.1	Measured HRT.....	90
4.5.2	Calculated HRT and comparison with measured HRT	90
5	Discussion	93
5.1	Used methods.....	93
5.1.1	Sieve analysis	93
5.1.2	Pycnometer experiments.....	93
5.1.3	k-value measurement.....	93
5.1.4	Column experiments	94
5.2	Filter materials	95
5.2.1	Criteria	95
5.2.1.1	Digression concerning BE	95
5.2.2	Slag.....	96
5.2.3	Perlit.....	97
5.2.4	Pumice	98
5.2.5	Turkish Sand.....	99
5.2.6	Turkish Zeolite	100
5.2.7	Crushed concrete.....	101
5.2.8	Ferro-Sorp©.....	102
5.2.9	Austrian Zeolite 1 (1.5-2.0 mm)	103
5.2.10	Austrian Zeolite 2 (2.0-2.5 mm)	104

5.2.11 Austrian Sand	105
5.2.12 Ferro-Sorp© + Turkish Zeolite	106
5.2.13 Mixtures	107
6 Summary	108
7 Indexes	112
7.1 References	112
7.2 List of figures.....	115
7.3 List of tables.....	118
8 Appendix	120
9 Curriculum vitae	127

List of abbreviations

A	Area
Al ₂ O ₃	Aluminium oxide
AS	Austrian sand
ATV	Abwassertechnische Vereinigung
AZ1	Austrian Zeolite with a grain size from 1.5 mm to 2.0 mm
AZ2	Austrian Zeolite with a grain size from 2.0 mm to 2.5 mm
BE	Crushed concrete
BOD	Biochemical oxygen demand
BOKU	Universität für Bodenkultur
CaO	Calcium oxide
C _{in}	Concentration input
C _{out}	Concentration output
C _U	Uniformity coefficient
C _C	Coefficient of gradation
CGr	Coarse gravel (essential part)
cgr	Coarse gravel (additional part)
Cl	Clay
CSa	Coarse sand (essential part)
csa	Coarse sand (additional part)
CSi	Coarse silt (essential part)
csi	Coarse silt (additional part)
CW	Constructed wetland
CW2D	Constructed wetland 2 – dimensional
d	Diameter
d ₁₀	Particle size corresponding to mass of through fraction of 10 % (Effective grain diameter)
d ₃₀	Particle size corresponding to mass of through fraction of 30 %
d ₅₀	Particle size corresponding to mass of through fraction of 50 %
d ₆₀	Particle size corresponding to mass of through fraction of 60 %
dL	Flow length
dH	Pressure head difference
DIN	Deutsches Institut für Normung
DWA	Deutsche Vereinigung für Wasserwirtschaft, Wasser und Abfall
Δh	Difference of hydrostatic pressure head

Δs	Length of flow
FE	Ferro–Sorp ©
FE+TZ	Mixture of 50% Ferro–Sorp © and 50% Turkish zeolite
Fe_2O_3	Ferrous oxide
Fe_2O_2	Ferrous oxide
FeO	ferrous oxide
FGr	Fine gravel (essential part)
fgr	Fine gravel (additional part)
FSa	Fine sand (essential part)
fsa	Fine sand (additional part)
FSi	Fine silt (essential part)
fsi	Fine silt (additional part)
γ_w	Weight of water
H_2	Hydrogen
HF CW	Horizontal flow constructed wetlands
HLR	Hydraulic load rate
HRT	Hydraulic retention time
HSSF CW	Horizontal subsurface flow constructed wetlands
KCl	Potassium chloride
KBr	Potassium bromide
K_2O	Potassium oxide
k_f	Hydraulic conductivity
L	Solubility product
LiCl	Lithium chloride
M	Mass
MgO	Magnesium oxide
MGr	Medium gravel (essential part)
mgr	Medium gravel (additional part)
FSi	Fine silt (essential part)
fsi	Fine silt (additional part)
MnO	Manganese oxide
MO	Microorganism
MSa	Medium sand (essential part)
msa	Medium sand (additional part)
MX	Mixture
MX 30	Mixture with a filter height of 30 cm

MX 50.....	Mixture with a filter height of 50 cm
MX 75.....	Mixture with a filter height of 75 cm
n.....	Porosity
N ₂	Nitrogen
NaCl.....	Sodium chloride
Na ₂ O	Sodium oxide
NH ₄	Ammonium
NO ₂	Nitrite
NO ₃	Nitrate
O ₂	Oxygen
ONUREM	Optimization of nutrient removal
p.....	Pressure
PE	Perlit
P ₂ O ₂	Phosphorus dioxide
PVC.....	Polyvinyl chloride
PU.....	Pumice
Q.....	Flow rate
Re	Reynolds number
RO	Reversal osmosis
rpm.....	Rounds per minutes
ρ _d	Bulk density
ρ _s	Particle density
ρ _{TW}	Density of water
S	Sulfur
SF CW	Surface flow constructed wetland
SIG.....	Institut für Siedlungswasserbau und Gewässerschutz
SiO ₂	Silicon dioxide
SL	Slag
SSF CW	Subsurface flow constructed wetland
t.....	Time
TiO ₂	Titanium dioxide
TS	Turkish sand
TZ	Turkish zeolite
V	Volume
V _p	Pore volume
v _{fl}	Kinematical viscosity

v_f Filtration rate
VSSF CW.....Vertical subsurface flow constructed wetlands
 z Geodetical height

1 Introduction

1.1 General

Constructed wetlands (CWs) are a further development of wastewater sprinkling and broad irrigation of wastewater (GELLER and HÖNER, 2003). Main types of CWs include surface flow and subsurface flow CWs (KADLEC and KNIGHT, 1996). CWs are soil filters, planted with helophytes. Mechanical pre-treated wastewater is led through the wetland for the purpose of treatment (ÖNORM B 2505, 1997). Concerning the operation method two types of SSF CWs can be distinguished. HSSF CWs and VSSF CWs. At first, almost exclusive, HF CWs with a number of different filter materials were applied. Since, about 1990, VF CWs are built on a large scale. Nowadays, the most CWs are VF CWs because they have a lower specific surface demand and because of there, better oxygen supply a better potential of purification. Nowadays CWs are a state-of-the-art technology. The development of CWs has been enabled due to numerous research projects (amongst others BÖRNER (1992; ct. at GELLER and HÖNER, 2003), GELLER et al. (1992; ct. at GELLER and HÖNER, 2003), HAGENDORF and HAHN (1994; ct. at GELLER and HÖNER, 2003), KUNST and FLASCHE (1995; ct. at GELLER and HÖNER, 2003), KRAUT (1995; ct. at GELLER and HÖNER, 2003), BAHLO (1997; ct. at GELLER and HÖNER, 2003), PLATZER (1998; ct. at GELLER and HÖNER, 2003), HABERL et al. (2000; ct. at GELLER and HÖNER, 2003)). In these projects, capabilities of different types of CWs were researched and different designs for different purification processes and different wastewater parameters were developed (GELLER and HÖNER, 2003).

The mechanisms in CWs are characterised by complex physical, chemical, and biological processes, which result from interactions between helophytes, filter material, microorganisms, wastewater, and air within the pores of the filter material (DWA A 262, 2006). The meaning of the components of system and there relations among each other are well clarified today. The focus of this research was the selection of filter materials, which provide on the one hand a sufficient hydraulic conductivity, and on the other hand a sufficient hydraulic retention time. Mostly, in German speaking areas sand is applied as filter material.

According to experience a sufficient degradation of organic matter can be reached by HSSV CWs but to accomplish a sufficient nitrification the application of VSSF CWs with intermittent loading is necessary (ÖNORM B 2505, 1997).

Additional, in comparison with HSSF CWs, VSSF CWs with intermittent loading have further advantages (RÖSKE and UHLMANN, 2005):

- lower risk of clogging
- less surface demand
- lower risk of short circuit flow
- frost proof
- a better controllable oxygen supply
- shorter start-up-time and longer operation time
- lower technical complexity
- lower investment costs

The main use of VSSF CWs has been the removal of organic matter, total suspended solids, ammonium, and microbiological contaminations. Although, VSSF CWs with intermittent loading are state-of-the art in Europe it is sometimes impossible to apply them in small to medium

communities (<2000 PE), where land is valuable, because of their extensive surface requirement from three to 10 m² /PE. To enhance the capabilities of VSSF CWs concerning surface requirement and nutrient removal the project called ONUREM was developed (KORKUSUZ and LANGERGRABER, 2006).

1.2 The project ONUREM

The project ONUREM (Project No. 515515) was funded by the European Commission by a “Marie Curie Intra European Individual Fellowship” of Dr. Elif Asuman Korkusuz from Turkey (KORKUSUZ and LANGERGRABER, 2006). In the framework of ONUREM, different natural and artificial materials, commercially available in Turkey and Austria, with potential application as filter substrates in VSSF CWs, were investigated. The materials were provided from Turkey (slag, perlit, pumice, sand, zeolite) and Austria (crushed concrete, Ferro-Sorp®, zeolite in two grain sizes and sand). Moreover a mixture of all materials in equal parts and one of Ferro-Sorp® and Turkish zeolite half-and-half was composed.

The objectives of the ONUREM project were (KORKUSUZ and LANGERGRABER, 2006):

- Quantification of the effect of different materials mentioned above on the removal performance of organic matter and nutrients in a lab-scale VSSF CWs.
- Development of a catalogue of materials suitable as filter materials including a database of their hydraulic, physical, and chemical characteristics and of their transport parameters.
- Integration of the assayed parameters to the simulation tool CW2D in order to be used in an optimal way as a design tool for CWs.
- Improvement of the reliability of CW2D
- Fostering the use of CW2D for optimal SSF CWs design

This diploma thesis was conducted within the framework of the ONUREM project.

1.3 Goals of the diploma thesis

The objective of this diploma thesis was the analysis and evaluation of physical and hydrological characteristics of the single materials and the compositions mentioned above in terms of application in VSSF CWs.

Analysed physical characteristics:

- Grading curve
- Particle density
- Bulk density

Analysed hydrological characteristics:

- Hydraulic conductivity
- Hydraulic retention time (HRT)
- Hydraulic load rate (HLR)
- Hydrograph
- Cumulative effluent

For the determination of these characteristics, the following experiments were carried out:

- Sieve analysis (grading curves)
- Pycnometer experiment (particle density, bulk density)
- Determination of permeability (k-value)
- Lab-scale column experiment (HLR, hydrographs, cumulative effluents)
- Tracer experiments at the lab-scale column experiment (HRT)

2 Fundamentals

Municipal and domestic wastewater contains solid and dissolved pollutants, which have to be removed. Among organic pollutants wastewater contains nutrients namely phosphorus and nitrate as well as hygienic relevant germs. In CWs the wastewater becomes treated by complex physical, chemical and biological processes, which result from interactions between helophytes, filter material, micro organisms, wastewater, and air within the pores of the filter material (cf. Figure 2-1) (GELLER and HÖNER, 2003).

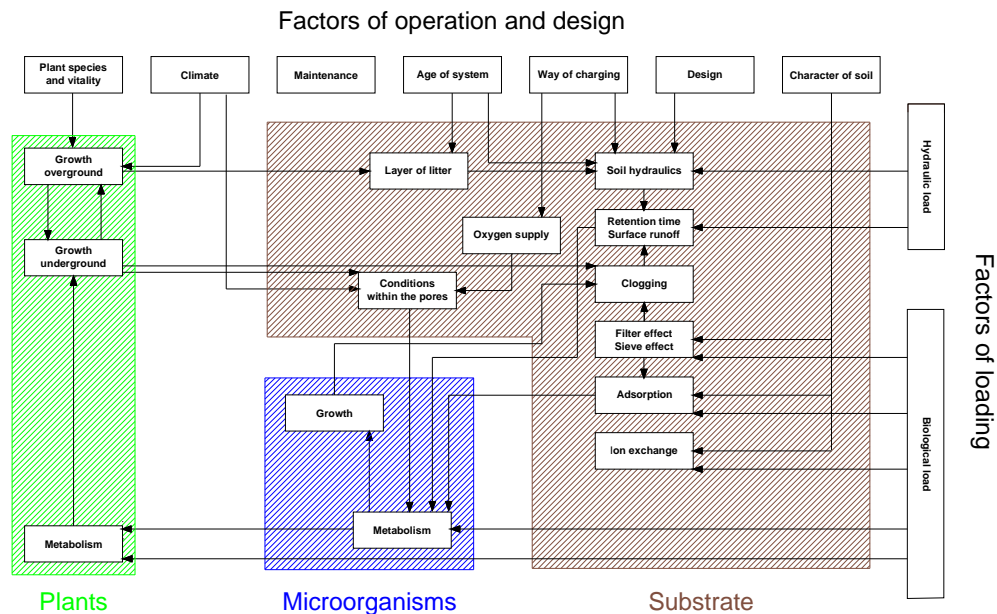


Figure 2-1: Mechanisms of action of CWs (BÖRNER, 1992)

Since, the physical and hydrological characteristics of the filter materials were investigated concerning their applicability for nutrient removal, subsequently, only processes concerning phosphorus and nitrogen removal are described.

2.1 Phosphorus removal

Substrate induced elimination processes are:

- Filtration
- Precipitation
- Adsorption

2.1.1 Filtration

Filtration is a physical process for separating particular matter. The substrate is the filter medium. Particular phosphorus retained within the substrate can be partially transformed into soluble compounds and therewith remobilised. Soluble phosphorus compounds, mainly orthophosphate, are available for subsequent precipitation and adsorption processes but can also become elutriated (LABER, 2001).

2.1.2 Precipitation

For precipitation, two types of substrates have to be distinguished:

- Ferrous and manganese containing substrates
- Calcium containing substrates

Ferrous and manganese containing substrates

Within this type of substrate, precipitation is mainly induced by iron (III) oxide and hydroxide. The equilibrium of dissolving and precipitating depends mainly on the solubility product (L) (MORTIMER, 1996; ct. at LABER, 2001). Due to external factors like pH-value, redox potential and oxygen content the equilibrium can be adjusted (BLUM, 1990; ct. at LABER, 2001).

If there are more phosphate anions dissolved than equating to capacity of iron (III), phosphate will precipitate together with iron (III). If the concentration of raw water changes and there are less phosphate anions dissolved than equating to the capacity of iron (III) the solution is unsaturated. Phosphate becomes dissolved and the concentration of phosphate within the solution rises (BLUM, 1990; ct. at LABER, 2001). This leads to recontamination of water.

Calcium containing substrates

Within substrates, which are rich in calcium, iron plays a secondary role. Precipitation of calcium carbonate is promoted by high temperatures and high pH-values. Orthophosphate can become adsorbed together with calcium carbonate. If the carbon dioxide concentration of the solution rises based on mineralization of organic matter, carbon dioxide becomes dissolved again for the most part consequently phosphate becomes dissolved again, too (BOSTRÖM et al., 1988; ct. at LABER, 2001).

The influence of redox potential on the solubility of phosphorus in substrates rich on calcium is low because of good buffering capacity (ANN et al., 2000; ct. at LABER, 2001).

2.1.3 Adsorption

Two ways of adsorption can be distinguished

- Specific adsorption
- Unspecific adsorption

Specific adsorption

Specific adsorption is based on the high affinity of the central lattice atom of complexes towards certain anions. Concerning phosphate, its affinity towards iron and aluminium is the determining factor. Due to this affinity phosphate is able to displace the ligands of iron or aluminium hydroxides respectively oxides. This leads to very stable bonds (BLUM, 1990; ct. at LABER, 2001).

Unspecific adsorption

Unspecific adsorption is based on mutual attraction of different charges. These bonds are loose. On the one hand because they are depending on pH – value and on the other hand because any other ion, can be bonded and used for adjustment of charges, according the concentration of solution (BLUM, 1990; ct. at LABER, 2001).

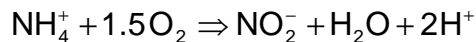
Phosphates are mainly adsorbed via specific adsorption.

2.2 Nitrogen removal

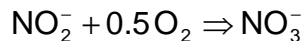
In domestic wastewater nitrogen occurs as ammonium (NH_4), nitrite (NO_2) and nitrate (NO_3). Nitrogen removal is based on nitrification and denitrification by microorganisms which grow at the surface of the particles of substrates in shape of bio films (RÖSKE and UHLMANN, 2005).

2.2.1 Nitrification

Nitrification is a two-stage process. In the first stage *Nitrosomonas* species oxidate NH_4 to NO_2 .



In the second stage *Nitrobacter* species oxidate NO_2 to NO_3 .



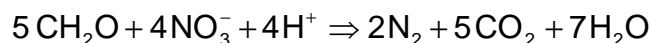
This process is very slow and requires a high amount of dissolved oxygen. Since *Nitrosomonas* and *Nitrobacter* species are autotrophic organisms no organic substance for their metabolism is needed (Universität Bremen, last visit 10.08.2011).

Influencing factors of nitrification are (Universität Bremen, last visit 10.08.2011):

- Temperature (28-36°C)
- Dissolved oxygen (≥ 2 mg/l)
- pH-value (7.5-8.3)
- Contact time
- Organic load

2.2.2 Denitrification

Denitrification is the microbial reduction of the nitrogen compounds NO_2 and NO_3 . The denitrifying *Pseudomonas* species are heterotrophic organisms. Thus *Pseudomonas* need organic substances, a carbon source, for metabolism. A redox reaction takes place. In this reaction carbon is the reducing agent. If no dissolved oxygen is available that means under anoxic conditions *Pseudomonas* species are able to take the oxygen of NO_3 respectively NO_2 for carbon oxidation. In this case NO_2 respectively NO_3 are the oxidants and become reduced. This process results to elementary nitrogen which leaks from CWs aerielly.



The energy yield of this reaction is low. As mentioned above for denitrification a carbon source is needed. The ideal ratio of biochemical oxygen demand (BOD) and NO_3 concentration is 4:1 (Universität Bremen, last visit 10.08.2011).

3 Materials and methods

3.1 Filter materials

3.1.1 Turkish filter materials

3.1.1.1 Slag (SL)

Blast furnace slag is a non-metallic by-product of the production of iron. It consists primarily of silicates, aluminium-silicates, and calcium-alumina-silicates. It also contains minor amounts of manganese, iron and sulphur compounds and trace quantities of heavy metals (MANN and BAVOR, 1993; ct. at KORKUSUZ, 2004).

The physical structure and gradation of granulated slag depends on its chemical composition, its temperature at the time of quenching, and the method of iron production. Treatment with controlled quantities of water during the cooling increases the vesicular nature of SL, and leads to a lightweight, porous material. SL is a material with good hydraulic conductivity and numerous sites for adsorption (MANN and BAVOR, 1993; ct. at KORKUSUZ, 2004), (SAKADEVAN and BAVOR, 1998; ct. at KORKUSUZ, 2004), (JOHANSSON, 1999; ct. at KORKUSUZ, 2004).



Figure 3.1-1: Slag

Slag is used in various applications as (KORKUSUZ, 2004):

- Aggregate for cement production (milled);
- Raw material for cement production (milled);
- Insulating material
- Sand blasting material (granulated).

The SL used in this experiment originates from KARDEMIR Iron and Steel Co (cf. Figure 3.1-1). Regarding its chemical composition, confer Table 3.1-1.

Table 3.1-1: Composition of SL

Chemical composition in (%) [*]											
FeO	Fe ₂ O ₃	SiO ₂	MnO	Al ₂ O ₃	CaO	MgO	S	Na ₂ O	K ₂ O	TiO ₂	Bazite
0.64	-	41.79	2.35	12.47	33.53	6.55	0.81	-	1.24	0.45	0.75

^{*}Reference: KARDEMIR Iron and Steel Ltd. Co. (2001; cited in KORKUSUZ, 2004)

3.1.1.2 Perlite (PE)

Raw Perlite is a natural glass, which is formed by cooling down lava very rapidly in contact with water or steam under high pressure. PE belongs to the group of volcanic rhyolites or quartz porphyry glasses. It is an aluminium silicate, which contains more than 70% silicon dioxide (KNAUF PERLITE GMBH, last visit 29.10.2010).

Raw Perlite has to be broken up and graded at a processing plant, after mining. Afterwards, a homogeneous and balanced water distribution within the granules of the mineral has to be obtained. This is important because it is the base to reach a sufficient expansion by heating it to a temperature of about

1000 °C and to reach a homogeneous pore distribution by evaporation of water. The result is a very light and porous granular material with a greyish brown colour and a pH-value of 6 to 8. 5.

PE can be used in a wide range of application:

- Filtration
- Horticulture
- Cryogenic Insulation
- Construction industry

The PE used in this experiment originates from POMZA EXPORT LTD. CO. in Menderes, Izmir, Turkey (cf. Figure 3.1-2). Regarding its chemical composition, confer Table 3.1-2.



Figure 3.1-2: Perlite

Table 3.1-2: Composition of PE

Chemical composition in (%) [*]							
SiO ₂	Al ₂ O ₃	Na ₂ O	K ₂ O	CaO	MgO	Fe ₂ O ₂	Bound H ₂ O
60-75	12-16	5-10	2-5	0-2	0-1	0-1	1-2

^{*}Reference: POMZA EXPORT Ltd. co, last visit 30.10.2010

3.1.1.3 Pumice (PU)

PU results from gassy and viscous lava. It is a frothy volcanic glass with an amorphous structure because solidification occurs too fast for crystallisation. Acid lava promotes the building of Pumice. That is the reason why the most types are rich on silicon dioxide and can be classified as Rhyolite.

During the solidification process at the surface, a sudden venting induces an outgasing which leads to a high porosity that can reach up to 85%. The whole matrix is griddled with not interconnected, irregular, or oval shaped pores. PU has a very high specific surface, is very light and its colour ranges from light grey to yellow and sometimes red (SCHUMANN, 2009).



Figure 3.1-3: Pumice

Range of application (AKTIENGESELLSCHAFT FÜR STEININDUSTRIE, last visit 30.10.2010):

- Construction material
- Soil stabilisation
- Filling material
- Abrasive material
- Carrier in fertiliser industry

The PU used in this experiment originates from POMZA EXPORT Ltd. co. in Menderes, Izmir, Turkey (cf. Figure 3.1-3). Regarding its chemical composition, confer Table 3.1-3.

Table 3.1-3: Composition of PU

Chemical composition in (%)*									
SiO ₂	Al ₂ O ₃	Fe ₂ O ₃	MnO	MgO	CaO	Na ₂ O	K ₂ O	TiO ₂	P ₂ O ₂
0.64	-	41.79	2.35	12.47	33.53	6.55	0.81	-	1.24

*Reference: POMZA EXPORT Ltd. co, last visit 30.10.2010

3.1.1.4 Turkish sand (TS)

Sand is clastic sediment. These sediments are a product of predominant physical alteration and they can be classified concerning grain size. Corresponding to the classification system, sand is a loose mixture of clastic sediments where at least 50% of mass have a grain size from 0.063 mm to 2.0 mm. Its chemical composition depends on parent material but main constituents are quartz, feldspar, and mica. The longer the natural transport of sand is, for example in rivers, the higher is the share in quartz (silicon dioxide), because it has the highest chemical resistance, is not divisible, and it is the hardest of these minerals (SCHUMANN, 2009).



Figure 3.1-4: Turkish sand

TS used in the experiment has been supplied from the riverbed of “Kizilirmak”, which is one of the largest rivers of Turkey meandering near Ankara (cf. Figure 3.1-4). The Kizilirmak (the red river), is 842 miles long and flowing into the Black Sea. The name Red River indicates that the water of Kizilirmak is rich in alluvium. As mentioned above, TS is very rich in silica.

Range of application (SCHUMANN, 2009):

- Construction material
- Concrete industry
- Glass industry
- Sandblast material
- Abrasive material

3.1.1.5 Turkish zeolite (TZ)

The name “Zeolite” originates from Greek and means, “boiling stone”. The name indicates its frothing when heated to a temperature of about 200°C. The group of Zeolites belong to the class of silicates and include minerals with similar properties, structure, and chemical composition. The Zeolite, used in the experiment, is a Clinoptilolite, one of the most useful natural Zeolites (ENLIMINING CORP., last visit 30.10.2010).

Clinoptilolite is a hydrated sodium potassium calcium aluminium silicate. Due to its high porosity the specific gravity is very low, approximately 2.2 and the surface area is very high. Half a

kilogram represents the surface of a football field. This large surface area in combination with a negative charge of structure leads to a high cation exchange capacity. Because of its physical properties, Clinoptilolite can absorb specific gas molecules selectively and water reversibly without any physical changes within the matrix.

Range of application:

- Pollution-Control
- Energy-Conservation
- Agriculture
- Mining
- Medicine
- Construction

The TZ used in this experiment originates from ENLI MINING CORPORATION, a mining company in Bayrakli, Izmir, Turkey that produces modified types of Zeolite for several and specific fields of application (cf. Figure 3.1-5). Regarding its chemical composition, confer Table 3.1-4.



Figure 3.1-5: Turkish zeolite

Table 3.1-4: Composition of TZ

Chemical composition in (%)*									
SiO ₂	Al ₂ O ₃	Fe ₂ O ₃	K ₂ O	MgO	Na ₂ O	CaO	TiO ₂	MnO	P ₂ O ₂
70.90	12.40	1.21	4.46	0.83	0.28	2.54	0.089	<0.01	0.02

*Reference: ENLI MINING CORPORATION, last visit 30.10.2010

3.1.2 Austrian filter materials

3.1.2.1 Crushed concrete (BE)

Concrete is a conglomerate, which consists of hardened cement paste, natural or artificial aggregates, mostly lime stone or quartz, and additives. This conglomerate has a wide range of application in construction industry. To meet the special requirements of different applications the chemical and mineralogical composition has to be modified and differs in a wide range (GRÜBL et al., 2001).

Cement consists of Portland cement clinker. This cement clinker is burned in a rotary kiln. Due to the chemical processes within this rotary kiln, cement always contains water-soluble salts mainly sulphates, chlorides, hydroxides and in the worst-case even chromate which is toxic. The amount of salts varies and can be higher than 1% of mass (MÜLLER, 2010).



Figure 3.1-6: Crushed concrete

BE is a waste product of construction industry. Concrete elements of pulled down buildings have to be crushed and homogenized to reach a certain range of particle size (cf. Figure 3.1-6).

Thus, the chemical and mineralogical composition of crushed concrete depends on its origin and is uncertain.

Additionally, depending on the former use of pulled down buildings, crushed concrete can contain pollutants, which are harmful to health and environment and can be washed out by water. Pollutants can be such as arsenic, lead, cadmium, copper, nickel, mercury, zinc, arenes and PAH (TECHNISCHE HOCHSCHULE DARMSTADT, last visit 25.11.2010).

Therefore, it is necessary to know the origin and to analyse the chemical and mineralogical composition of BE before using in CWs to prevent any recontamination of treated water by BE.

3.1.2.2 Ferro-Sorp® (FE)

FE is an artificial grained anion adsorber, which is based on ferric oxide hydrate. In general, ferric oxide occurs pasty. Via a patented process, ferric oxide is produced granular and available in different grain sizes after several milling and sieving processes. The transformation from pasty to granular makes FE suitable as filter material and applicable in a wide range. Because of its high specific surface and its chemical characteristics, related to phosphorus, phosphate, silicate, nitrogen compounds, hydrogen sulphide, arsenic and heavy metals, FE has a high adsorption capacity. Preliminary, they are bonded to the surface and afterwards transformed to stable ferrous compounds (HEGO BIOTEC GMBH, last visit 30.11.2010).



Figure 3.1-7: Ferro-Sorp®

Range of application (HEGO BIOTEC GMBH, last visit 30.11.2010):

- Bonding of phosphate of rivers and lakes
- Treatment of heavy metal polluted industrial wastewater
- Treatment of contaminated groundwater
- Elimination of phosphate compounds in CWs
- As reactive barriers for retention of contaminations
- Bonding of nutrients in aquariums or garden ponds

Advantages of FE (ZEOLITH UMWELTECHNIK GMBH, last visit 30.11.2010).

- Low costs
- High specific surface
- No change of pH-value of treated water
- No yield of anions to treated water

The FE used in this experiment originates from BIOTOP Landschaftsgestaltung, in Klosterneuburg-Weidling, Hauptstrasse 285, Lower Austria, Austria (cf. Figure 3.1-7). This company is a specialist in landscape design and pond construction.

Due to the patented production process, the chemical composition of FE was not available.

3.1.2.3 Austrian zeolite 1 (AZ1)

Since the differentiation between Austrian and Turkish zeolite refers only to their commercial source of supply, the characteristics and the geological genesis of the Austrian equals the Turkish zeolite (cf. chapter 3.1.1.5). The differentiation between Austrian Zeolite 1 and 2 refers to particle size distribution. This distinction was made to evaluate the influence of grain size on physical and hydrological characteristics and on cleaning performance.

The particle size of AZ1 ranged from 1.5 to 2.0 mm. It originated from PANACEO International Active Mineral Production GmbH, in Gödersdorf, Carinthia, Austria (cf. Figure 3.1-8). This company works in the field of alternative medicine and sells and develops products for health enhancement, which are based on zeolite.



Figure 3.1-8: Austrian zeolite 1

3.1.2.4 Austrian zeolite 2 (AZ2)

Concerning material description and source of supply confer chapter 3.1.1.5 and chapter 3.1.2.3.

The particle size of AZ2 ranged from 2.0 to 2.5 mm (cf. Figure 3.1-9).



Figure 3.1-9: Austrian zeolite 2

3.1.2.5 Austrian sand (AS)

AS is natural silica sand, free of clay and other impurities. Sand has a wide range of application in construction industry. The AS used in this experiment originates from LUSIT Betonelemente Löhne GmbH & Co. KG (cf. Figure 3.1-10), a company which produces concrete elements for application in landscape design. The particle size ranged from 0 mm to 4.0 mm.



Figure 3.1-10: Austrian sand

3.1.3 Mixed materials

Compositions were made to research if the combination of specific characteristics of different filter materials have any influence on the purification performance.

3.1.3.1 Ferro-Sorp® + Turkish zeolite (FE+TZ)

FE+TZ is a composition of 50% FE and 50% TZ (cf. Figure 3.1-11) where the characteristics of FE and TZ are represented. As mentioned above, FE is an anion adsorber (cf. chapter 3.1.2.2) and TZ a cation adsorber (cf. chapter 3.1.1.5). Both have a high specific surface.



Figure 3.1-11: Ferro-Sorp® + Turkish zeolite

3.1.3.2 Mixture (MX)

MX is a mixture of nine different filter materials, 1 kg each (cf. Figure 3.1-12). Therefore, the characteristics of this nine filter materials are represented in MX. Nine because there was no material of AZ2 left for adding to MX.



Figure 3.1-12: Mixture

3.2 Experimental set-up

The experimental set-up was placed at the technical laboratory hall of the Institute of Sanitary Engineering and Water Pollution Control of the University of Natural Resources and Life Sciences, Vienna (BOKU). It consisted of 14 columns, to represent unplanted VSSF CWs.

3.2.1 Design of the column experiment

The columns were made of PVC-pipes, which had a length of 1 m and a diameter of 20 cm. The bottoms of the pipes were sealed with stoppers, which were drilled in the middle to enable effluent. The drilled holes had a diameter of 1 cm. They were supported by grids in order to prevent any wash-out of filter material. The PVC-pipes were mounted to a rack (cf. Figure 3.2-1).



Figure 3.2-1: Experimental set-up

At the bottom of each of the columns, there was a supporting layer of 5 cm washed gravel with a particle size of 15/30 mm. The layer above consisted of filter materials. Ten of the columns were filled with a single material (SL, PE, PU, TS, TZ, BE, FE, AZ1, AZ2, AS) in a height of 50 cm (column numbers 1-10). The remaining four columns were filled with mixtures of various filter materials. One of them, with a composition of 50 % FE and 50 % TZ (FE+TZ) and in a height of 50 cm (column number 11) to question whether there will be an improved removal of ammonium - nitrogen (concerning the objectives of ONUREM) and whether there is any influence on the physical and hydrological characteristics. Three columns were filled with a mixture composed of SL, PE, PU, TS, TZ, BE, FE, AZ1, and AS in equal parts. In order to ascertain the influence of the height of filter on the removal performance of the columns (concerning the objectives of ONUREM) and the influence on the physical and hydrological characteristics, these three columns were filled in a different height of 30 cm, 50 cm and 75 cm, (MX 30, MX 50, MX 75, column numbers 12-14) (cf. Figure 3.2-2).

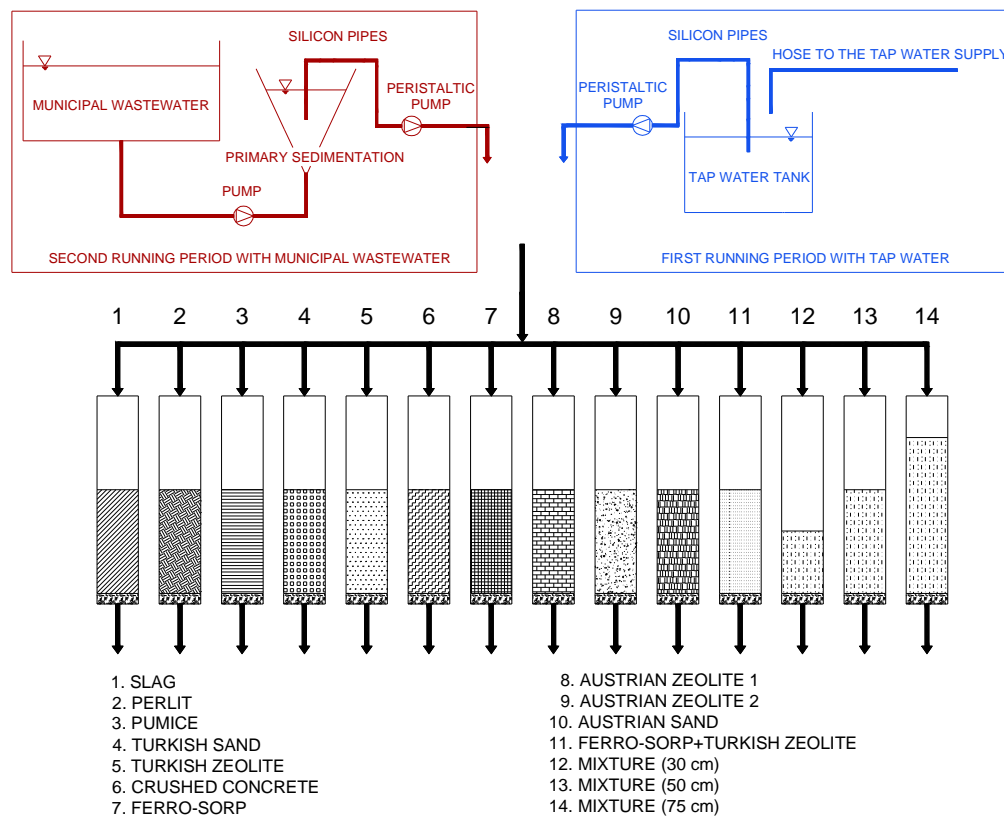


Figure 3.2-2: Scheme of experimental set up

3.2.2 Operation of the column experiment

In order to check if the columns are operating properly, they were operated with tap water during the first running period of the experiments. Tap water was provided from the water supply system of Vienna and, before applied, stored in a PVC tank beside the experiment.

Afterwards, columns were operated with primarily treated municipal wastewater, supplied from the sewer system of Vienna. The fresh wastewater, taken from the sewer line, was treated primarily in a sedimentation tank, located in the technical laboratory hall.

The water was applied from tanks (tap water tank or sedimentation tank) intermittently with a peristaltic pump using silicon pipes. The pump was operated at 220 rpm automatically. The duration of loadings was 10 minutes, four times a day, at 9:00 am; 3:00 pm; 9:00 pm, and 3:00 am. Time and duration of loading was controlled with a timer. Thus, and with the given diameter of the silicon pipes, a theoretical hydraulic loading rate (HLR) of approximately 60 mm/day for each of the columns was insured. A HLR of exactly 60 mm/day was not possible because the peristaltic pump did not provide the same water volume for each of the columns. It varied in a range of 490 ml/load to 550 ml/load (cf. Table 3.2-1). The reason was the design of the pump (cf. Figure 3.2-3). The pipes were mounted to the top of the columns (cf. Figure 3.2-4).



Figure 3.2-3: Peristaltic pump



Figure 3.2-4: Top view (inlet)

Table 3.2-1: Characteristics of the columns

Turkish filter material			Height of filter [cm]	Volume per loading [ml/load]	HLR
1	Slag	SL	50	520	66
2	Perlit	PE	50	520	66
3	Pumice	PU	50	519	66
4	Turkish Sand	TS	50	550	70
5	Turkish Zeolite	TZ	50	530	68
Austrian filter material					
6	Crushed concrete	BE	50	530	68
7	Ferro-Sorp®	FE	50	530	69
8	Austrian Zeolite 1	AZ1	50	546	70
9	Austrian Zeolite 2	AZ2	50	520	66
10	Austrian Sand	AS	50	520	66
Compositions					
11	Ferro-Sorp®+Turkish Zeolite	FE+TZ	50	520	66
12	Mixture	MX 30	30	490	62
13	Mixture	MX 50	50	530	68
14	Mixture	MX 75	75	520	66

To prevent erosion of filter material, induced by influent, Plexiglas baffle plates were placed on the surface of the filter materials in each of the columns (cf. Figure 3.2-5).

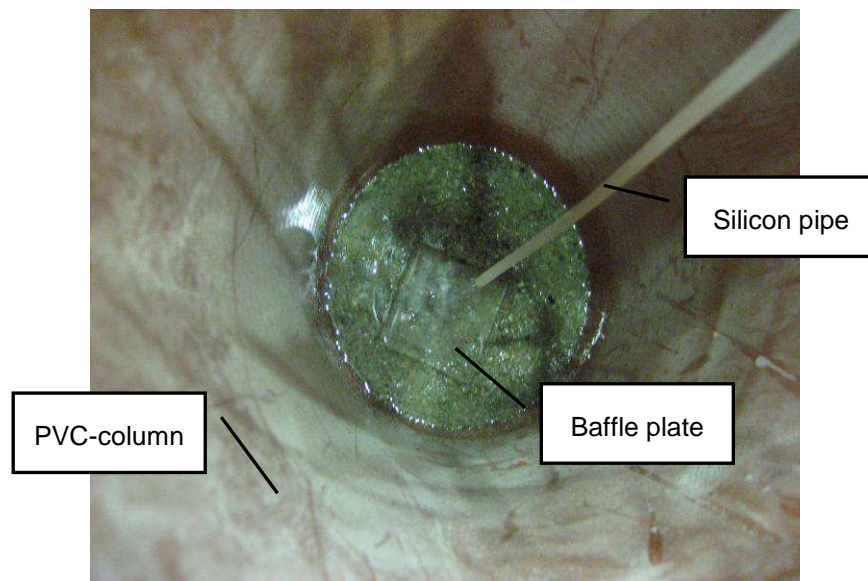


Figure 3.2-5: Interior view of a column

From the inlet water percolated, through the substrates, to the outlet, where the effluent was collected for measurements and analysis (cf. Figure 3.2-6).



Figure 3.2-6: Bottom view (outlet)

3.3 Measurements

For determination of physical and hydrological characteristic different methods were applied. These methods were:

- Sieve analysis (grading curves)
- Pycnometer experiment (particle density, bulk density)
- Determination of permeability (k-value)
- Water flow at column experiments (HLR, hydrographs, summation curves)
- Tracer experiment at the lab-scale column experiment (HRT)

Table 3.3-1 shows the times when the different measurements have been carried out.

Table 3.3-1: Operating schedule

K-value measurements		07.06.2006
Pycnometer experiments		14.06.2006
Tracer experiments	SL	04.08.2006 - 10.08.2006
	PE	14.08.2006 - 19.08.2006
	PU	21.08.2006 - 01.09.2006
	TS	01.09.2006 - 05.01.2006
	TZ	15.09.2006 - 19.09.2006
	BE	15.09.2006 - 20.09.2006
	FE	22.09.2006 - 26.09.2006
	AZ1	22.09.2006 - 26.09.2006
Hydrograph measurements tap water		28.09.2006
Tracer exp.	AZ2	29.09.2006 - 02.10.2006
	AS	01.02.2007 - 05.02.2007
	FE+TZ	01.02.2007 - 06.02.2007
	MX 30	01.02.2007 - 08.02.2007
	MX 50	14.02.2007 - 20.02.2007
	MX 75	14.02.2007 - 22.02.2007
Hydrograph measurements wastewater		24.04.2007

3.3.1 Sieve analysis

Sieve analysis is a method to determine the particle size distribution of a sample of granular materials by sieving through sieves with different mesh sizes. The sieving was carried out with a sieving machine (cf. Figure 3.3-1). The particles of a sample become classified according to the mesh size of the last sieve, which the particles pass. The result is a grading curve where the cumulative percentage of mass is plotted versus the according logarithm of mesh size (SMOLTCZYK et al, 2001).



Figure 3.3-1: Sieving machine

3.3.1.1 Grading curve

Sieve analysis was done with all filter materials except AZ1, AZ2, and MX. With AZ1 and AZ2, no sieve analysis was done because of the uniformity of grain sizes. The grading curve of MX equals the average of its components and no significant change due to the mix of single materials was expected. The filter materials were sieved through seven sieves with different mesh-sizes of 4.00, 2.00, 1.40, 1.00, 0.71, 0.50, 0.25 mm. Each filter material was sieved three times, two times with a sample size of 450 g and once with a sample size of 1000 g. The sieving analysis with a sample size of 1000 g was carried out in order to see, if there is an influence of sample size on resulting particle size distribution. After that, the average was built. Sieve analyses were carried out by Dr. Korkusuz.

Procedure (CEN ISO/TS 17892 – 4, 2004):

- 1) Samples of each filter material were taken.
- 2) The samples were dried in an incubator oven (105 °C) until the mass constants was reached.
- 3) The largest sieve size, through which all particles passed, was found.
- 4) The smallest sieve size, through which none of the particles passed, was found.
- 5) Five different sieves with sizes between the two extremes were placed onto the sieving machine and the samples were sieved for five minutes.
- 6) The fractions retained by the individual sieves were weighed.
- 7) The cumulative percentage by weight, passing a sieve with a defined mesh size, was calculated by subtracting cumulative percentage by weight of retained particles from 100 %.
- 8) Logarithm of sieve size versus cumulative percentage passing values was plotted.

The shape of the grading curve is characterised by two coefficients. The uniformity coefficient describes the average inclination and the coefficient of gradation the run of the curve between d_{10} and d_{60} (SMOLTCZYK et al., 2001).

The uniformity coefficient is determined as:

$$C_U = \frac{d_{60}}{d_{10}} \quad (\text{Eq. 1})$$

The coefficient of gradation is determined as:

$$C_C = \frac{d_{30}^2}{d_{10} \cdot d_{60}} \quad (\text{Eq. 2})$$

Where:

C_UUniformity Coefficient [-]

d_{60} Particle size corresponding to mass of through fraction of 60%

d_{10} Particle size corresponding to mass of through fraction of 10%

d_{30} Particle size corresponding to mass of through fraction of 30%

C_CCoefficient of gradation [-]

The resulting grading curves were compared to the grading curves of Platzer who recommended lower (Platzer 1) and upper (Platzer 2) limits of grain size distribution of materials which are suitable for the use as filters in VF CWs (cf. Figure 3.3-2). The comparison was done graphically and in terms of uniformity coefficient, coefficient of gradation, and effective grain size. Furthermore, the results of sieving analysis were compared in terms of requirements of DWA A 262 (2006) and ATV A 262 (1997). The DWA A 262 (2006) guidelines are the updated version of the ATV A 262 (1997) guidelines. Both guidelines are referred to as they include different requirements regarding selection of the filter material.

The borders Platzer 1 and Platzer 2 imply a classification of the filter material as sand respectively sandy gravel. Furthermore, recommended Platzer specific ranges of d_{10} , C_U and C_C .

$$0.1 \text{ mm} \leq d_{10} \leq 0.5 \text{ mm}$$

$$2 \leq C_U \leq 6$$

$$C_C \leq 1$$

Fulfilment of the recommendations concerning C_U and C_C means that the filter material is poorly graded (BIEHL, 2009). A property recommended in relevant standards.

The DWA A 262 (2006) requires poorly graded filter materials consisting of sand or sandy gravel with a steady grading curve. For fulfilment of this requirement, borders concerning d_{10} , C_U are defined.

$$0.2 \text{ mm} \leq d_{10} \leq 0.4 \text{ mm}$$

$$C_U \leq 5$$

ATV A 262 (1997) requires poorly graded filter materials. This requirement is fulfilled by materials with values of d_{10} and C_U of

$$d_{10} > 0.2$$

$$C_U \leq 5$$

Intermittent graded materials are some with $C_U > 5$ **and** $1 > C_C > 3$. These materials should not be used in CWs because they have a disposition to compaction due to particle displacement (LABER, 2001).

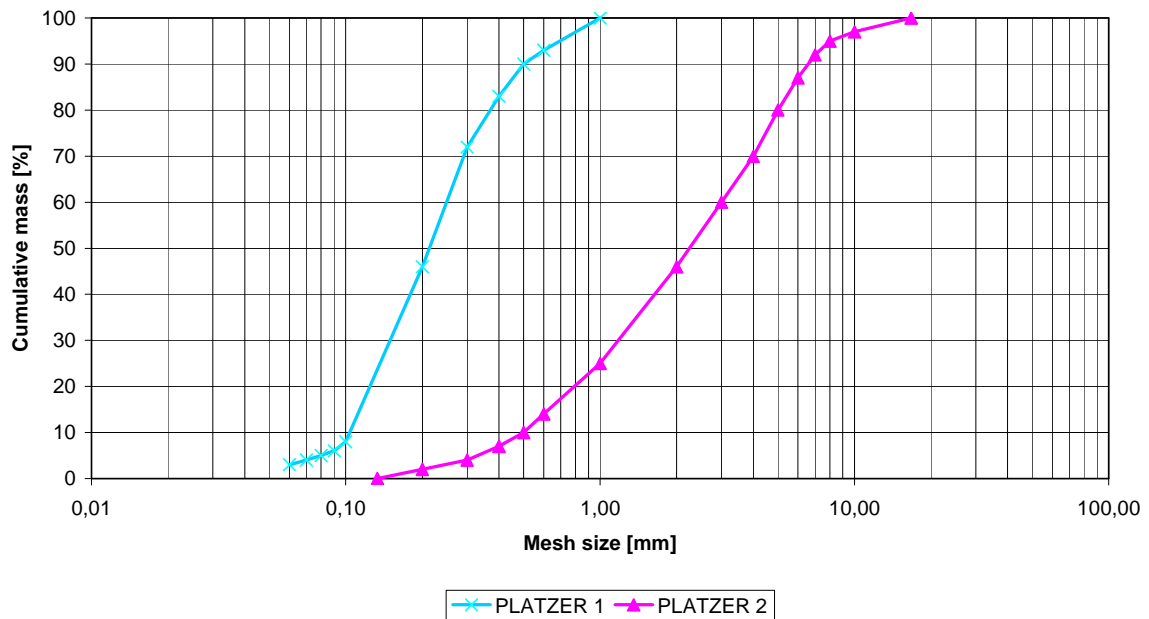


Figure 3.3-2: Recommended grain size distribution (PLATZER, 1997)

The filter materials were classified according ÖNORM EN ISO 14688-1 (2002).

Table 3.3-2: Soil classification (ÖNORM EN ISO 14688-1, 2002)

Group	Class	Subclass	Abbr.	Grain size (Mesh size) [mm]
Coarse grained	Gravel	Coarse gravel	CGr	> 20 - 63
		Medium gravel	MGr	> 6.3 - 20
		Fine gravel	FGr	> 2.0 – 6.3
	Sand	Coarse sand	CSa	> 0.63 – 2.0
		Medium sand	MSa	> 0.2 – 0.63
		Fine sand	FSa	> 0.063 – 0.2
Fine grained	Silt	Coarse silt	CSi	> 0.02 – 0.063
		Medium silt	MSi	> 0.0063 – 0.02
		Fine silt	FSi	> 0.002 – 0.0063
	Clay	Clay	Cl	< 0.002

3.3.2 Pycnometer experiments

The experiments for the determination of bulk densities and particle densities of the filter materials were carried out at the laboratory of the Institute at BOKU. For these measurements, capillary pycnometers with a volume of 50 ml were used (cf. Figure 3.3-3). Each of the filter materials was measured three times. The mean value and the standard deviation of the results were calculated.



Figure 3.3-3: Pycnometers

Materials and pycnometers had to be cooled down in a desiccator (cf. Figure 3.3-4) and weighed (cf. Figure 3.3-5).



Figure 3.3-4: Desiccator



Figure 3.3-5: Scale, type Sartorius

3.3.2.1 Particle density

Particle density of soils refers to the density of the solid particles collectively. It is expressed as the ratio of the total mass of solid particles to their total volume, excluding pore spaces between the particles but including voids within the grains (SMOLTCHYK et al., 2001)

Because of the influence of temperature on the density of water, the temperature had to be constant during measurement. The water used had a temperature of 21.4 °C during the entire measurement. This temperature corresponds to a density of 0.998 g·m⁻³ (DIN 18124, 1997).

Procedure (DIN 18124, 1997):

- 1) The capillary pycnometer was washed (with RO-water).
- 2) It was dried in an incubator oven (105 °C).
- 3) The pycnometer was cooled down in a desiccator.
- 4) The cooled down pycnometer with its stopper was weighed (cf. Figure 3.3-5).
- 5) Then, the pycnometer filled with RO-water and its stopper was weighted.
- 6) The pycnometer was filled with approximately 20 mg of the filter material and weighed with its stopper.
- 7) The pycnometer with approximately 20 mg filter material was filled with RO-water, shaken until no bubbles were rising to prevent the occurrence of air within the pores, and weighed with its stopper.

The particle density was calculated by:

$$\rho_s = \frac{(M_3 - M_1)}{(M_2 - M_1) - (M_4 - M_3)} \cdot \rho_{TW} \quad (\text{Eq. 3})$$

Where:

ρ_s Particle density [g/m³]

M_1 Mass of the empty pycnometer with stopper [g]

M_2 Mass of the pycnometer filled with RO-water plus stopper [g]

M_3 Mass of the pycnometer plus stopper and app. 20 mg of the filter material [g]

M_4 Mass of the pycnometer plus stopper, and Filter material and filled with water [g]

ρ_{TW} Density of water at a certain temperature [g/cm³]

3.3.2.2 Bulk density

Bulk density and porosity describe soil compactness. With increasing soil compactness the bulk density increases and correspondingly the porosity decreases (KELLER and HÅKANSON, 2010).

Procedure:

- 1) The pycnometers were washed with RO-water.
- 2) The filter materials and pycnometers were dried in an incubator oven at a temperature of 105 °C for 1 hour until the constants of mass was reached.
- 3) The pycnometers were weighted with stopper after they were cooled down in a desiccator.
- 4) The pycnometers were filled with one filter material and weighed with its stopper.

The bulk density was calculated by:

$$\rho_d = \frac{M_2 - M_1}{V_p} \quad (\text{Eq. 4})$$

Where:

ρ_dBulk density [g/cm³]

M_1Mass of the empty pycnometer with stopper [g]

M_2Mass of the pycnometer with stopper, filled with filter material [g]

V_pVolume of the pycnometer [cm³]

The porosity was calculated with the results of bulk density and particle density calculation. The resulting values were averaged, and the standard deviation was calculated.

The porosity was calculated by:

$$n = 1 - \frac{\rho_d}{\rho_s} \quad (\text{Eq. 5})$$

Where:

nPorosity [-]

ρ_dBulk density [g/m³]

ρ_sParticle density [g/m³]

3.3.3 Determination of permeability

The method for determination of permeability is based on Darcy's Law.

To describe groundwater flow in porous media quantitatively, Henry Darcy (1803 - 1858) a French scientist, carried out experimental studies (Figure 3.3-6). In these studies, he let water flow through sand filled pipes and found 1856 the law named after him. He determined that a perpendicular flow (Q) through a certain area (A) is proportional to the difference of hydrostatic pressure head (Δh) and the hydraulic conductivity (k_f) and inverse proportional to the length of flow (Δs). The ratio $\Delta h/\Delta s$ is denominated as hydraulic gradient and the ratio Q/A as filtration rate (LECHER et al, 2001).

Darcy's Law is only valid for laminar flow. For flows through granular materials with a grain size lower than coarse gravel laminar flow can be assumed (KOLYMBAS, 2007).

The criterion for laminar flow is the Reynolds number. It has to be ≤ 10 (SMOLTCZYK et al, 2001):

$$Re = \frac{d_{50} \cdot v_f}{v_{fl}} \leq 10 \quad (\text{Eq. 6})$$

Where:

Re Reynolds number [-]

d_{50} Medium grain diameter [m]

v_{fl} Kinematical viscosity [m^2/s]

v_f Filtration rate [m/s]

The kinematical viscosity depends on temperature and it amounts to $1.310 \cdot 10^{-6} \text{ m}^2/\text{s}$, at 10°C . This is also the temperature where the k_f -value is defined.

Darcy's law can be written as follows (LECHER et al, 2001):

$$\frac{Q}{A} = k_f \cdot \frac{\Delta h}{\Delta s} \quad (\text{Eq. 7})$$

Where:

Q Flow rate [m^3/s]

A Area [m^2]

k_f Hydraulic conductivity [m/s]

Δh Difference of hydrostatic pressure head [m]

Δs Length of flow [m]

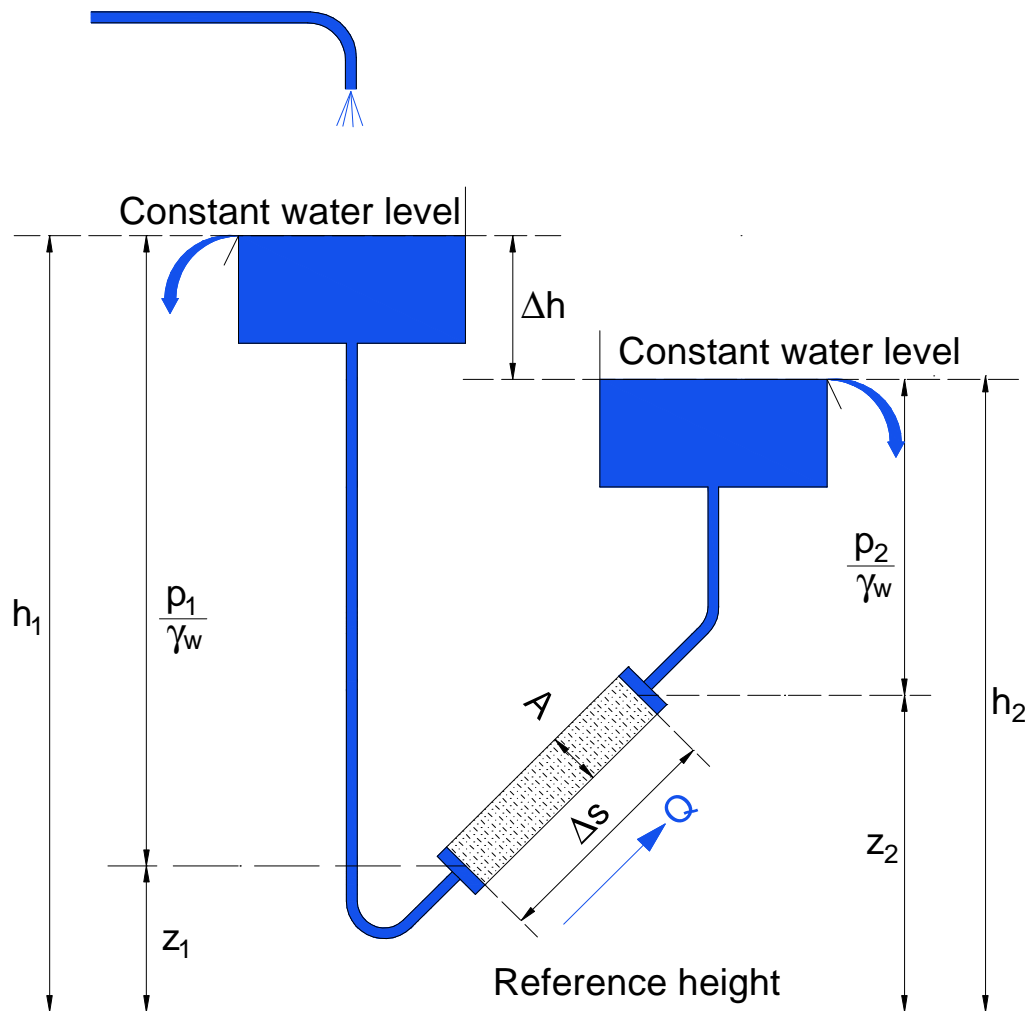


Figure 3.3-6: Scheme of Darcy's experiment (LECHER et al, 2001)

Where:

$z_{1,2}$ Geodetical height [m]

$\frac{p_{1,2}}{\gamma_w}$ Pressure head [m]

3.3.3.1 Measurement of k -value

The k -value can be measured with an invariant pressure head gradient and with a variant pressure head gradient. Mentioned first is preferred for granular materials. Supposition for a correct measurement is steady flow, which is insured by measuring under saturated conditions (SMOLTCZYK et al, 2001).

The used k_f measurement device consisted of a 300 mm long PVC-pipe with an inner diameter of 100 mm and a cross section area of 7854 mm². As support layer for the filter material, there was a horizontal grid within the pipe in a distance from the bottom of 55 mm. Two Plexiglas tubes with a diameter of 5 mm were mounted to the pipe. To prevent any escape of filter material, the inlets of these tubes were supported by grids. The vertical distance of the inlets of tubes was 100 mm. This determines the flow length (dL). To insure saturated conditions, the inflow hose was at the bottom of the pipe. The discharge hose was 50 mm under the top of the pipe and determined a constant water level within the PVC-pipe (cf. Figure 3.3-7).

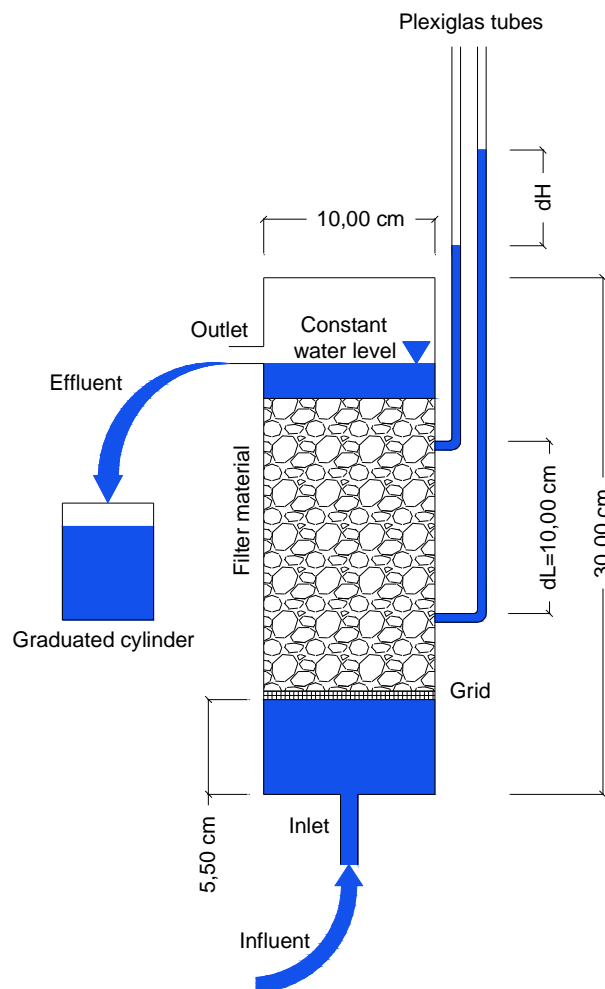


Figure 3.3-7: Scheme of experimental set up

Procedure (cf. Figure 3.3-8), (CEN ISO/TS 17892-11, 2004):

- 1) Water was led from the bottom, through the material, to the outlet.
- 2) When the effluent equalled the influent, saturated conditions were reached and the water level within the PVC-pipe was constant.
- 3) After a while, a constant difference of water levels within the Plexiglas tubes adjusted. This difference determined the pressure head difference (dH).
- 4) The effluent was measured with a graduated cylinder and the time until the volume of one litre was reached was recorded.

For each filter material, this procedure was repeated five times and the k-values were calculated. The results were averaged and the standard deviation was calculated.

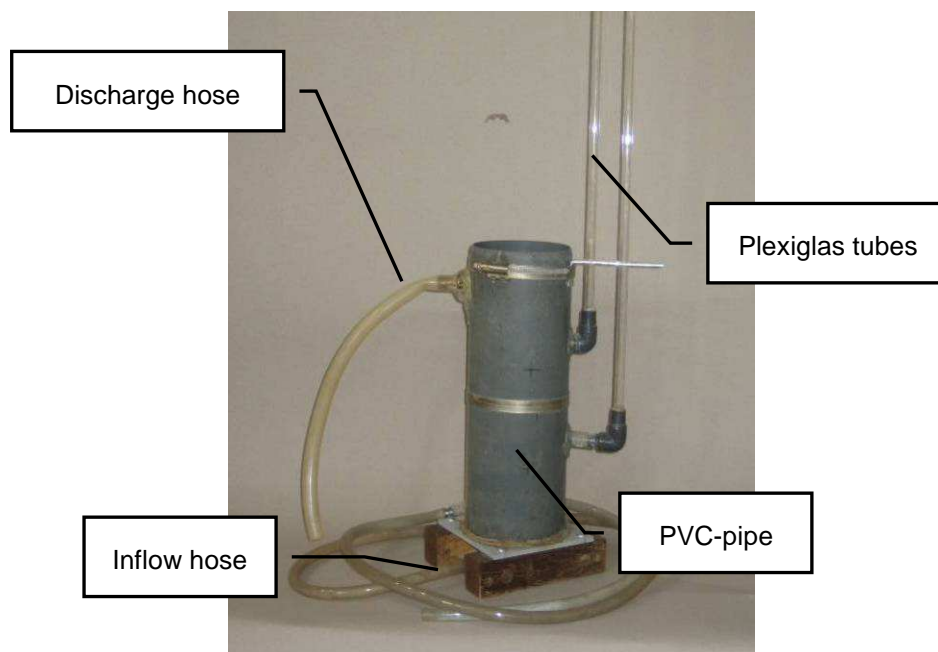


Figure 3.3-8: Device for k-value measurement

K-value was calculated by:

$$k = \frac{Q}{A} \cdot \frac{dL}{dH} \quad (\text{Eq. 8})$$

$$Q = \frac{V}{t} \quad (\text{Eq. 9})$$

$$k = \frac{\frac{V}{t}}{A} \cdot \frac{dL}{dH} \quad (\text{Eq. 10})$$

Where:

k k-value [m/s]

Q Effluent (one litre)

A Cross section area [mm²]

dL Flow length [mm]

dH Pressure head difference [mm]

V Volume [mm³]

t Measured time for reaching a volume of one litre [s]

3.3.3.2 k-value calculation based on effective grain diameter

Additional to the measurement of the k-value it was calculated based on effective grain diameter (d_{10}). This calculation is suggested in DWA A 262 (2006) because d_{10} determines the permeability of granular materials.

$$k = \frac{d_{10}^2}{100}$$

Where

k k-value [m/s]

d_{10} Effective grain diameter [mm]

3.3.4 Water flow at column experiments

At the column experiment, placed at the technical laboratory hall of the Institute (cf. chapter 3.2) hydrographs and cumulative effluent were measured, and, according to the given daily flow rate, the hydraulic load rate was calculated.

3.3.4.1 Hydraulic load rate

If CWs are operated with intermittent loading, the term hydraulic loading rate refers to the flow rate averaged over time. It does not imply the physical distribution of water uniformly over the wetland surface (KADLEC and KNIGHT, 1996).

The HLR was calculated by:

$$HLR = \frac{Q}{A} \quad (\text{Eq. 11})$$

Where:

HLR..... Hydraulic load rate [mm/d]

Q Water flow rate [mm³/d]

A Surface area [mm²]

HLR of columns, confer Table 3.2-1.

3.3.4.2 Hydrographs and cumulative effluent

Hydrographs are graphs of data in their temporal occurrence and summation curves are the progressive summation of hydrographs data versus time (MANIAK, 1997).

The hydrographs were measured to develop an idea on how long the applied water volume needs to pass through the columns and an idea about hydraulic capacity and infiltration dynamics of different filter materials. By defining, a certain minimum effluent the ratio of infiltration time and diffusion time can be calculated. Diffusion time is the time, which is available for oxygen supply of filter materials during resting time. Furthermore, a minimum sample size for later chemical analysis was essential. With hydrographs data of each column, the necessary time for reaching a sufficient volume of effluent was known. Finally, effluent hydrographs represent one of the basic data for a computer simulation of the experiment.

In order to see, the change of infiltration conditions between columns operated with tap water, and columns operated with wastewater, the measurements for each of the columns were carried out twice. The first measurement, with tap water and the second with municipal wastewater (cf. Table 3.3-1).

First measurement (tap water.)

Water was applied from a tank with a peristaltic pump via silicon pipes. The pump operated with 220 rpm. It was applied for ten minutes four times per day with an interval of 6 hours (Intermittent load). Within this 6 hours period, the measurement took place. The beginning of the measurement ($t=0$) was the start of loading of the peristaltic pump at 3 pm. During the resting period, the 10 minutes effluents of each column were collected in cups and measured with a graduated cylinder (cf. Figure 3.3-9 and Figure 3.3-10). With resulting 36 values the hydrographs and summation curves of the effluents were plotted.



Figure 3.3-9: Columns; cups for effluent collection

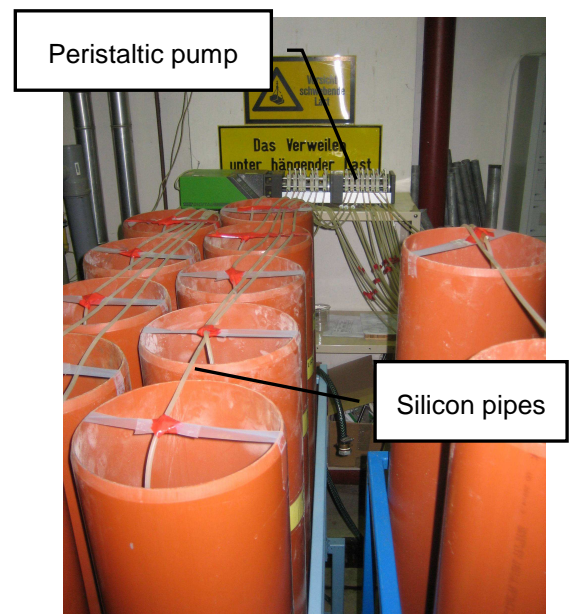


Figure 3.3-10: Columns, silicon pipes and peristaltic pump

Second measurement (wastewater)

Due to the occurrence of accumulation of sludge within the silicon pipes, which led to clogging, the loading conditions were not steady and loading volumes decreased. This effect was intensified by growth of microorganisms because, in combination with a high nutrient amount, the diaphanous silicon pipes provided them with good living conditions. To eliminate the effect on loading volume, the water volume which equals one loading period (10 minutes) was measured with a graduated cylinder for each column and applied manually (cf. Figure 3.3-). With this procedure, the same application volume as at measurement one was ensured. Thereafter, the 10 minutes effluents induced by loading were collected during a period of 6 hours and measured with a graduated cylinder. The measurement started at 3 pm. With resulting 36 values, the hydrographs and the summation curves were plotted.

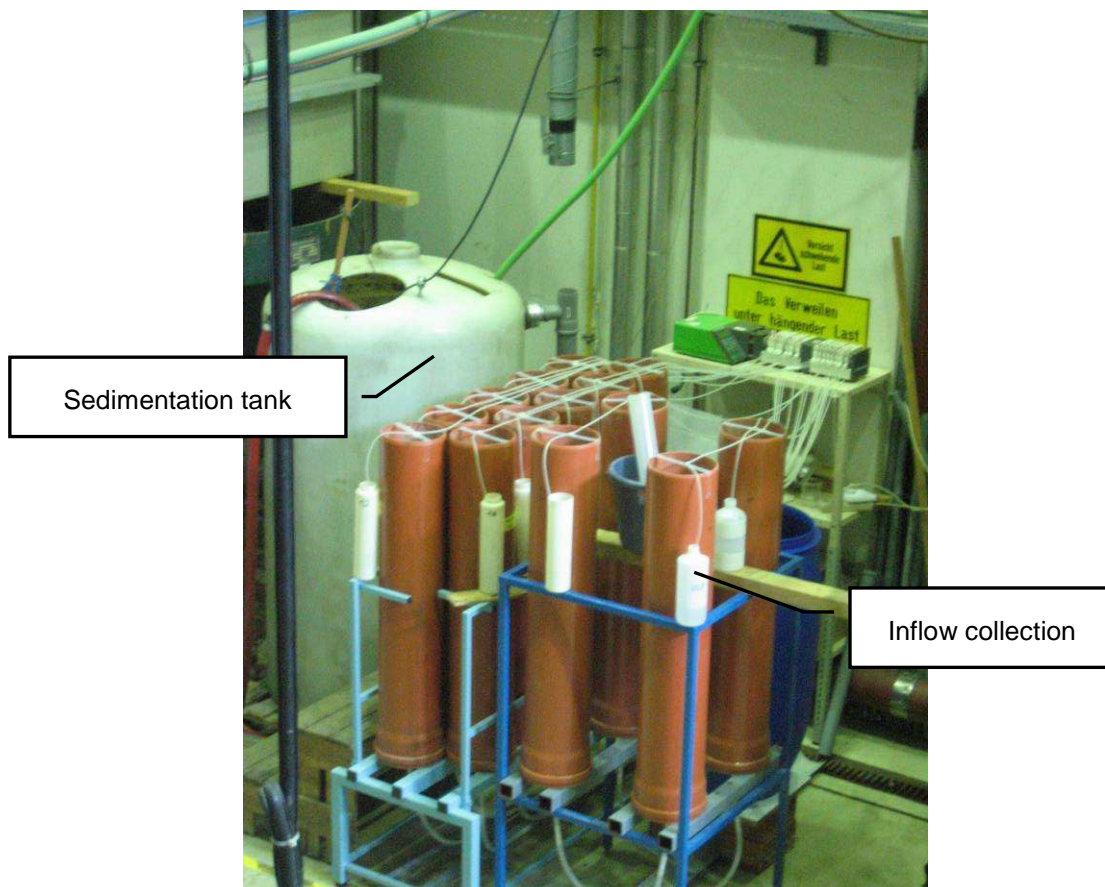


Figure 3.3-11: Collection of inflow

3.3.5 Tracer studies

Tracing is applied for tracking floating water. The main field of application are groundwater studies. Tracer experiments are applicable to assay direction and velocity of water flow and for analysis of hydrological characteristics like dispersion, porosity, hydraulic conductivity etc. Tracing can be conducted in two ways, either by using native occurring substances, which equal tracer properties, or by adding artificial substances (KÄSS et al., 1992)

Artificial tracer substances have to fulfil specific requirements (KÄSS et al., 1992):

- Absence in natural water or presence in very low concentrations
- low limit of detection
- Harmless for men, animals and plants
- Good water solubility and dispersible
- Stability concerning oxidising, reducing, acidic or basic reactions, resistant to microbiological degradation and to light and temperature
- Free of sorption and ion exchange properties
- Economical concerning acquisition, application and analysis

Applied artificial tracers are (KÄSS et al., 1992):

- Water soluble substances
 - Dyestuffs
 - Salts
 - Other chemicals
 - Isotopes
- Floats
 - Lycopod spores
 - Fluorescent pellets
 - Bacteria
 - Bacteriophages

Salts, frequently used as tracer substances, are for example KCl, NaCl, LiCl, and KBr.

Accomplishing tracer experiments, there are two options of tracer application. The impulse input and the continuous input.

1. Impulse input:

In the case of impulse input, the tracer solution is added to the inlet all at once. The effluent concentration is measured at the outlet continuously. Effluent concentration, respectively conductivity, plotted versus time results to the output function (cf. Figure 3.3-12) (TAUSENDSCHÖN, 1998).

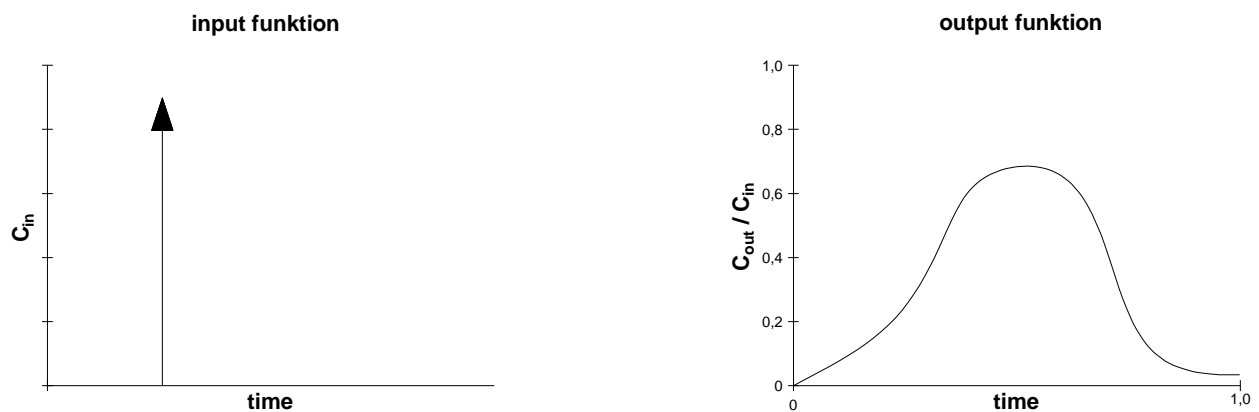


Figure 3.3-12: Impulse input and output function
(CLARK, 1996; adapted by TAUSENDSCHÖN, 1998)

2. Continuous input:

In the case of continuous input, from the beginning of the experiment, a constant amount of tracer solution is added at the inlet. The concentration at the outlet is measured continuously again. Effluent concentration versus time results to the output function (cf. Figure 3.3-13) (TAUSENDSCHÖN, 1998).

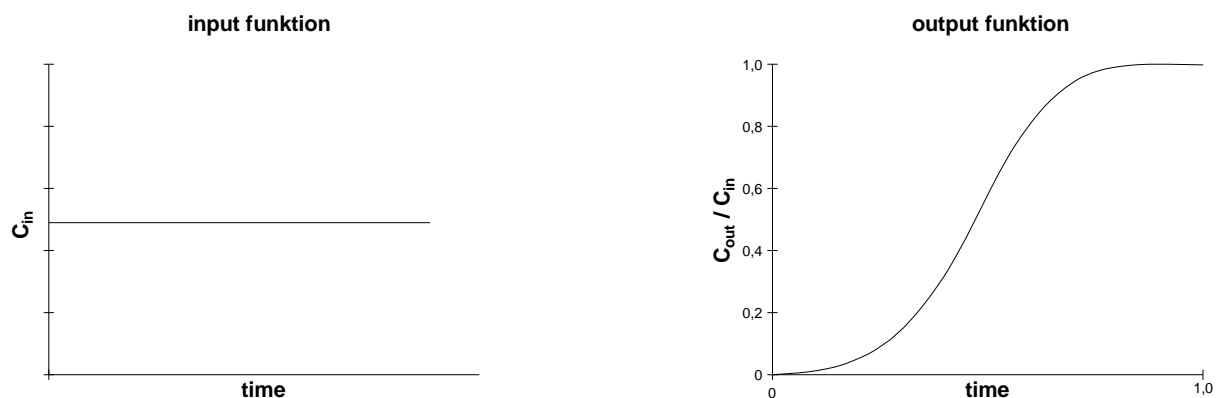


Figure 3.3-13: Continuous input and output function
(CLARK, 1996; adapted by TAUSENDSCHÖN, 1998)

3.3.5.1 Method

One tracer experiment was conducted for each column at the lab-scale column experiment for HRT determination and for later simulation studies. The used tracer was KCl.

To get an idea about the correlation of added mass of KCl, respectively concentration, and the electrical conductivity of solution a standard diagram was developed. For this purpose, one gram of KCl was added in progressive stages to a vessel filled with one litre of RO-water. At each stage, the electrical conductivity was measured with the conductivity meter WTW LF-196 (cf. Figure 3.3-14).



Figure 3.3-14: Conductivity meter WTW LF-196

This procedure led to 13 pairs of values (cf. Table 3.3-3). The background conductivity of solution was 0.005 mS cm^{-1} (RO–water).

Table 3.3-3: Pairs of value of the standard diagram

Concentration [mg/l]	0	1000	2000	3000	4000	5000	6000	7000	8000	9000	10000	11000	12000
Conductivity [mS/cm]	0.005	1.880	3.610	5.360	7.040	8.700	10.400	12.020	13.630	15.190	16.890	18.510	19.940

The plotting of conductivity versus concentration of KCl resulted in a standard diagram (cf. Figure 3.3-).

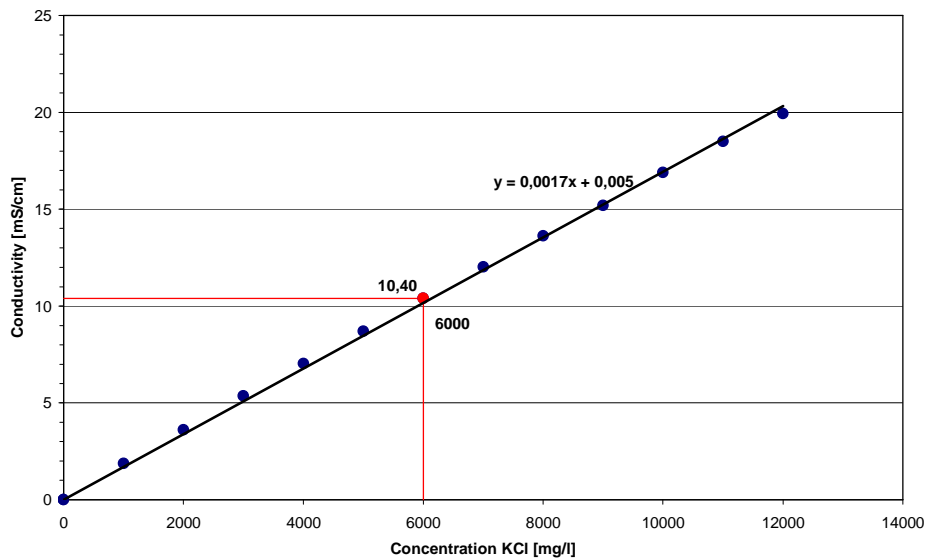


Figure 3.3-15: Standard diagram conductivity

The experiment started on the 4th of August 2006. Two columns were measured simultaneously. According to the standard diagram a tracer solution with a volume of two litres of water and a conductivity of 10.40 mS cm^{-1} (12 g KCl) was prepared. With this solution, one loading of two columns with water from the tap water tank was substituted (cf. Figure 3.3-16). The loadings of the 12 remaining columns were done with tap water.

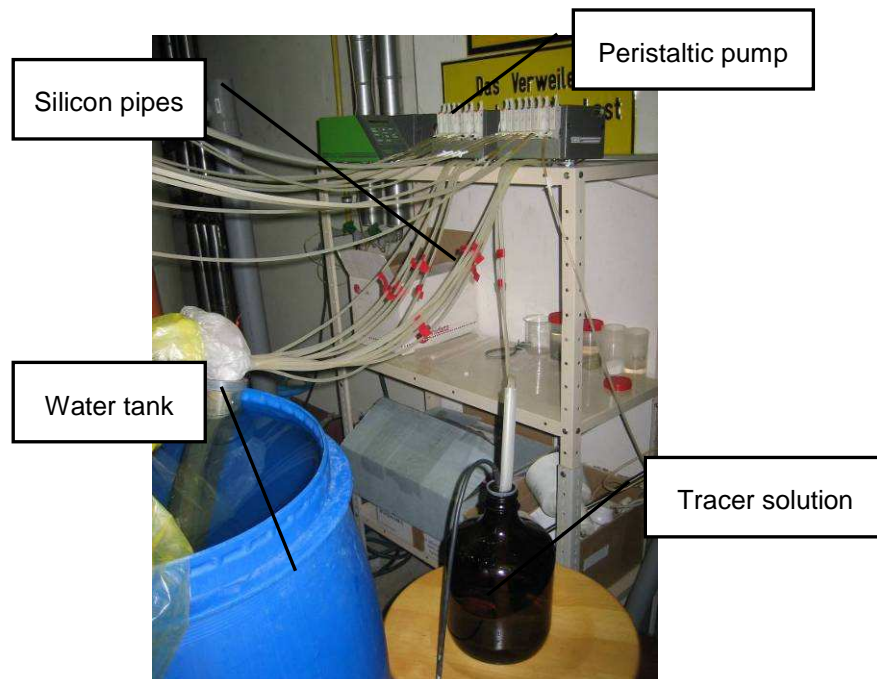


Figure 3.3-16: Application of tracer

After application of tracer, a back flushing, to prevent the occurrence of any residuals of KCl within the silicon pipes, was necessary. Any further loads were accomplished with water from the tap water tank. The conductivity of tap water was measured over the entire duration of the experiment to differentiate the background conductivity from the overall conductivity, which results in the tracer induced conductivity.

The effluent was collected with a collection cup and measured with the probe of the conductivity meter within the cup. (cf. Figure 3.3-17).

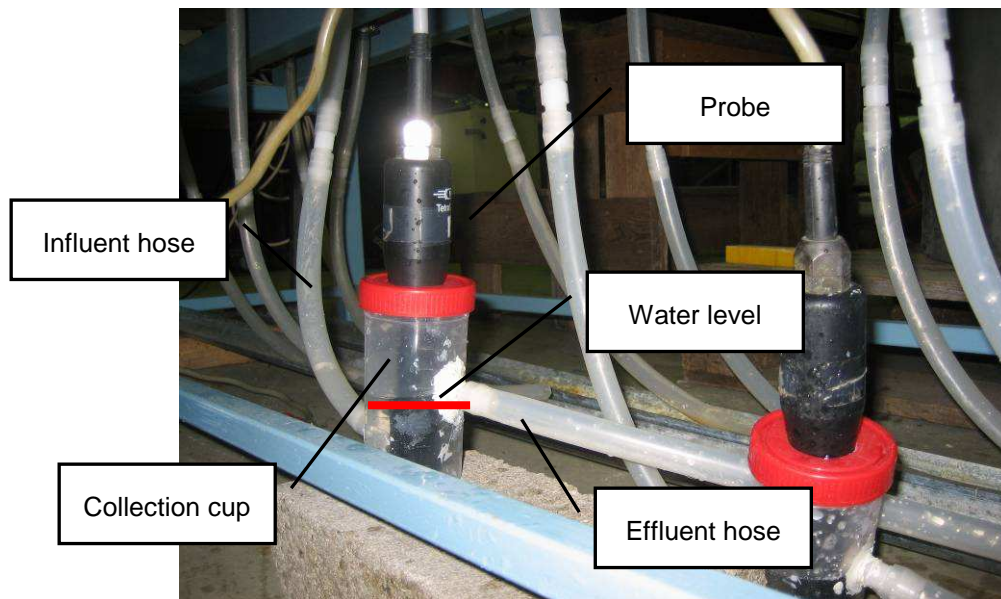


Figure 3.3-17: Effluent measurement

To insure a constant circulation of tracer solution around the probe, the influent hose of the cup was situated 1 cm above the bottom and the effluent hose 5 cm above the influent hose on the opposite side. The height of the effluent hose determined the water level and therewith a constant water volume (cf. Figure 3.3-18). It has to be as small as possible because the smaller the water volume the bigger is the impact of the potassium chloride solution on conductivity and the better the change of conductivity is measurable. The water volume within the cup was approximately 100 ml. The change of conductivity was measured continuously with a probe. To insure the submergence of the probe from the very first, the collection cup was filled with tap water manually before starting the measurement.

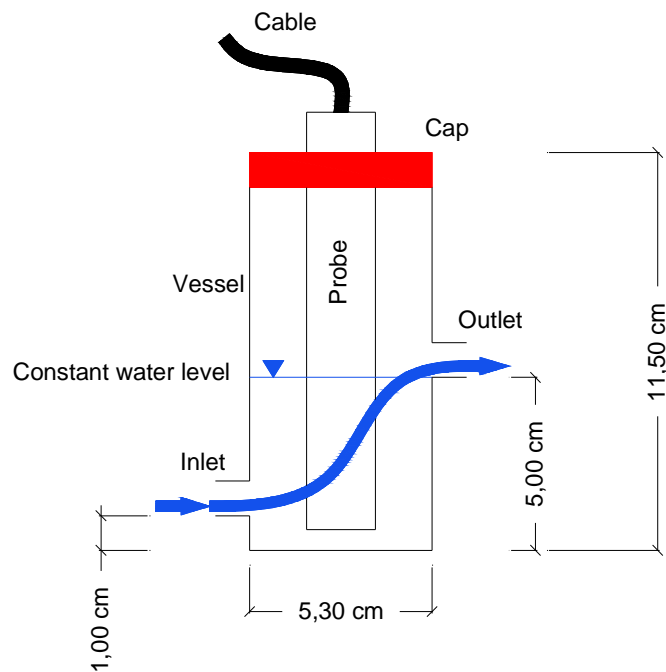


Figure 3.3-18: Scheme of conductivity measurement of effluent

The data were registered and saved automatically by a data logger (cf. Figure 3.3-19), transferred to a notebook and processed by using the computer program MSExcel®.

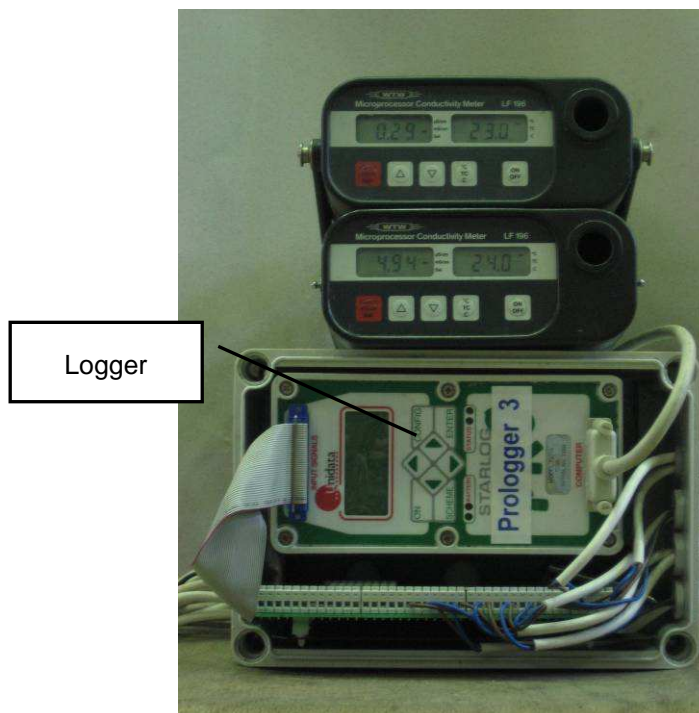


Figure 3.3-19: Data logger

3.3.5.2 Data processing

The measured data have to be processed for differentiation of background conductivity from the tracer-induced conductivity, for elimination of outliers, and in the case of change of the background conductivity, which leads to a negative tracer induced conductivity, for elimination of the negative values. The tracer-induced conductivity was calculated by subtracting influent conductivity from effluent conductivity. The outliers were eliminated by calculation of median and mean values. The negative values were eliminated by subtracting the trends of influent and effluent conductivity. At the end of processing, the cumulative conductivity was calculated and plotted versus time.

The processing of data is illustrated using the example of AS

1. Raw data

Starting point of evaluation was plotting the raw data of conductivity versus time (cf. Figure 3.3-20).

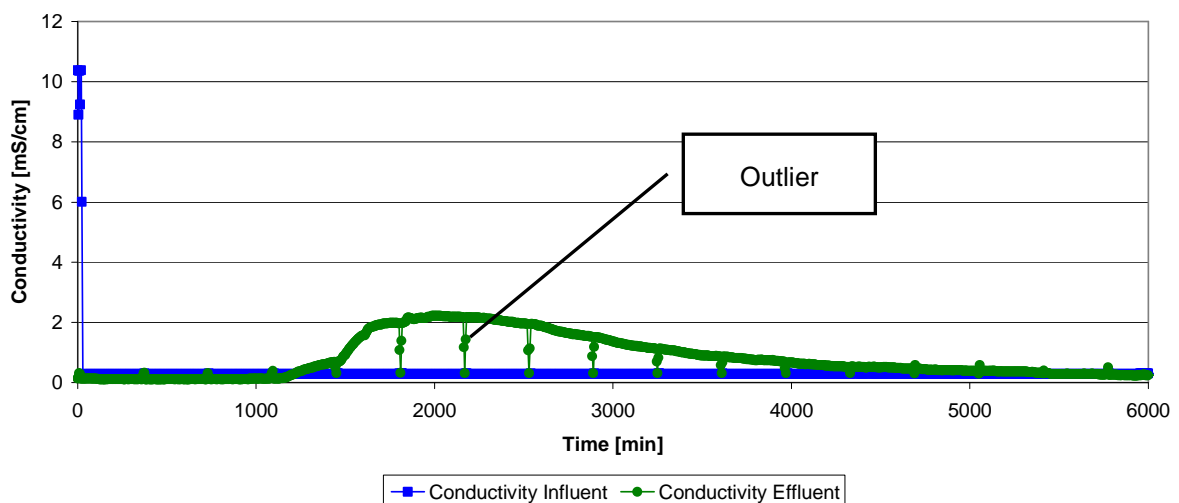


Figure 3.3-20: Tracer raw data

2. Calculation of median values

In a first step, to eliminate outliers, the median values of a period of 360 minutes (the loading interval of six hours) were calculated and again plotted versus time. With calculation of median values, most of the outliers were eliminated, but not completely (cf. Figure 3.3-21). Hence, a second step for elimination of outliers was necessary. It was done by calculating the average values.

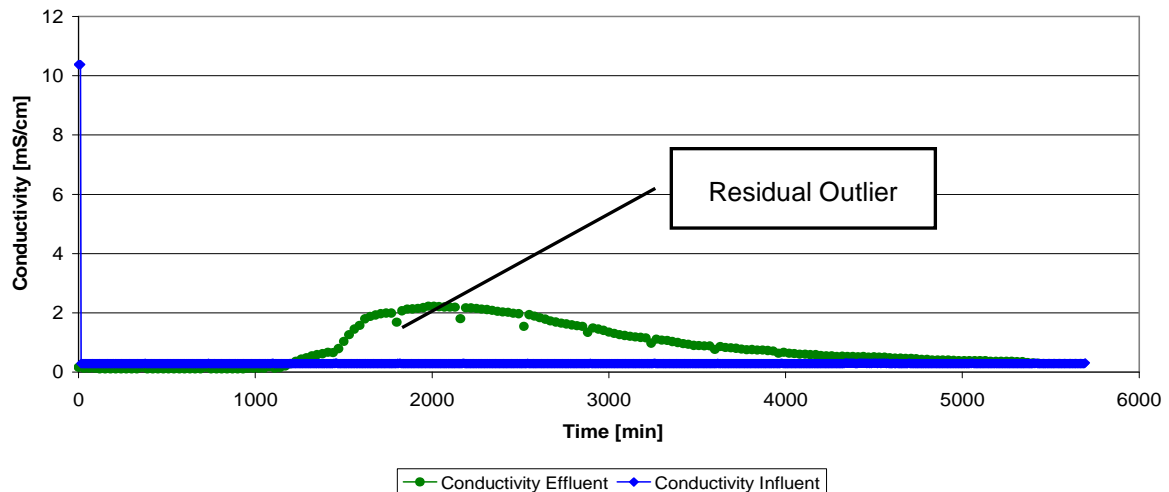


Figure 3.3-21: Tracer median-data

3. Calculation of mean values

To eliminate the residual outliers the mean of twelve median values was calculated. After that, the effluent conductivity was subtracted from the one of the influent to isolate the tracer-induced conductivity from the background conductivity (cf. Figure 3.3-22). In the case of increasing background conductivity of wastewater (the conductivity of influent) during the measurement period, the subtraction could lead to negative conductivity values. Hence, a correction by eliminating the trends of influent and effluent was necessary. This correction was done with median data.

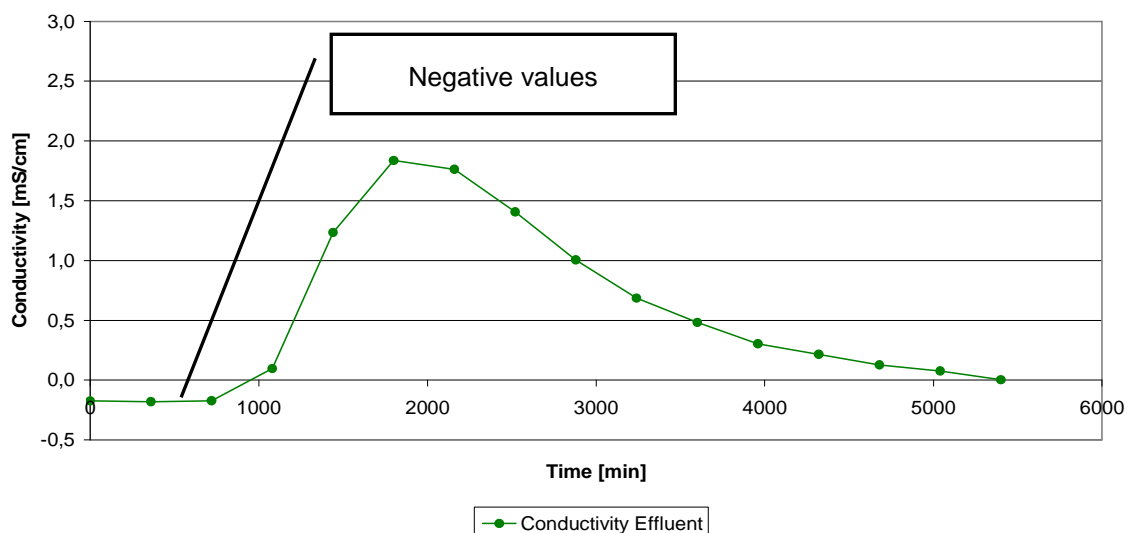


Figure 3.3-22: Tracer mean-data

4. Elimination of negative conductivity

The trend of conductivity of effluent and influent was calculated and subtracted from the aggregate conductivities of both (cf. Figure 3.3-23).

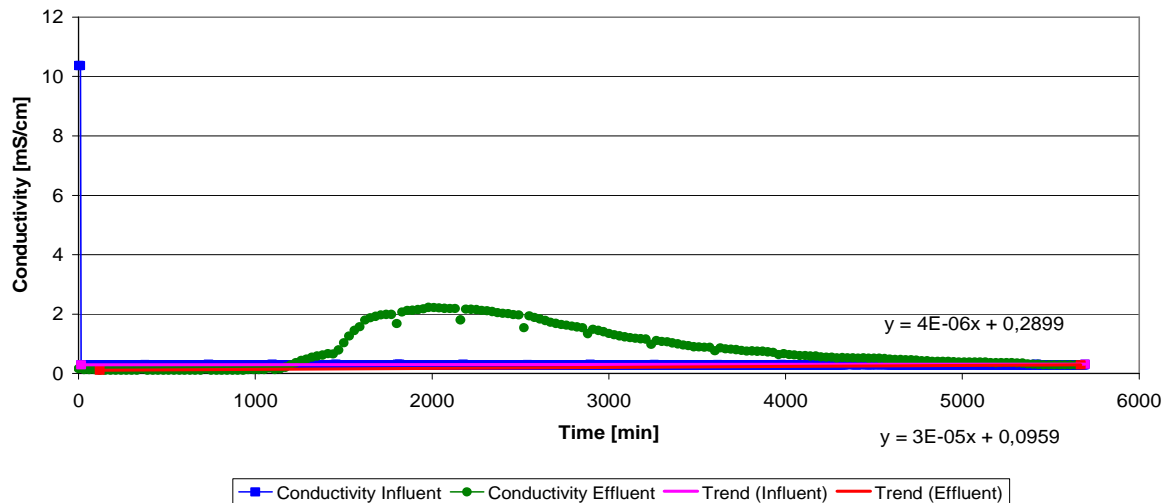


Figure 3.3-23: Correction of tracer median-data

5. Calculation of mean data after correction

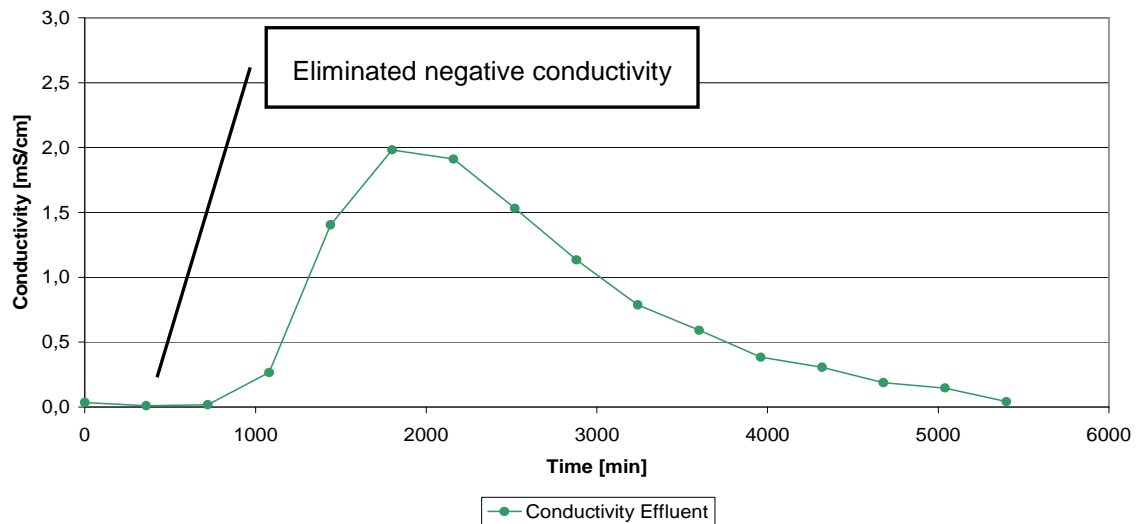


Figure: 3.3-24: Corrected tracer mean-data

6. Calculation of cumulative conductivity and HRT

The HRT is reached when 50% of the cumulative conductivity of the effluent is measured (cf. Figure 3.3-25).

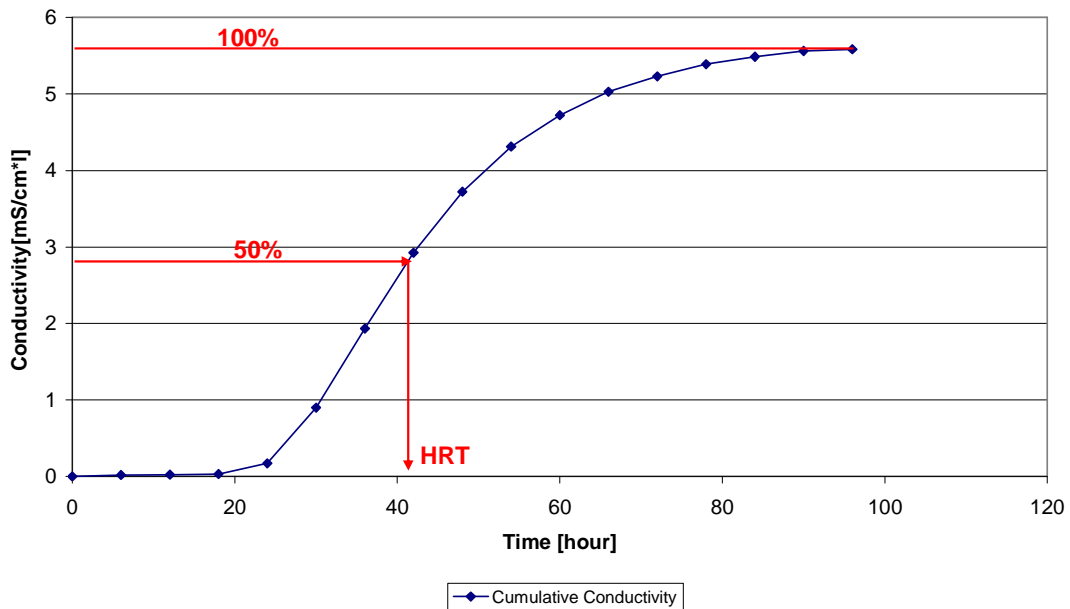


Figure 3.3-25: Cumulative conductivity

3.3.6 HRT calculation

Additional to the HRT determination via tracer experiments the HRT were calculated based on pore volume of the filter materials and the hydraulic load rate of the columns.

The comparison of calculated and measured HRT is suitable to identify short circuit flow.

The HRT was calculated by:

$$\text{HRT} = \frac{V_p}{Q} \quad (\text{Eq. 12})$$

$$V_p = n \cdot V \quad (\text{Eq. 13})$$

$$V = A \cdot h \quad (\text{Eq. 14})$$

$$A = \frac{d^2 \cdot \pi}{4} \quad (\text{Eq. 15})$$

Where

HRT..... Hydraulic retention time [d]

V_P Pore volume [m^3]

Q Influent volume [m^3/d]

n Porosity [-]

V Filter volume [m^3]

A Cross section surface of filter [m^2]

d Diameter of filter [m]

4 Results

4.1 Sieve analysis

4.1.1 Slag

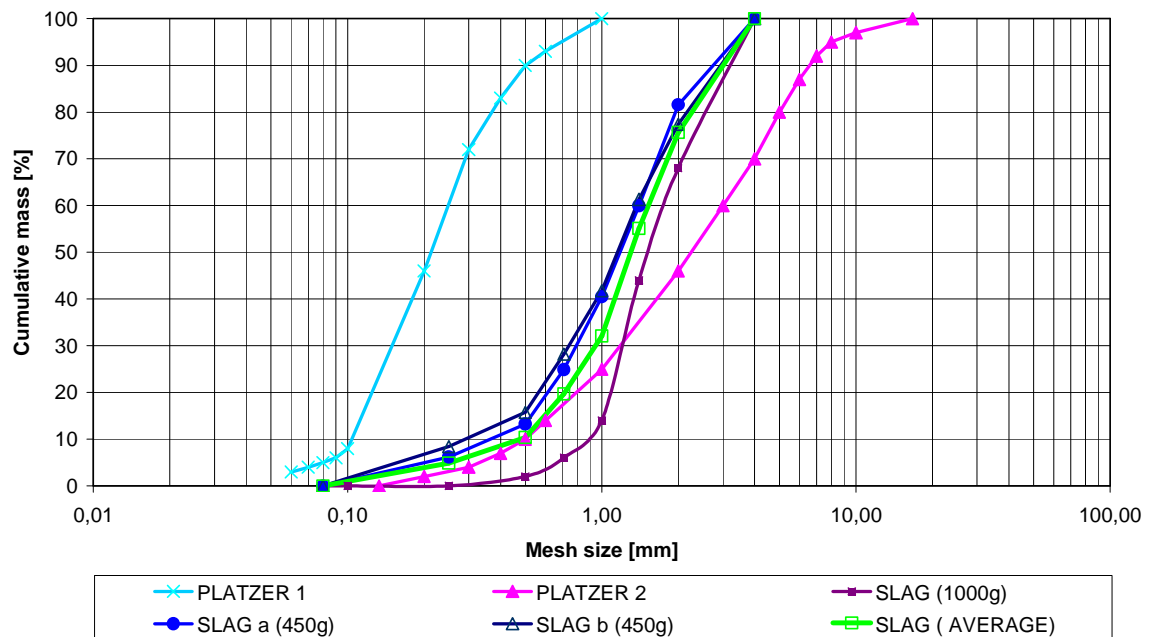


Figure 4.1-1: Grading curve SL vs. Platzer

The different sample sizes have an influence on the particle size distribution. In comparison to the sample sizes of 450 g, is the amount of fine and medium sand fractions of the sample of 1000 g lower. This leads to a higher porosity. The differences occur within a range that does not affect classification decisively (cf. Table 4.1-1 and Figure 4.1-1).

The classification of measured samples leads to a range of classes from fgrCSa to fgrCSaMSa. Essential parts are given in capitals, additional parts in small letters.

Table 4.1-1: Classification SL

d [mm]	Abbr. [-]	Sample			
		1000g	450g a	450g b	Average
> 2-6,3	FGr	32	18	24	24
> 0,63-2	CSa	64	57	47	57
> 0,2-0,63	MSa	4	20	23	16
> 0,063-0,2	FSa	0	4	5	3
	Σ	100	100	100	100
	Classification	fgrCSa	fgrCSaMSa	fgrCSaMSa	fgrCSaMSa

For explanation of abbreviations, confer Table 3.3-2.

The range of the parameters d_{10} , d_{30} , and d_{60} of the samples with a weight of 450 g is very small. They are almost the same. In comparison to those, the parameters of the samples with a weight of 1000 g differ decisively. They are all higher. This difference influences the values of C_u and C_c directly. Higher values of d_{10} and d_{30} lead to lower values of C_u and C_c (cf. Table 4.1-2).

Table 4.1-2: Measured parameters SL

Sample	d_{10} [mm]	d_{30} [mm]	d_{60} [mm]	C_u [-]	C_c [-]
1000g	0.86	1.21	1.80	2.11	0.96
450g	0.38	0.81	1.40	3.64	1.20
450g	0.30	0.75	1.37	4.52	1.34
Average	0.48	0.95	1.54	3.19	1.21

Compared to PLATZER (1997) and standards SL meets all requirements and recommendations (cf. Table 4.1-3)

Table 4.1-3: Comparison of SL parameters with recommendations and standards

	Recommendations Platzer	Requirements DWA A 262 (2006)	Requirements ATV A 262 (1997)	Measured parameters SL	Fulfillment
Classification	Sand, Sandy Gravel	Sand, Sandy Gravel	n.r	fgrCSaMSa	Ok
d_{10} [mm]	$0.1 \leq d_{10} \leq 0.5$	$0.2 \leq d_{10} \leq 0.4$	> 0.2	0.5	Ok
C_u [-]	$2 \leq C_u \leq 6$	≤ 5	≤ 5	3.2	Ok
C_c [-]	≤ 1	n.r	n.r	1.2	Too high

n.r..... No requirements are defined

4.1.2 Perlit

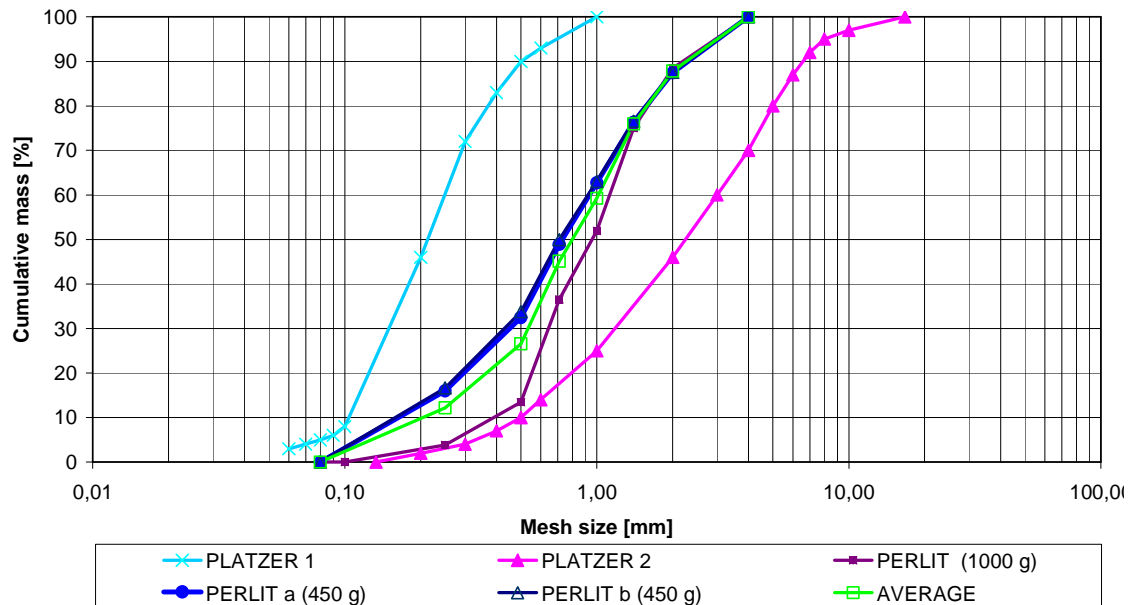


Figure 4.1-2: Grading curve PE vs. Platzer

The different sample sizes have an influence on the particle size distribution. In comparison to the sample size of 450 g, is the amount of coarse sand higher and the amount of medium sand fraction of the sample of 1000 g lower. This leads to a higher porosity. The differences occur within a range, which does almost not affect classification (cf. Figure 4.1-2 and Table 4.1-4).

The classification of measured samples leads to a range of classes from fgrMSaCSa to fgrCSaMSa. Essential parts are given in capitals, additional parts in small letters.

Table 4.1-4: Classification PE

D [mm]	Abbr. [-]	Sample			
		1000g	450g a	450g b	Average
> 2-6,3	FGr	12	13	12	12
> 0,63-2	CSa	58	35	34	42
> 0,2-0,63	MSa	28	43	44	38
> 0,063-0,2	FSa	2	10	10	7
	Σ	100	100	100	100
	Classification	fgrCSaMSa	fgrMSaCSa	fgrMSaCSa	fgrCSaMSa

For explanation of abbreviations, confer Table 3.3-2

The range of the parameters d_{10} , d_{30} , and d_{60} of the samples with a weight of 450 g is very small. They are almost the same. In comparison to those, the parameters of the samples with a weight of 1000 g differ. They are all higher. This difference influences the values of C_u and C_c directly. Higher values of d_{10} and d_{30} lead to lower values of C_u and C_c (cf. Table 4.1-5).

Table 4.1-5: Measured parameters PE

Sample	d_{10} [mm]	d_{30} [mm]	d_{60} [mm]	C_u [-]	C_c [-]
1000g	0.41	0.65	1.14	2.78	0.91
450g	0.20	0.46	0.94	4.64	1.12
450g	0.20	0.45	0.93	4.66	1.06
Average	0.23	0.54	1.02	4.47	1.25

Compared to PLATZER (1997) and standards PE meets all requirements and recommendations (cf. Table 4.1-6)

Table 4.1-6: Comparison of PE parameters with recommendations and standards

	Recommendations Platzer	Requirements DWA A 262 (2006)	Requirements ATV A 262 (1997)	Measured parameters PE	Fulfillment
Classification	Sand, Sandy Gravel	Sand, Sandy Gravel	n.r	fgrCSaMSa	Ok
d_{10} [mm]	$0.1 \leq d_{10} \leq 0.5$	$0.2 \leq d_{10} \leq 0.4$	> 0.2	0.2	Ok
C_u [-]	$2 \leq C_u \leq 6$	≤ 5	≤ 5	4.5	Ok
C_c [-]	≤ 1	n.r	n.r	1.3	Too high

n.r..... No requirements are defined

4.1.3 Pumice

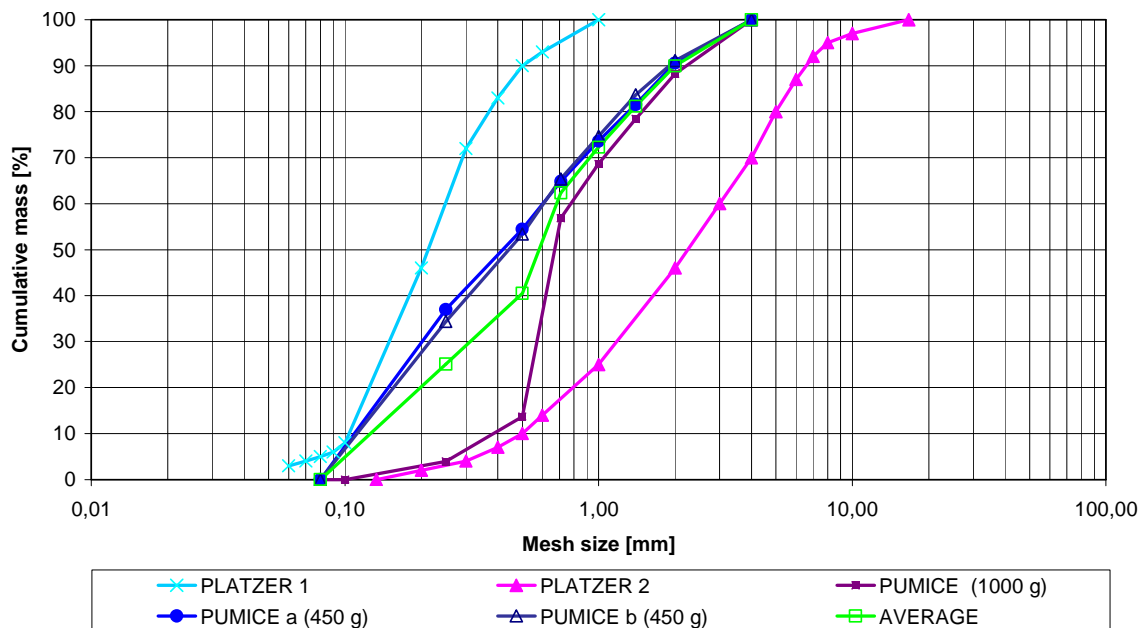


Figure 4.1-3: Grading curve PU vs. Platzer

The different sample sizes have an influence on the particle size distribution. In contrast to sample sizes of 450 g, is the fine sand fraction in sample of 1000 g almost not available additionally is the amount of medium sand lower and the amount of coarse sand higher. This leads to a higher porosity. The differences occur within a range, which does not affect classification decisively (cf. Figure 4.1-3 and Table 4.1-7).

The classification of measured samples leads to a range of classes from fgrMSaFSa to fgrMSaCSa. Essential parts are given in capitals, additional parts in small letters.

Table 4.1-7: Classification PU

d [mm]	Abbr. [-]	Sample			
		1000g	450g a	450g b	Average
> 2-6,3	FGr	12	9	9	10
> 0,63-2	CSa	45	7	10	21
> 0,2-0,63	MSa	40	61	61	54
> 0,063-0,2	FSa	2	22	21	15
Σ		100	100	100	100
Classification		fgrCSaMSa	fgrMSaFSa	fgrMSaFSa	fgrMSaCSa

For explanation of abbreviations, confer Table 3.3-2

The parameters d_{10} , d_{30} , and d_{60} of the samples with a weight of 450 g are almost the same. In comparison to those, the parameters of the samples with a weight of 1000 g differ decisively. They are all higher. This difference influences the values of C_u and C_c directly. Higher values of d_{10} and d_{30} lead to lower value of C_u and because of the low difference of d_{60} to a higher C_c (cf. Table 4.1-8).

Table 4.1-8: Measured parameters PU

Sample	d_{10} [mm]	d_{30} [mm]	d_{60} [mm]	C_u [-]	C_c [-]
1000g	0.41	0.58	0.79	1.94	1.05
450g	0.16	0.23	0.61	3.85	0.53
450g	0.16	0.23	0.62	3.82	0.55
Average	0.17	0.33	0.69	3.93	0.90

Compared to PLATZER (1997) and standards PU meets all requirements and recommendations (cf. Table 4.1-9)

Table 4.1-9: Comparison of PU parameters with recommendations and standards

	Recommendations Platzer	Requirements DWA A 262 (2006)	Requirements ATV A 262 (1997)	Measured parameters PU	Fulfillment
Classification	Sand, Sandy Gravel	Sand, Sandy Gravel	n.r	fgrMSaCSa	Ok
d_{10} [mm]	$0.1 \leq d_{10} \leq 0.5$	$0.2 \leq d_{10} \leq 0.4$	> 0.2	0.2	Ok
C_u [-]	$2 \leq C_u \leq 6$	≤ 5	≤ 5	3.9	Ok
C_c [-]	≤ 1	n.r	n.r	0.9	Ok

n.r..... No requirement are defined

4.1.4 Turkish Sand

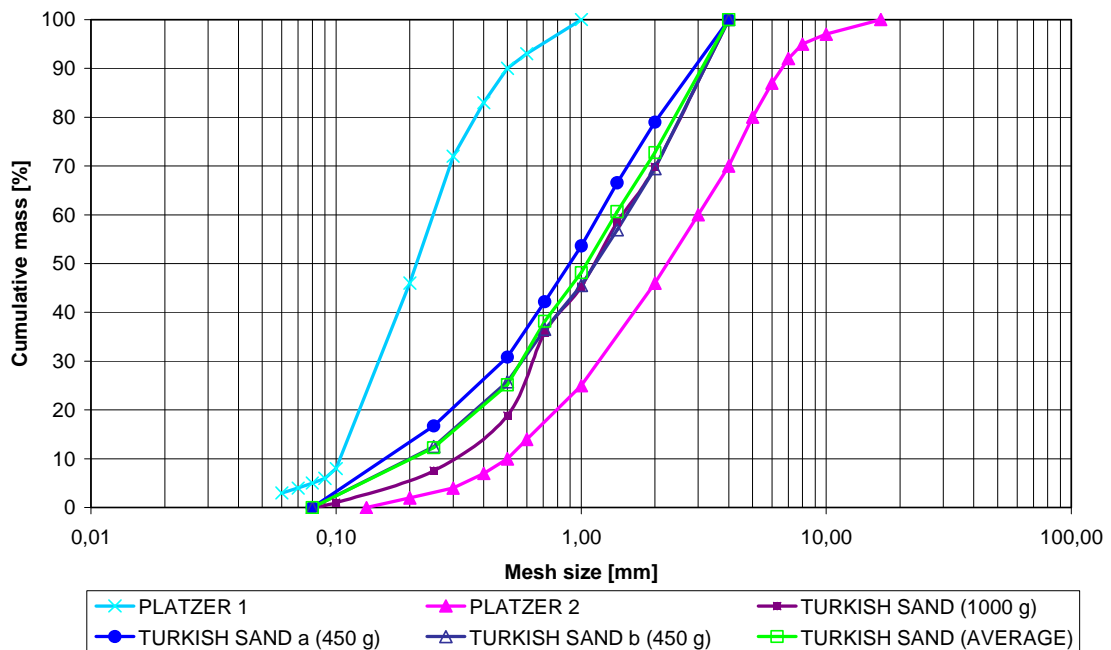


Figure 4.1-4: Grading curve TS vs. Platzer

Almost no difference occurs in grain size distribution due to different sample sizes. TS can be classified as fgrMSaCSa (cf. Figure 4.1-4 and Table 4.1-10).

Table 4.1-10: Classification TS

		Sample			
d [mm]	Abbr. [-]	1000g	450g a	450g b	Average
Through fraction [%]					
> 2-6,3	FGr	30	21	31	27
> 0,63-2	CSa	36	31	30	32
> 0,2-0,63	MSa	29	38	32	33
> 0,063-0,2	FSa	5	10	8	7
	Σ	100	100	100	100
	Classification	fgrCSaMSa	fgrMSaCSa	fgrMSaCSa	fgrMSaCSa

For explanation of abbreviations, confer Table 3.3-2

The parameters d_{10} , d_{30} , and d_{60} of the samples with a weight of 450 g are almost the same. In comparison to those, the parameters of the samples with a weight of 1000 g differ decisively. They are all higher. This difference influences the values of C_u and C_c directly. Higher values of d_{10} and d_{30} lead to lower values of C_u and C_c (cf. Table 4.1-11).

Table 4.1-11: Measured parameters TS

Sample	d_{10} [mm]	d_{30} [mm]	d_{60} [mm]	C_u [-]	C_c [-]
1000g	0.30	0.64	1.48	4.87	0.90
450g	0.20	0.49	1.20	5.99	0.98
450g	0.22	0.58	1.55	6.88	0.97
Average	0.23	0.58	1.38	6.08	1.07

TS meets the recommendations of PLATZER (1997). Concerning d_{10} is TS within the ranges of DWA A 262 (2006) and ATV A 262 (1997). Concerning C_u the value of TS is slight above the requirements. As the criterion $1 > C_c > 3$ and $C_u > 5$ is not fulfilled TS can still be characterised as poorly graded (cf. Table 4.1-12).

Table 4.1-12: Comparison of TS parameters with recommendations and standards

	Recommendations Platzer	Requirements DWA A 262 (2006)	Requirements ATV A 262 (1997)	Measured parameters TS	Fulfillment
Classification	Sand, Sandy Gravel	Sand, Sandy Gravel	n.r	fgrMSaCSa	Ok
d_{10} [mm]	$0.1 \leq d_{10} \leq 0.5$	$0.2 \leq d_{10} \leq 0.4$	> 0.2	0.2	Ok
C_u [-]	$2 \leq C_u \leq 6$	≤ 5	≤ 5	6.1	Too high
C_c [-]	≤ 1	n.r	n.r	1.1	Ok

n.r..... No requirements are defined

4.1.5 Turkish Zeolite

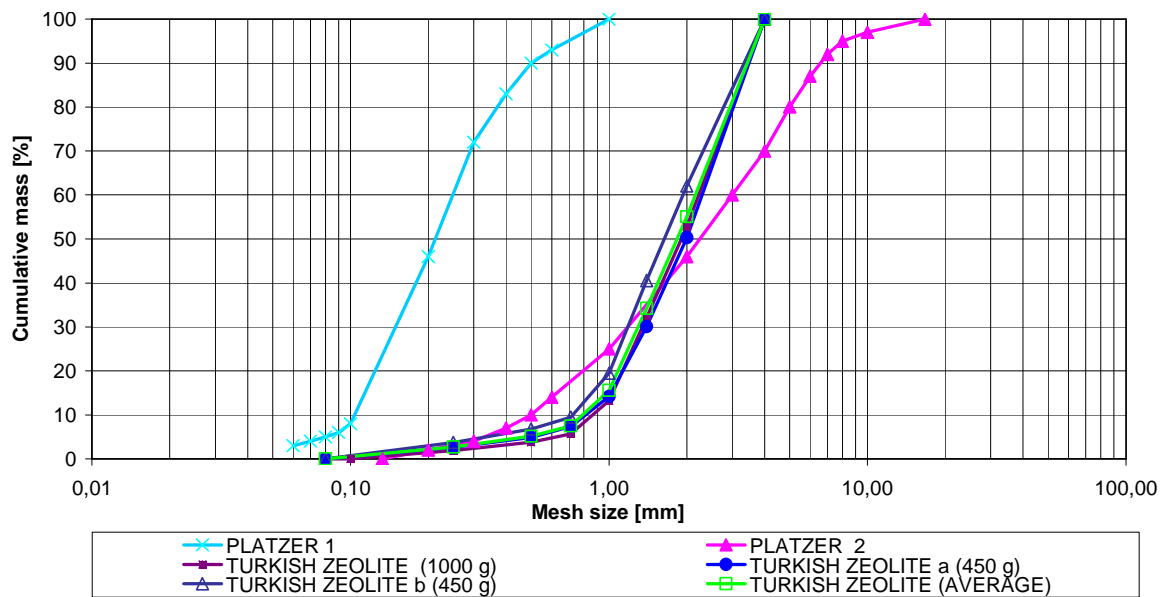


Figure 4.1-5: Grading curve TZ vs. Platzer

Almost no difference in grain size distribution due to different sample sizes occurs. TZ can be classified as FGrCSa (cf. Figure 4.1-5 and Table 4.1-13).

Table 4.1-13: Classification TZ

		Sample			
d [mm]	Abbr. [-]	1000g	450g a	450g b	Average
Through fraction [%]					
> 2-6,3	FGr	47	50	38	45
> 0,63-2	CSa	47	42	51	47
> 0,2-0,63	MSa	5	6	8	7
> 0,063-0,2	FSa	1	2	2	2
	Σ	100	100	100	100
	Classification	FGrCSa	FGrCSa	fgrCSa	CSaFGr

For explanation of abbreviations, confer Table 3.3-2

The parameters d_{10} , d_{30} , and d_{60} of the samples with a weight of 450 g and of the sample with a weight of 1000 g are almost the same. Therewith, C_u and C_c are quite similar (cf. Table 4.1-14).

Table 4.1-14: Measured parameters TZ

Sample	d_{10} [mm]	d_{30} [mm]	d_{60} [mm]	C_u [-]	C_c [-]
1000g	0.88	1.36	2.30	2.63	0.91
450g	0.82	1.40	2.39	2.90	0.99
450g	0.73	1.20	1.94	2.68	1.02
Average	0.80	1.31	2.22	2.78	0.97

Concerning C_u and C_c TZ fulfils the requirements. The value of d_{10} is distinct above the ranges of DWA A 262 (2006), ATV A 262 (1997) and PLATZER (1997). This means the amount of small particles within the sample is lower than recommended. This could lead to a higher porosity (cf. Table 4.1-15).

Table 4.1-15: Comparision of TZ parameters with recommendations and standards

	Recommendations Platzer	Requirements DWA A 262 (2006)	Requirements ATV A 262 (1997)	Measured parameters TZ	Fulfillment
Classification	Sand, Sandy Gravel	Sand, Sandy Gravel	n.r	CSaFGr	Ok
d_{10} [mm]	$0.1 \leq d_{10} \leq 0.5$	$0.2 \leq d_{10} \leq 0.4$	> 0.2	0.8	Too high
C_u [-]	$2 \leq C_u \leq 6$	≤ 5	≤ 5	2.8	Ok
C_c [-]	≤ 1	n.r	n.r	1.0	Ok

n.r..... No requirements are defined

4.1.6 Crushed concrete

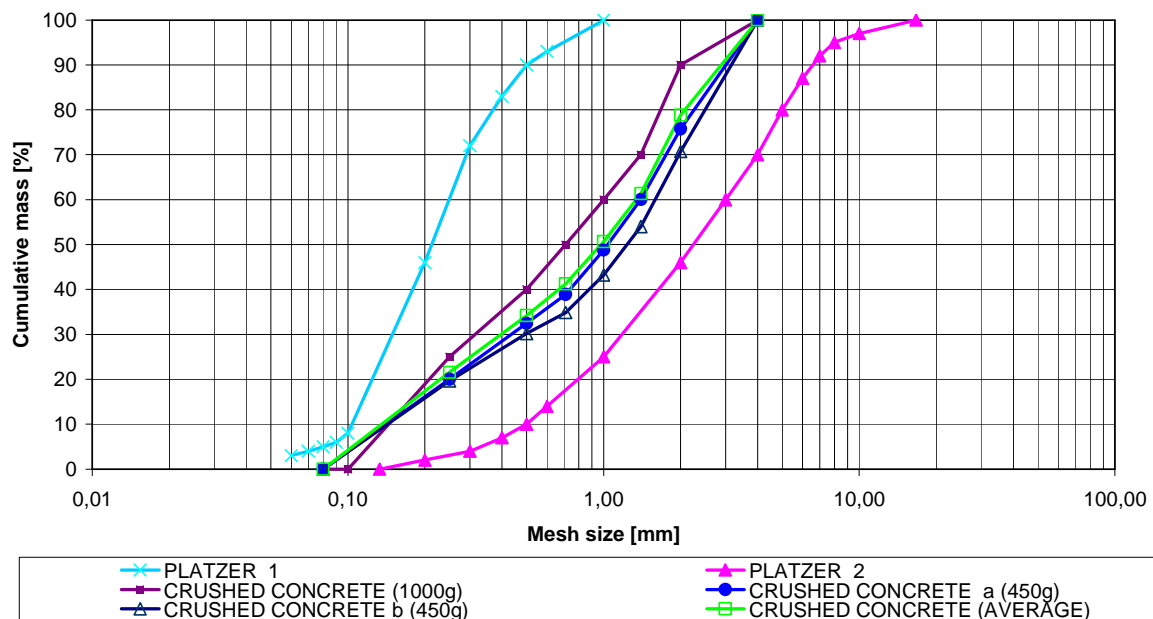


Figure 4.1-6: Grading curve BE vs. Platzer

Almost no difference in grain size distribution due to different sample sizes occurs. BE can be classified as fgrMSaCSa (cf. Figure 4.1-6 and Table 4.1-16).

Table 4.1-16: Classification BE

		Sample			
D [mm]	Abbr. [-]	1000g	450g a	450g b	Average
Through fraction [%]					
> 2-6,3	FGr	10	24	29	21
> 0,63-2	CSa	29	27	26	27
> 0,2-0,63	MSa	46	36	33	39
> 0,063-0,2	FSa	15	12	12	13
	Σ	100	100	100	100
	Classification	fgrMSaCSa	fgrMSaCSa	fgrMSaCSa	fgrMSaCSa

For explanation of abbreviations, confer Table 3.3-2

The parameters d_{10} , d_{30} , and d_{60} of the samples with a weight of 450 g and 1000 g differ slightly. The values show no influence of sample size on differences. The parameter C_U of the sample with a weight of 1000 g is notably lower (cf. Table 4.1-17).

Table 4.1-17: Measured parameters BE

Sample	d_{10} [mm]	d_{30} [mm]	d_{60} [mm]	C_U [-]	C_C [-]
1000g	0.18	0.33	1.00	5.71	0.63
450g	0.19	0.45	1.40	7.47	0.77
450g	0.25	0.50	1.62	6.46	0.61
Average	0.18	0.42	1.35	7.38	0.70

Concerning d_{10} and C_C BE meets all recommendations and requirements. Concerning C_U the value of BE is above the requirements. As the criterion $1 > C_C > 3$ **and** $C_U > 5$ is not fulfilled TS can still be characterised as poorly graded (cf. Table 4.1-18).

Table 4.1-18: Comparison of BE parameters with recommendations and standards

	Recommendations Platzer	Requirements DWA A 262 (2006)	Requirements ATV A 262 (1997)	Measured parameters BE	Fulfillment
Classification	Sand, Sandy Gravel	Sand, Sandy Gravel	n.r	fgrMSaCSa	Ok
d_{10} [mm]	$0.1 \leq d_{10} \leq 0.5$	$0.2 \leq d_{10} \leq 0.4$	> 0.2	0.2	Ok
C_U [-]	$2 \leq C_U \leq 6$	≤ 5	≤ 5	7.4	Too high
C_C [-]	≤ 1	n.r	n.r	0.7	Ok

n.r..... no requirements are defined

4.1.7 Ferro-Sorp©

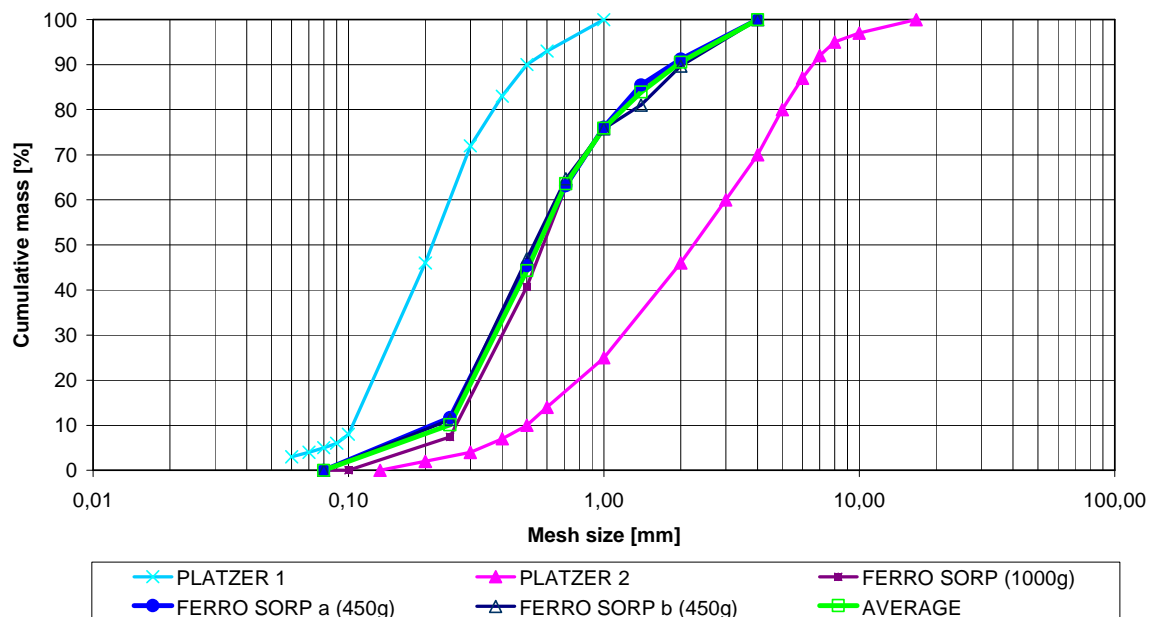


Figure 4.1-7: Grading curve FE vs. Platzer

No difference in grain size distribution due to different sample sizes occurs. FE can be classified as fgrMSaFSa (cf. Figure 4.1-7 and Table 4.1-19).

Table 4.1-19: Classification FE

d [mm]	Abbr. [-]	Sample			
		1000g	450g a	450g b	Average
> 2-6,3	FGr	9	9	10	9
> 0,63-2	CSa	32	28	25	28
> 0,2-0,63	MSa	54	56	58	56
> 0,063-0,2	FSa	4	7	7	6
	Σ	100	100	100	100
	Classification	fgrMSaFSa	fgrMSaFSa	fgrMSaFSa	fgrMSaFSa

For explanation of abbreviations, confer Table 3.3-2

The parameters d_{10} , d_{30} , and d_{60} of the samples with a weight of 450 g and of the sample with a weight of 1000 g are almost the same. Therewith, C_u and C_c are quite similar (cf. Table 4.1-20).

Table 4.1-20: Measured parameters FE

Sample	d_{10} [mm]	d_{30} [mm]	d_{60} [mm]	C_u [-]	C_c [-]
1000g	0.27	0.42	0.68	2.53	0.40
450g	0.23	0.39	0.67	2.90	0.37
450g	0.24	0.38	0.65	2.77	0.36
Average	0.25	0.40	0.67	2.70	0.37

Compared to PLATZER (1997) and standards FE meets all requirements and recommendations (cf. Table 4.1-21).

Table 4.1-21: Comparison of FE parameters with recommendations and standards

	Recommendations Platzer	Requirements DWA A 262 (2006)	Requirements ATV A 262 (1997)	Measured parameters FE	Fulfillment
Classification	Sand, Sandy Gravel	Sand, Sandy Gravel	n.r	fgrMSaFSa	Ok
d_{10} [mm]	$0.1 \leq d_{10} \leq 0.5$	$0.2 \leq d_{10} \leq 0.4$	> 0.2	0.3	Ok
C_u [-]	$2 \leq C_u \leq 6$	≤ 5	≤ 5	2.7	Ok
C_c [-]	≤ 1	n.r	n.r	0.4	Ok

n.r..... no requirements are defined

4.1.8 Austrian Zeolite 1

No sieving analysis was made (cf. chapter 3.3.1.1).

4.1.9 Austrian Zeolite 2

No sieving analysis was made (cf. chapter 3.3.1.1).

4.1.10 Austrian Sand

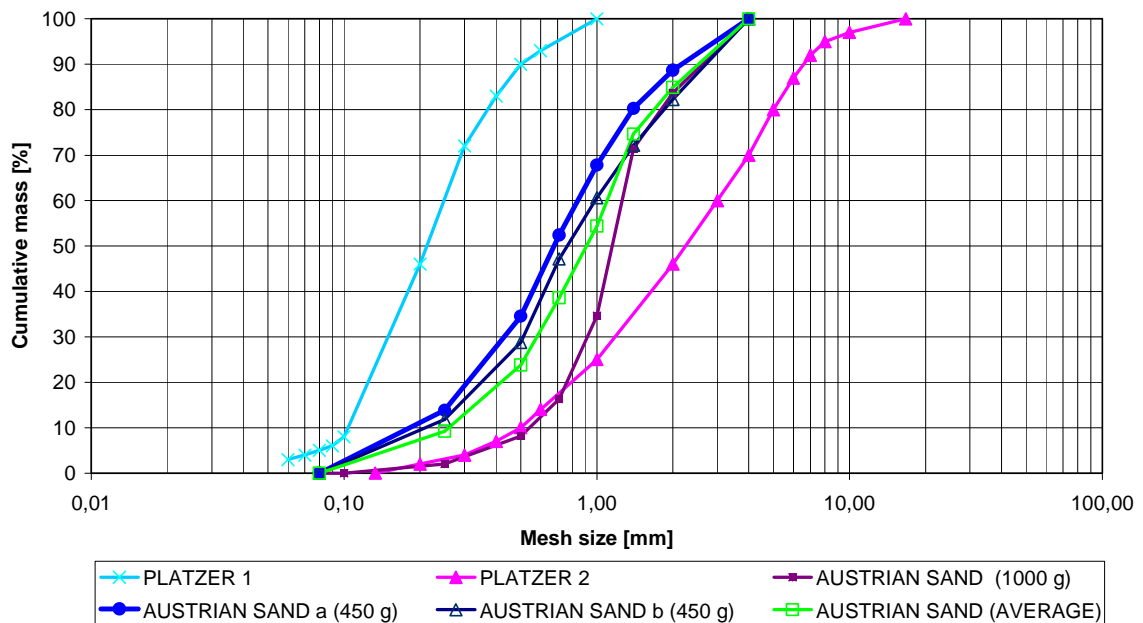


Figure 4.1-8: Grading curve AS vs. Platzer

The different sample sizes have an influence on the particle size distribution. In comparison to the sample sizes of 450 g, is in the sample of 1000 g the amount of medium sand lower and the amount of coarse sand higher (cf. Figure 4.1-8 and Table 4.1-22). This leads to a higher porosity. The differences occur within a range, which does not affect classification decisively.

The classification of measured samples leads to a range of classes from fgrMSaCSa to fgrCSaMSa. Essential parts are given in capitals, additional parts in small letters.

Table 4.1-22: Classification AS

d [mm]	Abbr. [-]	Sample			
		1000g	450g a	450g b	Average
> 2-6,3	FGr	16	11	18	15
> 0,63-2	CSa	69	35	35	46
> 0,2-0,63	MSa	13	46	40	33
> 0,063-0,2	FSa	1	8	7	6
Σ		100	100	100	100
Classification		fgrCSaMSa	fgrMSaCSa	fgrMSaCSa	fgrCSaMSa

For explanation of abbreviations, confer Table 3.3-2

The parameters d_{10} , d_{30} , and d_{60} of the samples with a weight of 450 g are almost the same. In comparison to those, for each of the columns, the parameters of the samples with a weight of 1000 g differ decisively. They are all higher. This difference influences the values of C_u and C_c directly. Higher values of d_{10} and d_{30} lead to lower value of C_u and because of the low difference of d_{60} to a higher C_c (cf. Table 4.1-23).

Table 4.1-23: Measured parameters AS

Sample	d_{10} [mm]	d_{30} [mm]	d_{60} [mm]	C_u [-]	C_c [-]
1000g	0.55	0.93	1.28	2.33	1.23
450g	0.22	0.45	0.85	3.96	1.08
450g	0.23	0.51	0.99	4.27	1.16
Average	0.26	0.59	1.11	4.22	1.18

Concerning d_{10} and C_u BE meets all recommendations and requirements. Concerning C_c the value of AS is above the requirements (cf. Table 4.1-24). As the criterion $1 > C_c > 3$ and $C_u > 5$ is not fulfilled AS can still be characterised as poorly graded.

Table 4.1-24: Comparison of AS parameters with recommendations and standards

	Recommendations Platzer	Requirements DWA A 262 (2006)	Requirements ATV A 262 (1997)	Measured parameters AS	Fulfillment
Classification	Sand, Sandy Gravel	Sand, Sandy Gravel	n.r	fgrCSaMSa	Ok
d_{10} [mm]	$0.1 \leq d_{10} \leq 0.5$	$0.2 \leq d_{10} \leq 0.4$	> 0.2	0.3	Ok
C_u [-]	$2 \leq d_{10} \leq 6$	≤ 5	≤ 5	4.2	Ok
C_c [-]	≤ 1	n.r	n.r	1.2	Too high

n.r..... no requirements are defined

4.1.11 Ferro-Sorp® + Turkish Zeolite

No sieving analysis was made (cf. chapter 3.3.1.1)

4.1.12 Mixtures

No sieving analysis was made (cf. chapter 3.3.1.1)

4.1.13 Summary

The grading curves of all analysed filter materials in comparison with the borders recommended by PLATZER (1997) are presented in Figure 4.1-9.

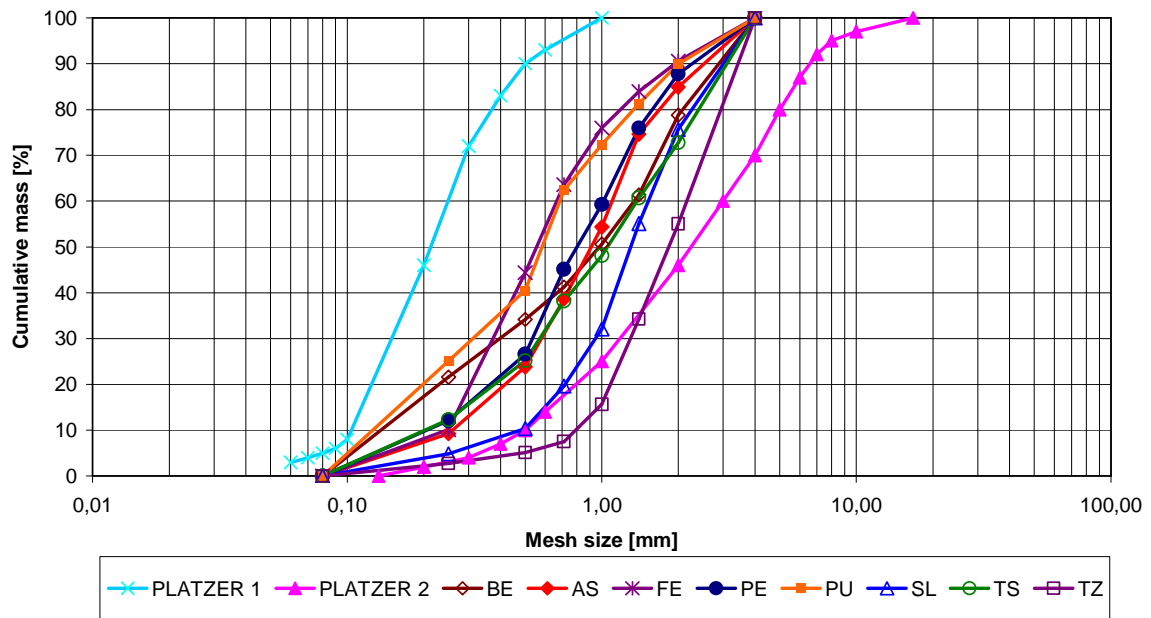


Figure 4.1-9: Grading curves of all analysed materials

4.2 Pycnometer Experiments

Bulk density and particle density were measured for subsequent calculation of porosity (cf. Table 4.2-1).

Table 4.2-1: Results Pycnometer experiments all materials

	Bulk density		Particle density		Porosity	
	Average [g/cm ³]	Standard deviation [-]	Average [g/cm ³]	Standard deviation [-]	Average [g/cm ³]	Standard deviation [-]
SL	1.0671	0.0233	2.1718	0.1468	0.5087	0.0301
PE	1.5237	0.0044	2.1930	0.0138	0.3052	0.0058
PU	1.3837	0.0222	2.1123	0.0206	0.3449	0.0121
TS	1.7179	0.0275	2.6903	0.0351	0.3614	0.0055
TZ	0.8907	0.0028	1.8723	0.0846	0.5243	0.0203
BE	1.5605	0.0223	2.9614	0.8147	0.4730	0.1377
FE	0.6856	0.0120	2.4044	0.4842	0.7149	0.0548
AZ1	1.0419	0.0168	2.3821	0.4256	0.5626	0.0669
AZ2	1.0119	0.0160	2.0751	0.0349	0.5123	0.0069
AS	1.7860	0.0172	2.5762	0.0597	0.3067	0.0212
FE+TZ	0.8116	0.0041	2.6848	0.0785	0.6977	0.0075
MX	1.2649	0.0222	2.4762	0.0186	0.4892	0.0124

4.2.1 General

Due to the classification of all filter materials as sand respectively sandy gravel according to LABER (2001) a certain range of porosity can be expected (cf.: Table 4.2-2). Ranges of porosity are only coarse clues.

Table 4.2-2: Expected porosity (LABER, 2001)

Classification	Porosity [-]	
	from	To
Sandy gravel	0.25	0.35
Pebbly sand	0.28	0.35
Medium sand	0.30	0.38

4.2.2 Particle density

Particle density of each filter material was measured three times and the average and standard deviation was calculated (cf. Table 4.2-3 and Figure 4.2-1).

Table 4.2-3: Particle density of all filter materials

	Particle density [g/cm ³]				Standard deviation
	1st sample	2nd sample	3rd sample	Average	
SL	2.2606	2.0024	2.2525	2.1718	0.1468
PE	2.1882	2.1822	2.2085	2.1930	0.0138
PU	2.1249	2.1235	2.0885	2.1123	0.0206
TS	2.7298	2.6627	2.6784	2.6903	0.0351
TZ	1.9669	1.8458	1.8041	1.8723	0.0846
BE	3.9000	2.4368	2.5476	2.9614	0.8147
FE	2.9585	2.0633	2.1912	2.4044	0.4842
AZ1	2.8730	2.1565	2.1167	2.3821	0.4256
AZ2	2.1083	2.0387	2.0782	2.0751	0.0349
AS	2.5129	2.6315	2.5842	2.5762	0.0597
FE+TZ	2.6317	2.6477	2.7749	2.6848	0.0785
MX	2.4972	2.4695	2.4618	2.4762	0.0186

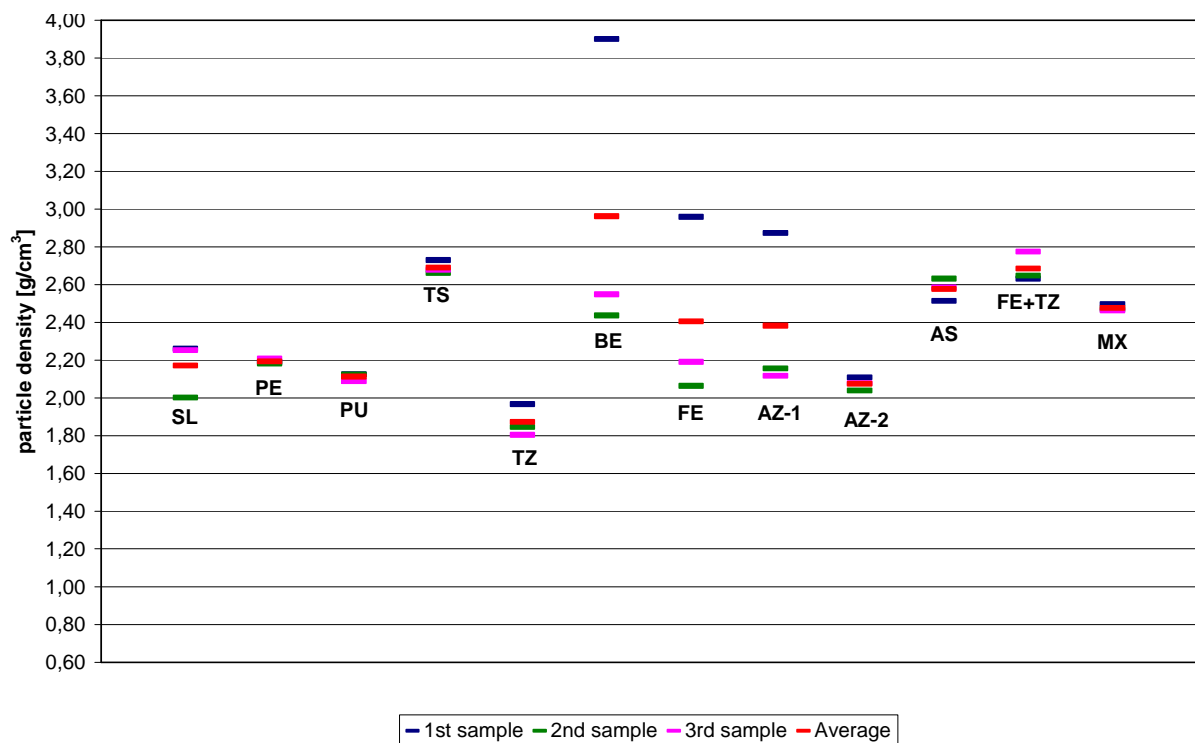


Figure 4.2-1: Particle density all materials

The standard deviation of the results of particle density measurement ranges, according to material, from 0.0138 g/cm³ (PE) to 0.8147 g/cm³ (BE). The comparatively high standard deviation of BE, FE and AZ1 is attracting attention. The reason could be that air bubbles remained within the pores of the material at some measurements. This would lead to unsaturated conditions and would have an influence on weight, therewith on particle density.

4.2.3 Bulk density

Particle density of each filter material was measured three times and the average was built (cf. Table 4.2-4 and Figure 4.2-2).

Table 4.2-4: Bulk density of all filter materials

	Bulk densities [g/cm ³]				Standard deviation
	1st sample	2nd sample	3rd sample	Average	
SL	1.0550	1.0524	1.0940	1.0671	0.0233
PE	1.5284	1.5228	1.5198	1.5237	0.0044
PU	1.4058	1.3614	1.3840	1.3837	0.0222
TS	1.7478	1.7122	1.6938	1.7179	0.0275
TZ	0.8932	0.8876	0.8912	0.8907	0.0028
BE	1.5394	1.5838	1.5584	1.5605	0.0223
FE	0.6790	0.6784	0.6994	0.6856	0.0120
AZ1	1.0574	1.0442	1.0240	1.0419	0.0168
AZ2	1.0244	1.0098	1.0016	1.0119	0.0160
AS	1.7928	1.7664	1.7988	1.7860	0.0172
FE+TZ	0.8072	0.8124	0.8152	0.8116	0.0041
MX	1.2458	1.2596	1.2892	1.2649	0.0222

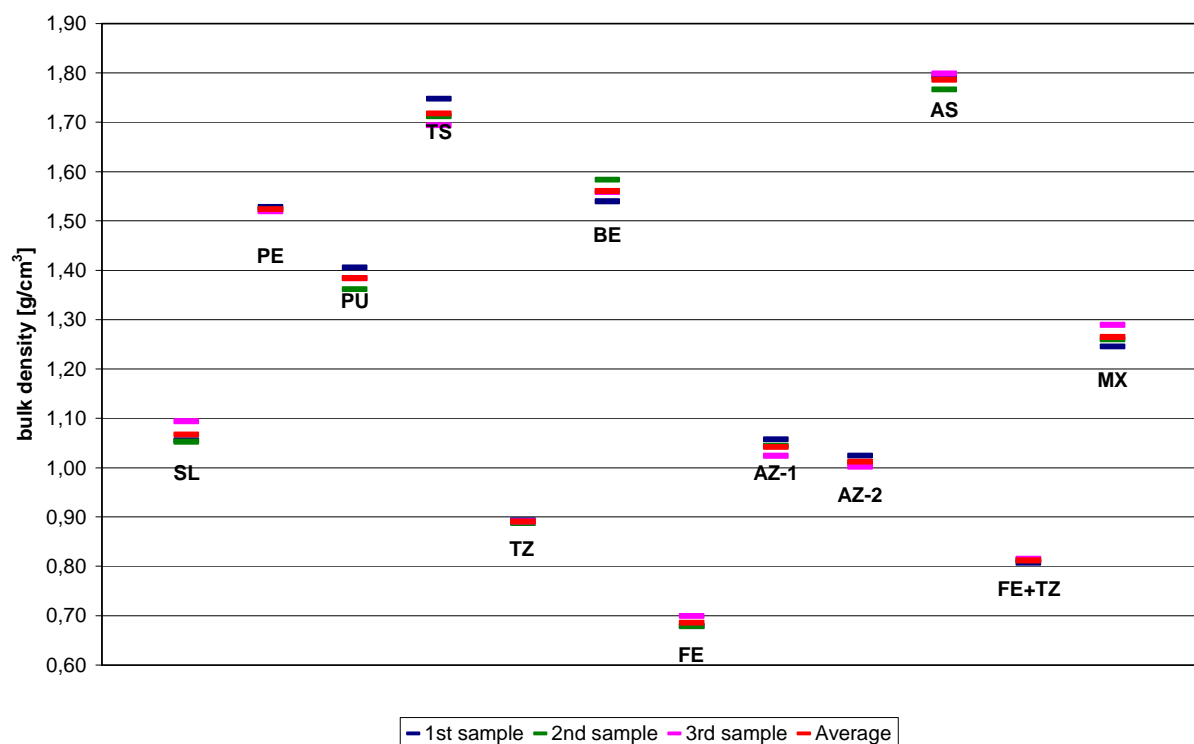


Figure 4.2-2: Bulk density all materials

The standard deviation of the results of bulk density measurement ranges, according to material, from 0.0028 g/cm³ (TZ) to 0.0275 g/cm³ (TS). It is very low especially in comparison to particle density. At bulk density, the pores are included.

4.2.4 Porosity

Porosity was calculated with the results of the measurement of particle density and bulk density. Afterwards the average was built (cf. Table 4.2-5 and Figure 4.2-3).

Table 4.2-5: Measured porosity of all filter materials

	Porosity [g/cm ³]				Standard deviation
	1st sample	2nd sample	3rd sample	Average	
SL	0.5333	0.4744	0.5143	0.5087	0.0301
PE	0.3015	0.3022	0.3119	0.3052	0.0058
PU	0.3384	0.3589	0.3373	0.3449	0.0121
TS	0.3597	0.3570	0.3676	0.3614	0.0055
TZ	0.5459	0.5191	0.5060	0.5243	0.0203
BE	0.6053	0.3500	0.3883	0.4730	0.1377
FE	0.7705	0.6712	0.6808	0.7149	0.0548
AZ1	0.6320	0.5158	0.5162	0.5626	0.0669
AZ2	0.5141	0.5047	0.5181	0.5123	0.0069
AS	0.2866	0.3287	0.3039	0.3067	0.0212
FE+TZ	0.6933	0.6932	0.7062	0.6977	0.0075
MX	0.5011	0.4899	0.4763	0.4892	0.0124

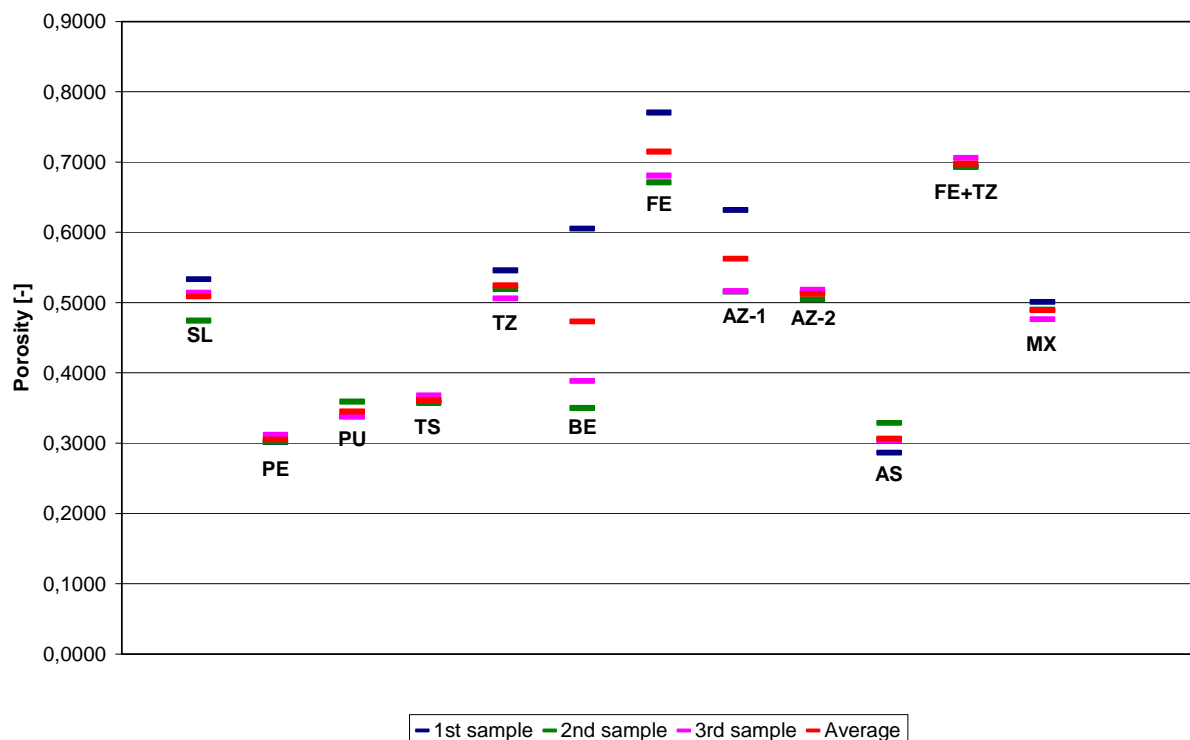


Figure 4.2-3: Porosity all materials

The standard deviation of porosity ranges from 0.0055 (TS) to 0.1377 (BE) and is mainly influenced by the standard deviation of particle density.

According to the filter material classification, a certain porosity can be expected. The porosity of materials with no correlation to the expectations according classification is at all materials higher. This is not an indication for higher k-values (cf. Table 4.2-6).

Table 4.2-6: Comparison of measured and expected porosity

	Classification	Porosity measured [-]	Expected porosity [-]		Match
			from	To	
SL	fgrCSaMSa	0.5087	0.28	0.35	-
PE	fgrCSaMSa	0.3052	0.28	0.35	+
PU	fgrMSaCSa	0.3449	0.28	0.35	+
TS	fgrMSaCSa	0.3614	0.28	0.35	++
TZ	CSaFGr	0.5243	0.28	0.35	-
BE	fgrMSaCSa	0.4730	0.28	0.35	-
FE	fgrMSaFSa	0.7149	0.28	0.35	-
AZ1	nsa	0.5626	*	*	*
AZ2	nsa	0.5123	*	*	*
AS	fgrCSaMSa	0.3067	0.28	0.35	+
FE+TZ	nsa	0.6977	*	*	*
MX	nsa	0.4892	*	*	*

+ Good match

- Bad match

++ Medium match

nsa No sieve analysis

* No comparison possible

4.3 Permeability

The k-value of each material, except AZ1, was measured five times. The average was built. For k-value measurement of AZ1, no material was available (cf. Table 4.3-1 and Figure 4.3-1).

Table 4.3-1: k-values of all filter materials

	k-value [m/s]					Average	Standard deviation
	1st sample	2nd sample	3rd sample	4th sample	5th sample		
SL	1.74E-02	1.66E-02	1.68E-02	1.11E-02	1.09E-02	1.46E-02	3.26E-03
PE	9.65E-03	9.83E-03	6.00E-03	9.43E-03	7.58E-03	8.50E-03	1.66E-03
PU	6.27E-03	5.53E-03	5.20E-03	4.74E-03	5.75E-03	5.50E-03	5.76E-04
TS	6.75E-03	4.37E-03	7.72E-03	7.07E-03	7.13E-03	6.61E-03	1.30E-03
TZ	1.96E-02	1.73E-02	1.65E-02	1.44E-02	1.35E-02	1.62E-02	2.42E-03
BE	9.87E-03	1.00E-02	9.66E-03	8.77E-03	8.08E-03	9.28E-03	8.23E-04
FE	6.06E-03	6.40E-03	5.64E-03	6.35E-03	7.20E-03	6.33E-03	5.74E-04
AZ1	-	-	-	-	-	-	-
AZ2	4.55E-02	6.56E-02	5.11E-02	2.60E-02	4.41E-02	4.64E-02	1.43E-02
AS	3.40E-03	3.04E-03	3.05E-03	2.84E-03	2.83E-03	3.03E-03	2.33E-04
FE+TZ	1.48E-02	2.00E-02	1.27E-02	1.59E-02	1.44E-02	1.56E-02	2.73E-03
MX	1.18E-02	1.25E-02	1.36E-02	1.27E-02	1.26E-02	1.26E-02	6.38E-04

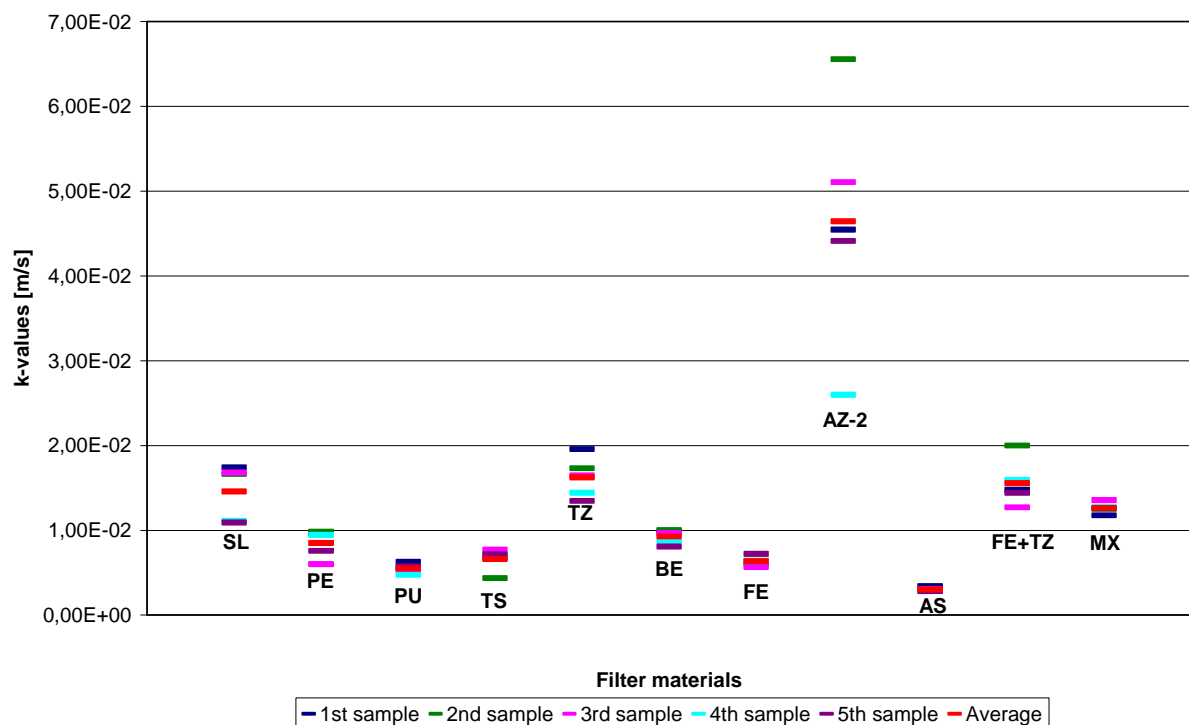


Figure 4.3-1: k-values all materials

The standard deviation of k-values ranges from 2.33E-04 (AS) to 1.43E-02 (AZ2) where the standard deviation of AZ2 is exceptional high. Standard deviation of all materials is high.

ÖNORM B 2505 (1997) and DWA A 262 (2006) recommend k-values in a range from 10^{-4} m/s to 10^{-3} m/s. At DWA A 262 (2006) the calculation based on effective grain diameter (d_{10}) is suggested.

At materials where a comparison between measured and calculated k- values is possible it is attracting attention that at any single filter material the averages of measured values are considerably higher than the calculated ones (cf. Table 4.3-2). The reason is that at the contact area between the stiff PVC-pipe of the measurement device and the filter material the porosity is enhanced (cf. Figure 3.3-8). This leads to an intensified flow along the contact area and to a higher measured permeability. This effect would not occur if the filter material within the pipe is welted by an elastic membrane and supported by external pressure (KOLYMBAS, 2007).

Calculated k-values of all materials are within the range recommended by ÖNORM B 2505 (1997) and DWA A 262 (2006).

Table 4.3-2: Comparison of measured and calculated k-values

	k- value		Difference [%]	d_{10} [mm]
	measured [m/s]	calculated [m/s]		
SL	1.46E-02	2.50E-03	584	0.5
PE	8.50E-03	4.00E-04	2125	0.2
PU	5.50E-03	4.00E-04	1375	0.2
TS	6.61E-03	4.00E-04	1525	0.2
TZ	1.62E-02	6.40E-03	250	0.8
BE	9.28E-03	4.00E-04	2300	0.2
FE	6.33E-03	4.00E-04	1580	0.2
AZ1	-	nsa	*	nsa
AZ2	4.64E-02	nsa	*	nsa
AS	3.03E-03	9.00E-04	373	0.3
FE+TZ	1.56E-02	nsa	*	nsa
MX	1.26E-02	nsa	*	nsa

-No k-value

nsaNo sieve analysis

*No comparison possible

4.4 Hydrographs and cumulative effluent

4.4.1 General

For assessment of hydrographs, three parameters are important:

- Maximum flow rate
- Skewness
- time until minimum value effluent flow rate is reached (minimum effluent has to be defined)

A very high maximum effluent flow rate with a skewed left hydrograph and a minimum effluent flow rate, which is reached very fast, indicates a high hydraulic capacity. On the one hand, a high hydraulic capacity leads to a fast drainage of coarse pores therewith a high diffusion of oxygen into the filter, on the other hand, it leads to a shorter contact time of water and biofilm and therefore to reduced purification performance. A compromise between contact time and hydraulic capacity has to be found. The ideal hydrograph should be skewed left with a ratio of infiltration time and diffusion time between 1:2 and 1:3. Infiltration time is the time that water needs to percolate through the column from the beginning of loading until the minimum effluent of 15 ml/10 minutes is reached. Diffusion time is the time, which is available for oxygen diffusion, after reaching the minimum effluent until the next loading. 3/4 of the time between two loadings should be available for oxygen diffusion (LABER, 2001).

Minimum effluent was assumed at 15 ml/10 minutes that equals the 10 minutes average over 6 hours of the loading volume of 520 ml.

4.4.2 Slag

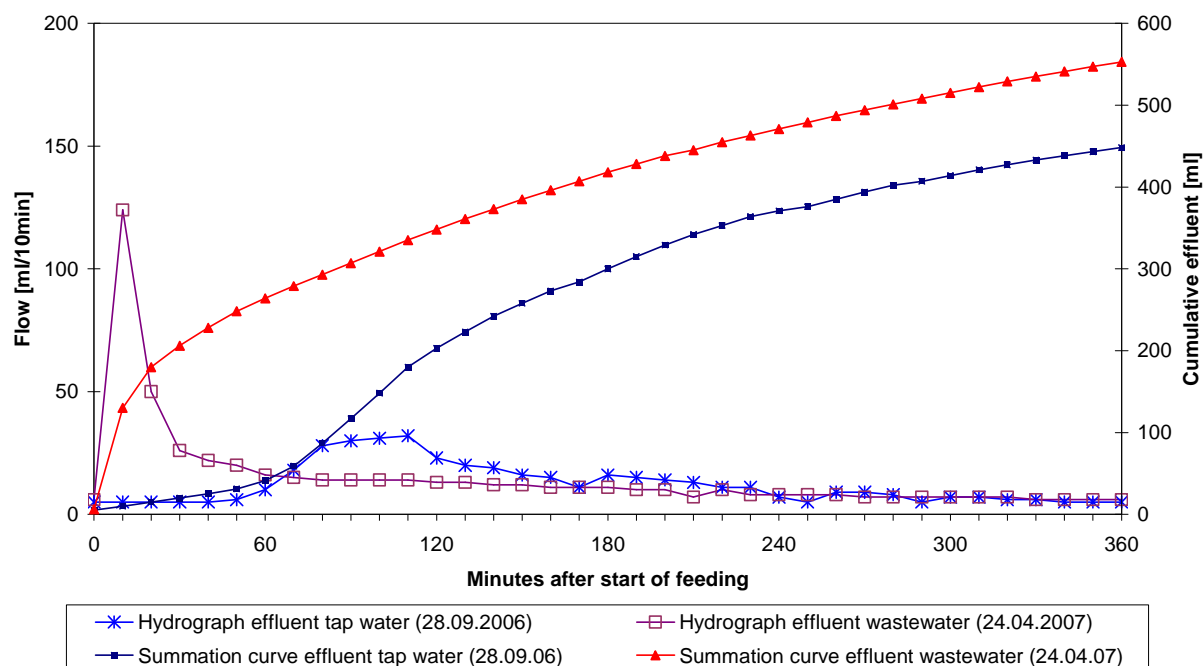


Figure 4.4-1: Hydrographs and cumulative effluent SL

The hydrograph of tap water is slightly skewed left. The maximum effluent of 32 ml/10 minutes is reached after 110 minutes. The minimum effluent is reached after 155 minutes. The ratio of infiltration time and diffusion time is 1:1.3. The more or less uniformity of effluent indicates an even distribution pores. Due to the fact that only 86 % of influent volume is discharged, water storage within the column occurred. This leads to accumulation of water due to insufficient permeability.

The hydrograph of wastewater was measured seven month later. It is notably skewed left. The maximum effluent of 124 ml/10 minutes is reached after 10 minutes. The minimum effluent is reached after 65 minutes. The ratio of infiltration time and diffusion time is 1:4.0. This indicates a fast dewatering of coarse pores. Therewith a change of pore size distribution due to particle displacement. The shape of summation curve shows that discharge is not ended until the next loading. This leads to accumulation of water within the fine pores of SL. The fact that the summation of effluent is higher than the loading volume indicates a mobilisation of preliminary accumulated water based on reopening of clogged pores. The infiltration condition changed towards a higher permeability (cf. Table 4.4-1 and Figure 4.4-1).

Table 4.4-1: Summary hydrographs and cumulative effluent SL

	Influent [ml/load]	Summation Effluent [ml]	Maximum effluent		Minimum effluent		Skewness left + right -
			Volume [ml /10 min]	Time [min]	Volume [ml /10 min]	Time [min]	
Tap water	520	448	32	110	15	155	1.204
Wastewater	520	553	124	10	15	65	4.840

4.4.3 Perlite

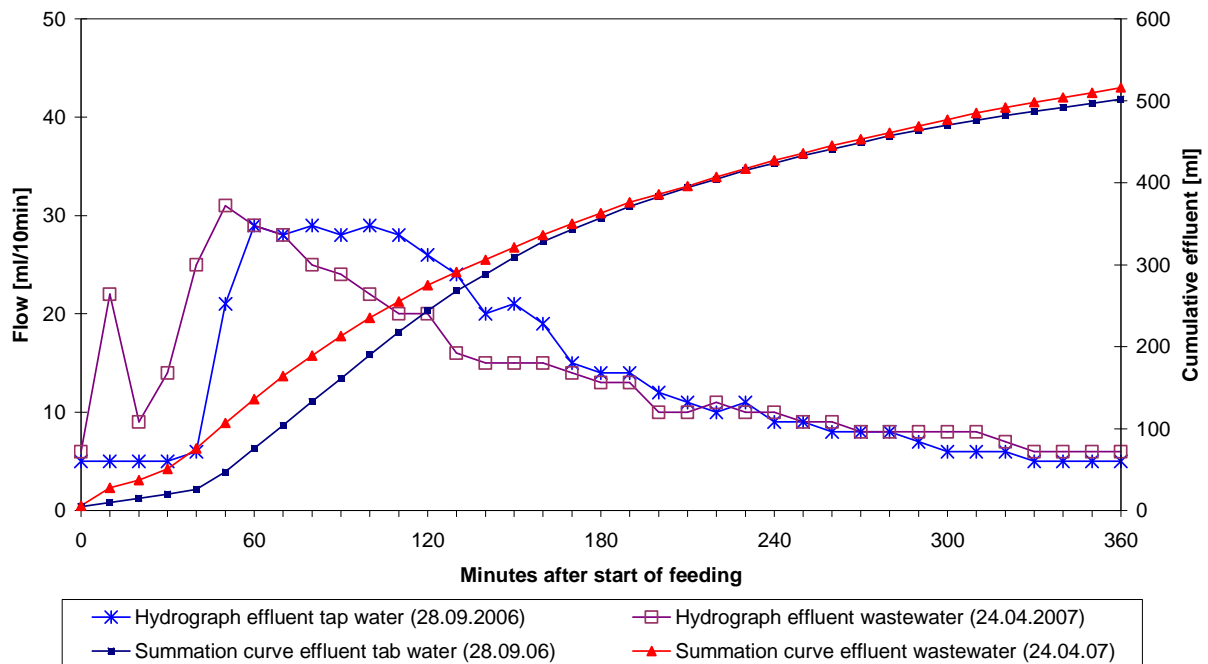


Figure 4.4-2: Hydrographs and cumulative effluent PE

The hydrograph of tap water is slightly skewed left. The maximum effluent of 29 ml/10 minutes is reached after 60 minutes. The minimum effluent is reached after 165 minutes. The ratio of infiltration time and diffusion time is 1:1.2. The more or less uniformity of effluent indicates a uniform pore size distribution. The summation of effluent is lower than the loading volume. Because the difference is low, it is explicable by evaporation.

The hydrograph of wastewater was measured seven month later. The maximum effluent of 31 ml/10 minutes is reached after 10 minutes. The minimum effluent is reached after 135 minutes. The ratio of infiltration time and diffusion time is 1:1.7. Although there is almost no difference between hydrographs and summation curves of wastewater and tap water the maximum effluent of hydrograph of wastewater shifted to the left and increased which means a slight increase of permeability. Nevertheless, the infiltration conditions did not change decisively during seven months (cf. Table 4.4-2 and Figure 4.4-2).

Table 4.4-2: Summary hydrographs and cumulative effluent PE

	Influent [ml/load]	Summation Effluent [ml]	Maximum effluent		Minimum effluent		Skewness left + right -
			Volume [ml /10 min]	Time [min]	Volume [ml /10 min]	Time [min]	
Tap water	520	502	29	60	15	165	0.704
Wastewater	520	516	31	50	15	135	0.867

4.4.4 Pumice

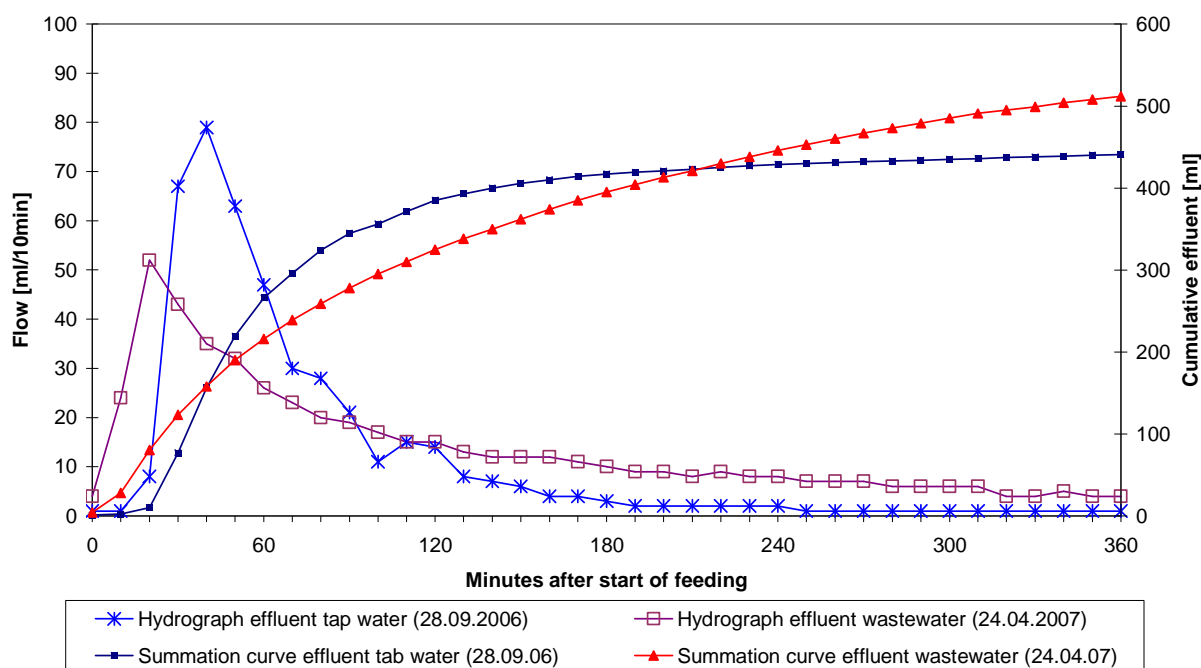


Figure 4.4-3: Hydrographs and cumulative effluent PU

The hydrograph of tap water is skewed left. The maximum effluent of 79 ml/10 minutes is reached after 40 minutes. The minimum effluent is reached after 105 minutes. The ratio of infiltration time and diffusion time is 1:2.4. The distinct peak of the effluent curve indicates a fast dewatering of coarse pores. The summation of effluent is lower than the summation of influent. Additionally shows the shape of the summation curve of tap water that the discharge is completed before influent volume is reached. This indicates a water accumulation within fine pores.

The hydrograph of wastewater, measured seven months later, shows a change of infiltration conditions. The maximum effluent shifted to the left and is reached after 20 minutes. However, it is with 52 ml/10 minutes lower than the maximum effluent of tap water. The skewness decreased. The minimum effluent is reached after 105 minutes. The ratio of infiltration time and diffusion time is 1:2.4. The pore size distribution becomes more regular due to particle displacement. The summation curve of wastewater shows that the loading volume is discharged almost completely. The difference is explicable by evaporation (cf. Figure 4.4-3 and Table 4.4-3).

Table 4.4-3: Summary hydrographs and cumulative effluent PU

	Influent [ml/load]	Summation Effluent [ml]	Maximum effluent Volume [ml /10 min]	Time [min]	Minimum effluent Volume [ml /10 min]	Time [min]	Skewness left + right -
Tap water	519	441	79	40	15	105	2.263
Wastewater	519	512	52	20	15	105	1.810

4.4.5 Turkish Sand

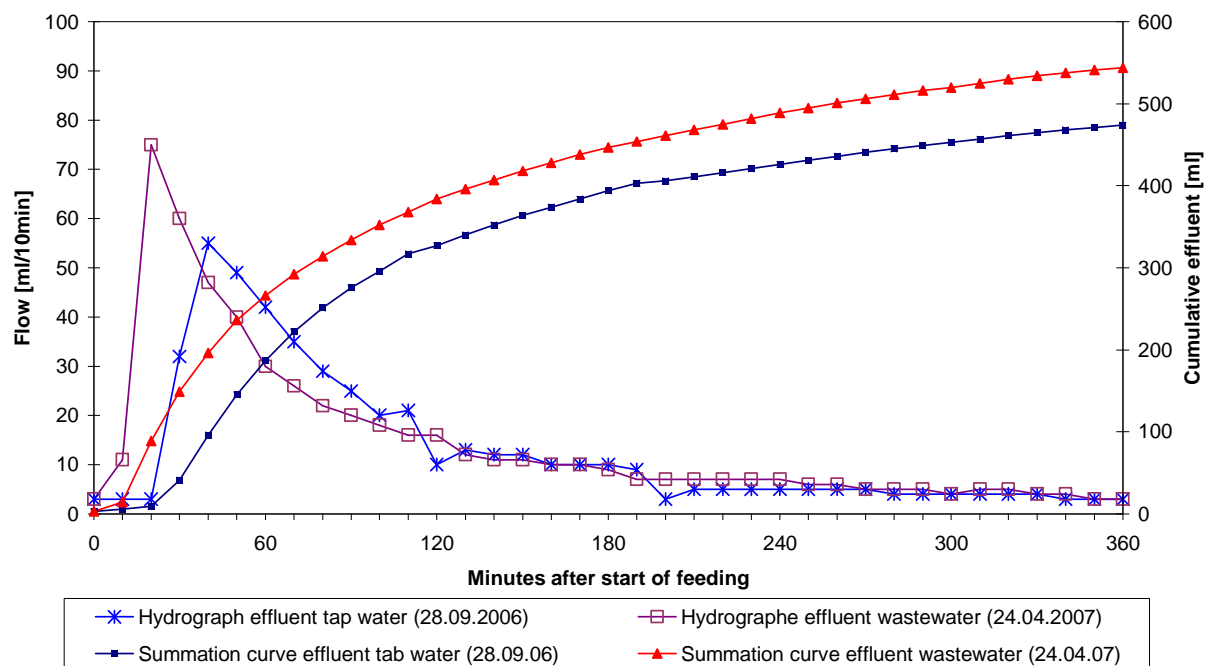


Figure 4.4-4: Hydrographs and cumulative effluent TS

The hydrograph of tap water is skewed left. The maximum effluent of 55 ml/10 minutes is reached after 40 minutes. The minimum effluent is reached after 125 minutes. The ratio of infiltration time and diffusion time is 1:1.9. The peak of the effluent curve indicates a fast dewatering of coarse pores. The summation of effluent is lower than the summation of influent. Additionally shows the shape of the summation curve of tap water that the discharge is not completed before next loading. This indicates that the permeability of fine pores is too low for complete discharge.

The hydrograph of wastewater, measured seven months later, shows a change of infiltration conditions. The maximum effluent of 75 ml/10 minutes shifted to the left and is reached after 20 minutes. It is higher than the maximum effluent of tap water. The skewness increased. The minimum effluent is reached after 115 minutes. The ratio of infiltration time and diffusion time is 1:2.1. This indicates a particle displacement and a change of pore size distribution towards coarse pores. The summation curve of wastewater shows that the loading volume is discharged almost completely. The difference is explicable by evaporation (cf. Figure 4.4-4 and Table 4.4-4)

Table 4.4-4: Summary hydrographs and cumulative effluent TS

	Influent [ml/load]	Summation Effluent [ml]	Maximum effluent		Minimum effluent		Skewness left + right -
			Volume [ml /10 min]	Time [min]	Volume [ml /10 min]	Time [min]	
Tap water	550	474	55	40	15	125	1.733
Wastewater	550	544	75	20	15	115	2.329

4.4.6 Turkish Zeolite

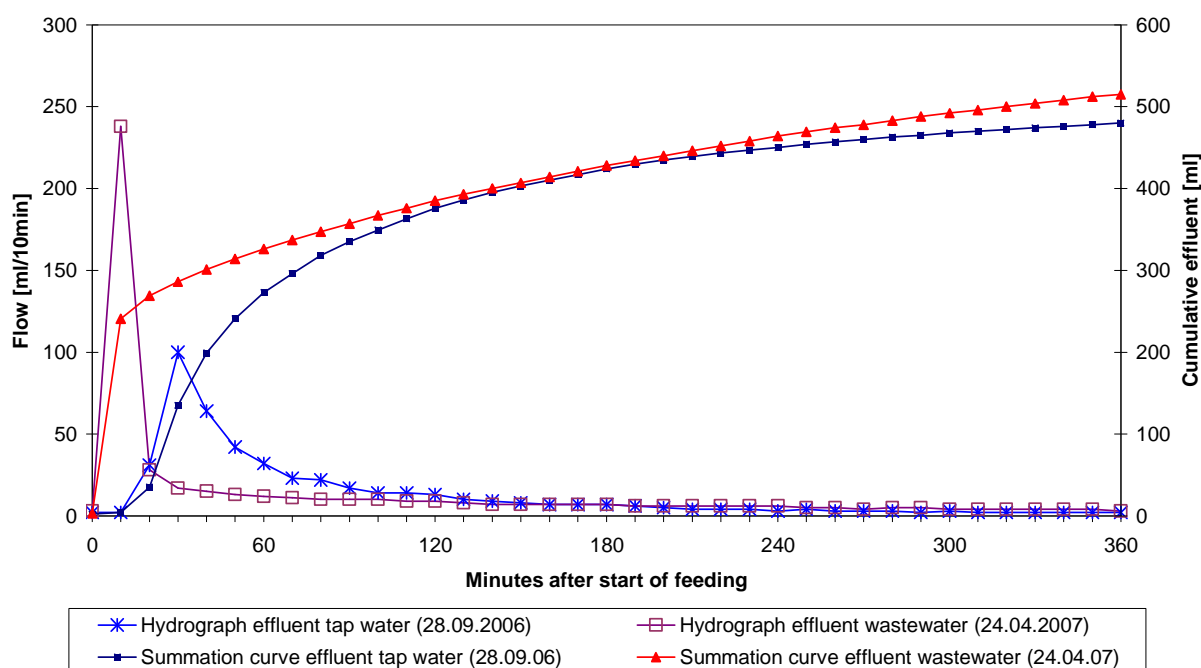


Figure 4.4-5: Hydrographs and cumulative effluent TZ

The hydrograph of tap water is skewed left. The maximum effluent of 100 ml/10 minutes is reached after 30 minutes. The minimum effluent is reached after 95 minutes. The ratio of infiltration time and diffusion time is 1:2.8. The peak of the effluent curve indicates a fast dewatering of coarse pores. The summation of effluent is lower than the summation of influent. Additional shows the shape of the summation curve of tap water that the discharge is not completed before next loading. This indicates that the permeability of fine pores is too low for complete discharge.

The hydrograph of wastewater, measured seven months later, shows a change of infiltration conditions. The maximum effluent of 238 ml/10 minutes shifted to the left and is reached after 10 minutes. It is more than two times higher than the maximum effluent of tap water. The skewness increased. The minimum effluent is reached after 35 minutes. The ratio of infiltration time and diffusion time is 1:9.3. The hydraulic capacity increased considerably. This indicates the development of fingers. The summation curve of wastewater shows that the loading volume is discharged almost completely. The difference is explicable by evaporation (cf. Figure 4.4-5 and Table 4.4-5)

Table 4.4-5: Summary hydrographs and cumulative effluent TZ

	Influent [ml/load]	Summation Effluent [ml]	Maximum effluent Volume [ml /10 min]	Time [min]	Minimum effluent Volume [ml /10 min]	Time [min]	Skewness left + right -
Tap water	530	480	100	30	15	95	3.074
Wastewater	530	515	238	10	15	35	5.938

4.4.7 Crushed Concrete

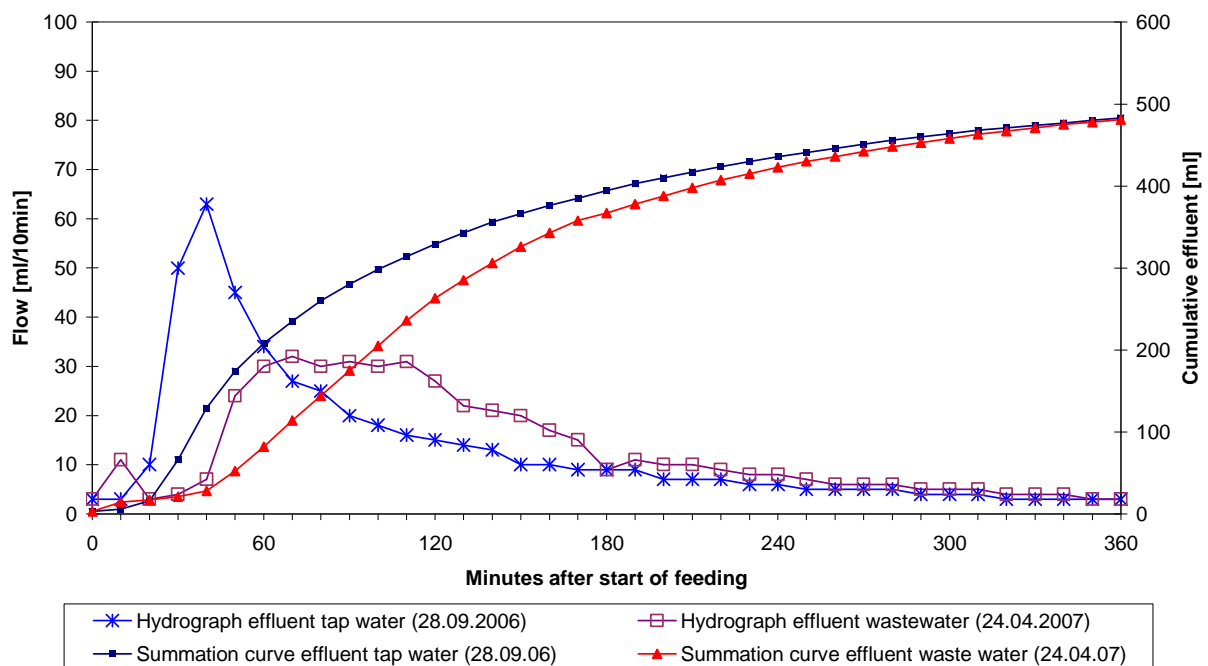


Figure 4.4-6: Hydrographs and cumulative effluent BE

The hydrograph of tap water is skewed left. The maximum effluent is 63 ml/10 minutes and is reached after 40 minutes. The minimum effluent is reached after 115 minutes. The ratio of infiltration time and diffusion time is 1:2.1. The summation of effluent is lower than loading volume. Additional shows the shape of summation curve that effluent is not completed before next loading. This is an indication for to low permeability.

The hydrograph of wastewater shows a change of infiltration conditions. The low maximum effluent with 32 ml/10 minutes shifted to the right and is reached after 70 minutes. It is with 32 ml/10 minutes two times lower than the maximum effluent of tap water. The minimum effluent is reached after 165 minutes. The curve shows a very low skewness. The ratio of infiltration time and diffusion time is 1:1.2. The infiltration is uniform. This indicates a uniform pore size distribution. Due to particle displacement, the average pore size decreased. The summation of effluent is lower than loading volume but equals the summation of effluent of the summation curve of tap water. This indicates a change of infiltration dynamics because of uniformity of pore size distribution. the hydraulic capacity decreased. Additional shows the shape of summation curve that effluent is not completed before next loading. This is an indication for to low permeability (cf. Figure 4.4-6 and Table 4.4-6).

Table 4.4-6: Summary hydrographs and cumulative effluent BE

	Influent [ml/load]	Summation	Maximum effluent		Minimum effluent		Skewness left + right -
		Effluent [ml]	Volume [ml /10 min]	Time [min]	Volume [ml /10 min]	Time [min]	
Tap water	530	483	63	40	15	115	2.147
Wastewater	530	481	32	70	15	165	0.824

4.4.8 Ferro-Sorp®

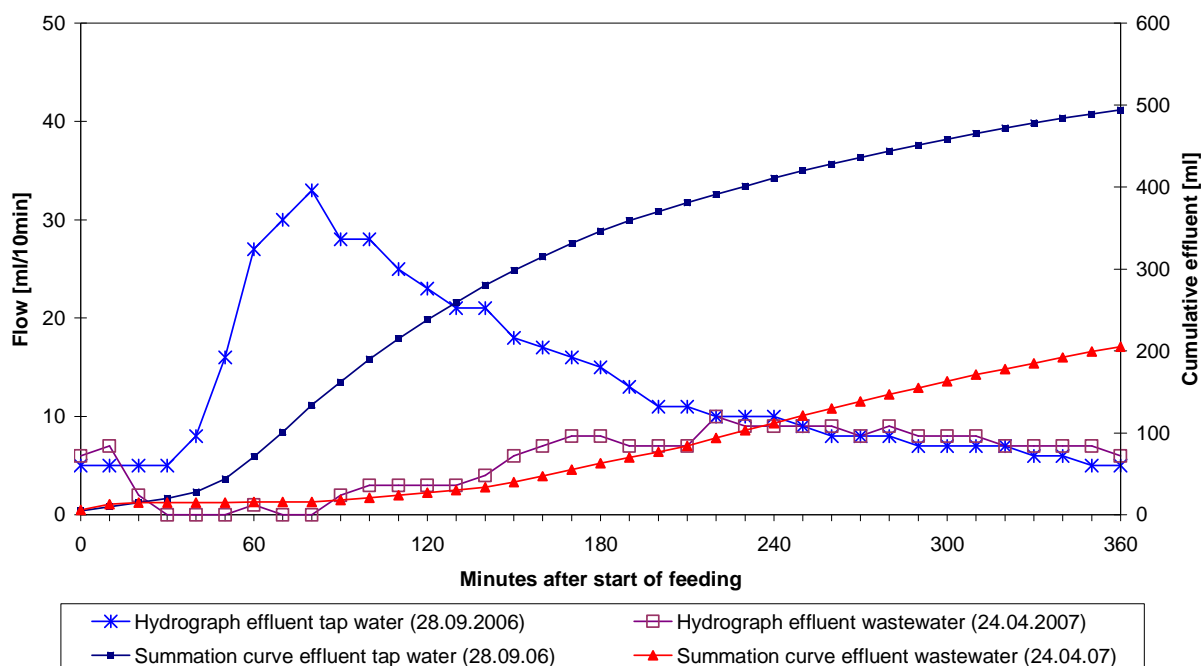


Figure 4.4-7: Hydrographs and cumulative effluent FE

The hydrograph of tap water is slight skewed left. The maximum effluent of 33 ml/10 minutes is reached after 80 minutes. The minimum effluent is reached after 175 minutes. The ratio of infiltration time and diffusion time is 1:1.1. The more or less uniformity of effluent indicates evenly distributed pores. The summation of effluent is lower than the loading volume. Because the difference is low, it is explicable by evaporation.

The effluent of wastewater is as low that the minimum effluent is not reached. The skewness of the hydrograph shifted from skewed left to skewed right. As the summation curve shows, not even 50 % of influent are discharged. This is an indication of clogging. The infiltration conditions became worse during the seven months between loading with tap water and loading with wastewater (cf. Figure 4.4-7 and Table 4.4-7).

Table 4.4-7: Summary hydrographs and cumulative effluent FE

	Influent [ml/load]	Summation Effluent [ml]	Maximum effluent		Minimum effluent		Skewness left + right -
			Volume [ml /10 min]	Time [min]	Volume [ml /10 min]	Time [min]	
Tap water	540	494	33	80	15	175	0.913
Wastewater	540	205	10	220	15	0	-0.631

4.4.9 Austrian Zeolite 1

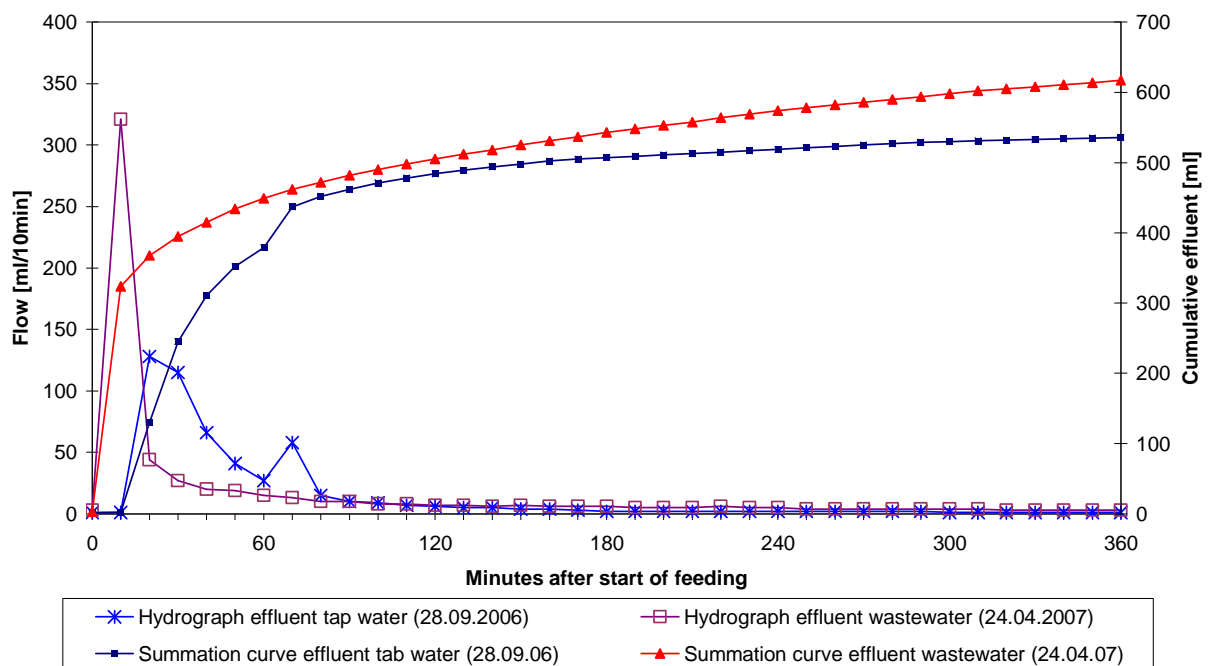


Figure 4.4-8: Hydrographs and cumulative effluent AZ1

The hydrograph of tap water is skewed left. The maximum effluent of 128 ml/10 minutes is reached after 20 minutes. After decrease of effluent, the curve shows a second peak, which is an indication of reopening of preliminary clogged pores. The minimum effluent is reached after 75 minutes. The ratio of infiltration time and time of diffusion time is 1:3.8. The peak of the effluent curve indicates a fast dewatering of coarse pores. The summation of effluent is lower than the summation of influent. The difference is Additional shows the shape of the summation curve of tap water. This is explicable by evaporation.

The hydrograph of wastewater, measured seven month later, shows a change of infiltration conditions. The skewness of the hydrograph of wastewater shifted to the left and the maximum effluent increased from 128 ml to 321 ml/10 minutes. The minimum effluent is reached after 55 minutes. The ratio of infiltration time and diffusion time is 1:5.6. The increase of maximum effluent indicates the development of fingers. The summation curve of wastewater shows that more water is discharged than loaded. Preliminary accumulated water is mobilised again (cf. Figure 4.4-8 and Table 4.4-8)

Table 4.4-8: Summary hydrographs and cumulative effluent AZ1

	Influent [ml/load]	Summation Effluent [ml]	Maximum effluent Volume [ml /10 min]	Time [min]	Minimum effluent Volume [ml /10 min]	Time [min]	Skewness left + right -
Tap water	546	536	128	20	15	75	2.871
Wastewater	546	617	321	10	15	55	5.865

4.4.10 Austrian Zeolite 2

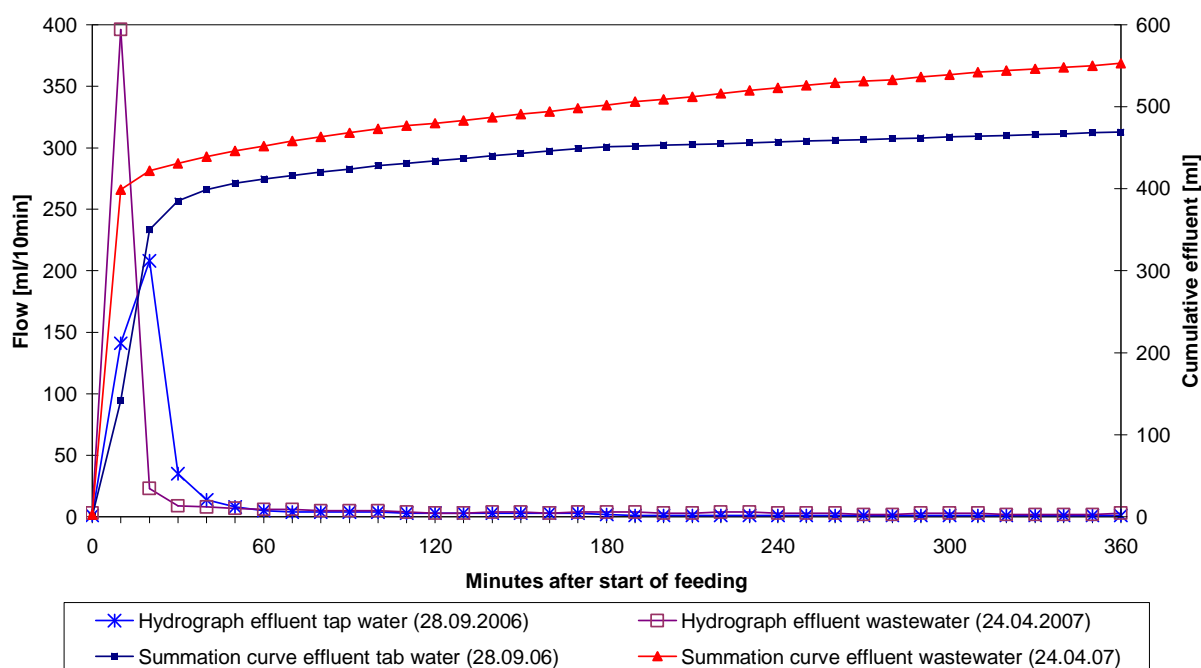


Figure 4.4-9: Hydrographs and cumulative effluent AZ2

The hydrograph of tap water is extremely skewed left. The maximum effluent of 208ml/10 minutes is reached after 20 minutes. The minimum effluent is reached after 35 minutes. The ratio of infiltration time and diffusion time is 1:9.3. The peak of the effluent curve indicates a fast dewatering of coarse pores. The hydraulic capacity is very high. The summation of effluent is lower than the summation of influent. Additionally shows the shape of the summation curve of tap water that the discharge is not completed before next loading. This indicates that the permeability of fine pores is too low for complete discharge.

In comparison to the hydrographs of tap water, the hydrograph of wastewater shows a change of infiltration conditions. The maximum effluent is reached after 10 minutes and increased from 208 ml/10 minutes to 553 ml/10 minutes. Additionally increased the skewness. The minimum effluent is reached after 15 minutes. The ratio of infiltration time and diffusion time is 1:23. The hydraulic capacity is extremely high. This indicates the development of fingers. The summation curve of wastewater shows that more water is discharged than loaded. Preliminary accumulated water is mobilised again by particle displacement (cf. Figure 4.4-9 and Table 4.4-9)

Table 4.4-9: Summary hydrographs and cumulative effluent AZ2

	Influent [ml/load]	Summation Effluent [ml]	Maximum effluent Volume [ml /10 min]	Time [min]	Minimum effluent Volume [ml /10 min]	Time [min]	Skewness left + right -
Tap water	520	469	208	20	15	35	4.235
Wastewater	520	553	396	10	15	15	6.054

4.4.11 Austrian Sand

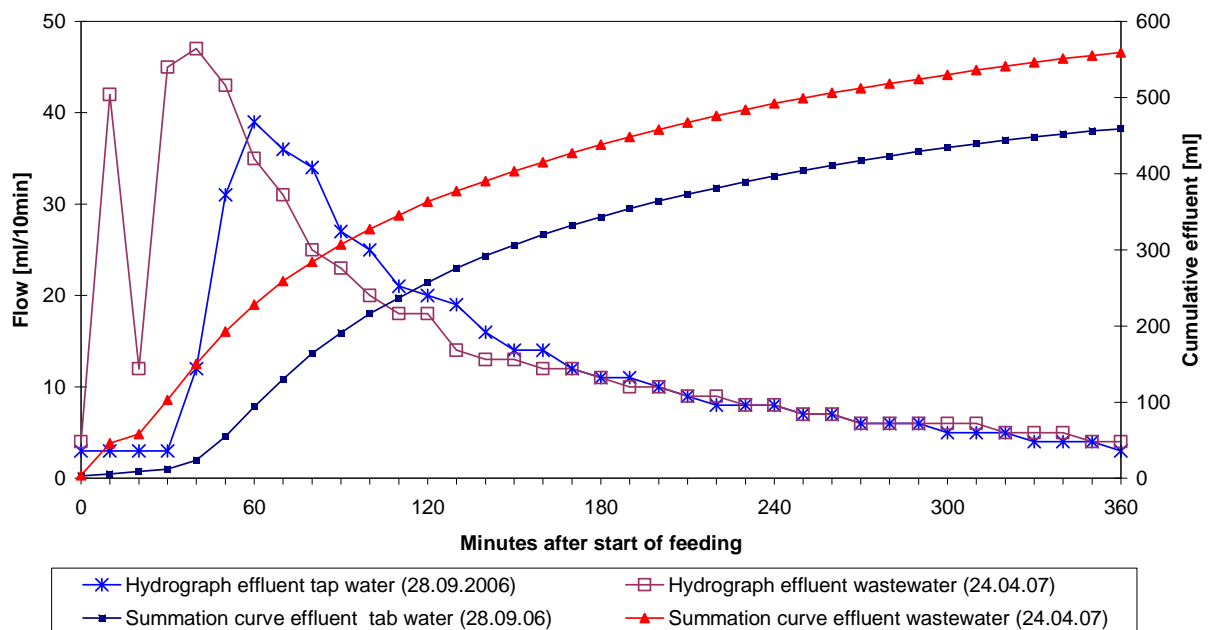


Figure 4.4-10: Hydrographs and cumulative effluent AS

The hydrograph of tap water is skewed left. The maximum effluent of 39 ml/10 minutes is reached after 60 minutes. The minimum effluent is reached after 145 minutes. The ratio of infiltration time and diffusion time is 1:1.5. The peak of the effluent curve indicates a fast dewatering of coarse pores. The summation of effluent is lower than the summation of influent. Additional shows the shape of the summation curve of tap water that the discharge is not completed before next loading. This indicates that the permeability of fine pores is too low for complete discharge.

The hydrograph of wastewater is skewed left and the maximum effluent of 47 ml/10 minutes is reached after 40 minutes. After decrease of effluent, the curve shows a second peak, which is an indication of reopening of preliminary clogged pores. The minimum effluent is reached after 125 minutes. The ratio of infiltration time and diffusion time is 1:1.9. The hydraulic capacity increased. The summation of effluent of wastewater is higher than the loading volume. Accumulated water of preliminary loadings is discharged (cf. Figure 4.4-10 and Table 4.4-10)

Table 4.4-10: Summary hydrographs and cumulative effluent AS

	Influent [ml/load]	Summation Effluent [ml]	Maximum effluent		Minimum effluent		Skewness left + right -
			Volume [ml /10 min]	Time [min]	Volume [ml /10 min]	Time [min]	
Tap water	520	459	39	60	15	145	1.296
Wastewater	520	559	47	40	15	125	1.450

4.4.12 Ferro-Sorp® + Turkish Zeolite

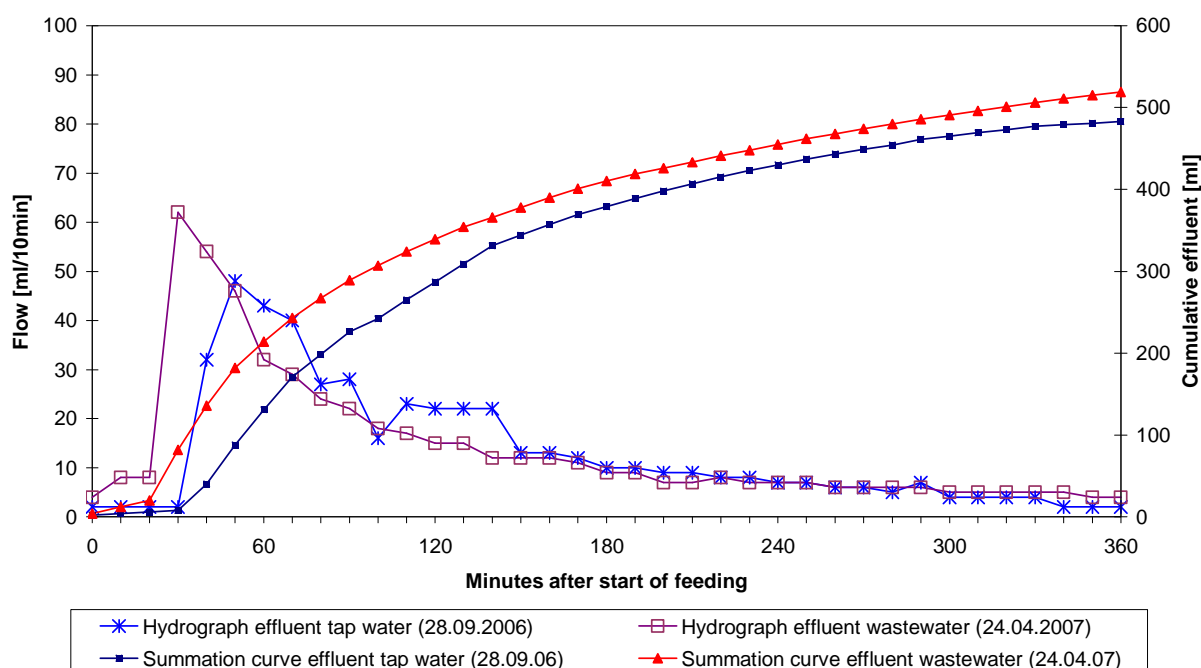


Figure 4.4-11: Hydrographs and cumulative effluent FE+TZ

The hydrograph of tap water is skewed left. The maximum effluent of 48 ml/10 minutes is reached after 50 minutes. The minimum effluent is reached after 175 minutes. The ratio of infiltration time and diffusion time is 1:1.1. The hydraulic capacity is low. The peak of the effluent curve indicates a fast dewatering of coarse pores. The summation of effluent is lower than the summation of influent. Additionally shows the shape of the summation curve of tap water that the discharge is not completed before next loading. This indicates that the permeability of fine pores is too low for complete discharge.

In comparison to the hydrograph of tap water, the hydrograph of wastewater shows a change of infiltration conditions. The maximum effluent of 62 ml/10 minutes shifted to the left and is reached after 30 minutes. It is higher than the maximum effluent of tap water. The skewness increased. The minimum effluent is reached after 115 minutes. This leads to a ratio of infiltration time and diffusion time of 1:2.1. This indicates a faster dewatering of coarse pores. The hydraulic capacity increased. The summation curve of wastewater shows that the loading volume is discharged almost completely. The difference is explicable by evaporation (cf. Figure 4.4-11 and Table 4.4-11).

Table 4.4-11: Summary hydrographs and cumulative effluent FE+TZ

	Influent [ml/load]	Summation	Maximum effluent		Minimum effluent		Skewness left + right -
		Effluent [ml]	Volume [ml /10 min]	Time [min]	Volume [ml /10 min]	Time [min]	
Tap water	520	483	48	50	15	175	1.393
Wastewater	520	519	62	30	15	115	2.209

4.4.13 Mixture 30

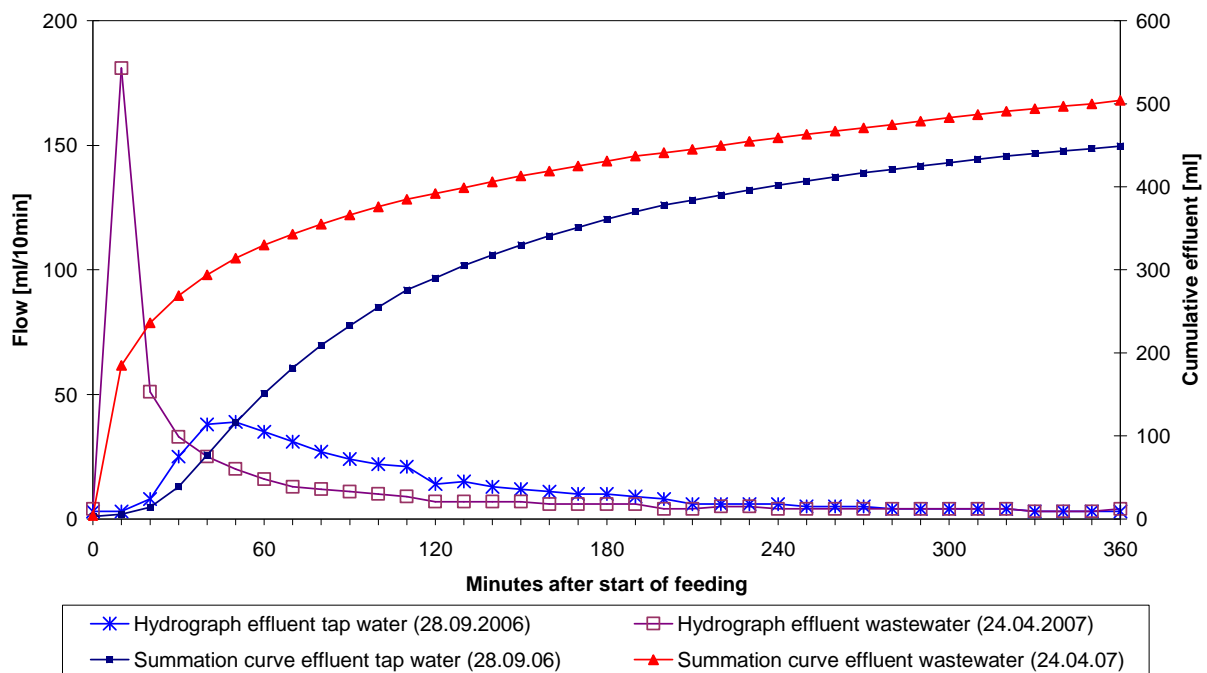


Figure 4.4-12: Hydrographs and cumulative effluent MX 30

The hydrograph of tap water is slight skewed left. The maximum effluent of 39 ml/10 minutes is reached after 50 minutes. The minimum effluent is reached after 125 minutes. The ratio of infiltration time and diffusion time is 1:1.9. The more or less uniformity of effluent indicates evenly distributed pores. The summation of effluent is lower than the loading volume. Because the difference is low, it is explicable by evaporation.

The hydrograph of wastewater was measured seven month later. It is notable skewed left. The maximum effluent of 181 ml/10 minutes is reached after 10 minutes. It is almost five times higher than the maximum effluent of tap water. The minimum effluent is reached after 55 minutes. The ratio of infiltration time and diffusion time is 1:5.6. The hydraulic capacity increased considerably. The distinct peak of the effluent curve indicates the development of fingers due to the displacement of particles. The fact that the summation of effluent is higher than the loading volume indicates a mobilisation of preliminary accumulated water based on reopening of clogged pores. The infiltration condition changed decisively (cf. Figure 4.4-12 and Table 4.4-12).

Table 4.4-12: Summary hydrographs and cumulative effluent MX 30

	Influent [ml/load]	Summation Effluent [ml]	Maximum effluent Volume [ml /10 min]	Time [min]	Minimum effluent Volume [ml /10 min]	Time [min]	Skewness left + right -
Tap water	490	449	39	50	15	125	1.285
Wastewater	490	504	181	10	15	55	5.216

4.4.14 Mixture 50

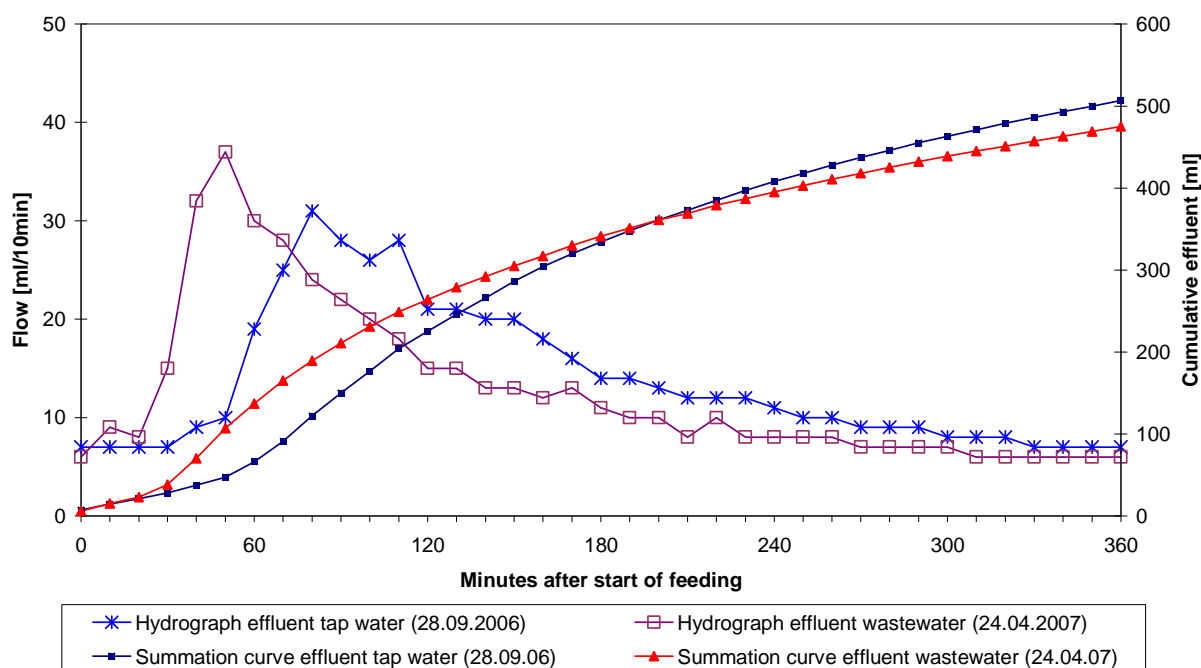


Figure 4.4-13: Hydrographs and cumulative effluent MX 50

The hydrograph of tap water is slight skewed left. The maximum effluent of 31 ml/10 minutes is reached after 80 minutes. The minimum effluent is reached after 165 minutes. The ratio of infiltration time and diffusion time is 1:1.2. The more or less uniformity of effluent indicates evenly distributed pores. The summation of effluent is lower than the summation of influent. This leads to accumulation of water due to insufficient permeability.

The hydrograph of wastewater shows as well as the hydrograph of tap water a very low permeability. The shape of the hydrograph of wastewater changed in comparison to the shape of the one of wastewater only slightly. The maximum effluent of 37 ml/10 minutes is reached after 50 minutes. The minimum effluent is reached after 165 minutes. The ratio of infiltration time and diffusion time is 1:1.2. The summation of effluent decreased from tap water to wastewater. At loading with wastewater, the whole loading volume was not discharged before next loading. This is an indication of too low permeability (cf. Figure 4.4-13 and Table 4.4-13). Because the column MX 50 consists of the same material as MX 30, the influence of filter height on infiltration conditions is obvious. The hydraulic capacity decreases with increasing height of filter (cf. chapter 4.4.13).

Table 4.4-13: Summary hydrographs and cumulative effluent MX 50

	Influent [ml/load]	Summation Effluent [ml]	Maximum effluent Volume [ml /10 min]	Time [min]	Minimum effluent Volume [ml /10 min]	Time [min]	Skewness left + right -
Tap water	530	507	31	80	15	165	0.996
Wastewater	530	475	37	50	15	115	1.517

4.4.15 Mixture 75

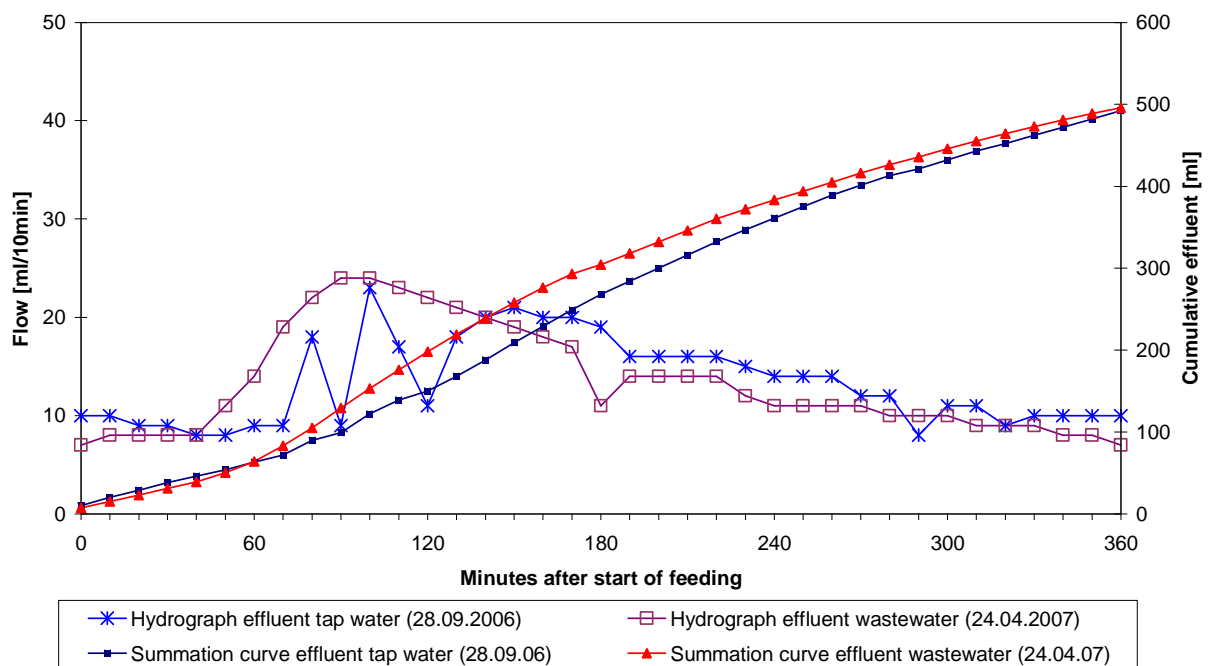


Figure 4.4-14: Hydrographs and cumulative effluent MX 75

Both hydrographs show more or less the same low permeability. The maximum effluents are low and the curves are very slight skewed left. The more or less uniformity of effluent indicates evenly distributed fine pores. The ratio of infiltration time and diffusion time amounts to 1:0.6. The ratio of wastewater amounts to 1:1.1. The hydraulic capacity of both is very low, but increased during the operation time of seven month, slightly. The summation of effluent is lower than the loading volume. Because the difference is low, it is explicable by evaporation (cf. Figure 4.4-14 and Table 4.4-14)

Because the column MX 75 consists of the same material as MX 30 and MX 50 the influence of filter height on infiltration condition is obvious (cf. chapter 4.4.13 and chapter 4.4.14).

Table 4.4-14: Summary hydrographs and cumulative effluent MX 75

	Influent [ml/load]	Summation Effluent [ml]	Maximum effluent		Minimum effluent		Skewness left + right -
			Volume [ml /10 min]	Time [min]	Volume [ml /10 min]	Time [min]	
Tap water	520	492	23	100	15	225	0.567
Wastewater	520	496	24	100	15	175	0.711

4.5 Tracer studies

4.5.1 Measured HRT

Concerning measured conductivities, it is noticeable that at any single filter material shows a difference between the cumulative conductivity of influent and effluent (cf. Table 4.5-1). That means either that KCl solution remained partially within the filter material because of sorption, in the case of lower conductivity of effluent, or in the case of higher conductivity of effluent, that dissolving processes took place. In other words, the results of HRT are falsified due to these processes. They cannot be avoided because an ideal tracer does not exist but they should be as little as possible.

For BE, MX 50, and MX 75 so many ions became dissolved that a statement about the HRT is not possible. Because the cumulative electrical conductivity of effluent of BE is 764 % higher than the cumulative conductivity of influent it is evident that the higher conductivity of MX 50 and MX 75 is induced by BE (cf. chapter 3.1.2.1). It is noticeable that at MX 30 the cumulative conductivity of effluent is lower than the one of influent. This can be explained by inhomogeneous mixing of its components. At FE 51 % of the tracer solution remained within the column. This is an amount, which makes a statement about the HRT of FE impossible, too

Table 4.5-1: Measured HRT

	Loading Volume [ml/load]	Cumulative cond. Influent [mS/cm*I]	Cumulative cond. Effluent [mS/cm*I]	Difference cond. Influent-Effluent [%]	Cumulative cond. Effluent/2 [mS/cm*I]	HRT	
						[hours]	[days]
SL	520	5.37	5.58	3.97	2.79	41.2	1.7
PE	520	5.37	6.11	13.79	3.06	41.0	1.7
PU	519	5.36	6.34	18.17	3.17	30.7	1.3
TS	550	5.68	5.44	-4.27	2.72	67.5	2.8
TZ	530	5.68	4.78	15.83	2.39	30.6	1.3
BE	530	5.47	47.29	763.72	23.64	89.0	3.7
FE	530	5.47	2.68	-51.00	1.34	99.3	4.1
AZ1	546	5.64	4.20	-25.61	2.10	30.0	1.3
AZ2	520	5.42	4.17	-23.00	2.09	53.6	2.2
AS	520	5.37	5.99	11.43	2.99	41.4	1.7
FE+TZ	520	5.37	3.55	-33.89	1.78	52.6	2.2
MX 30	490	5.17	5.12	-0.92	2.56	29.1	1.2
MX 50	530	5.37	9.09	69.16	4.54	32.0	1.3
MX 75	520	5.37	8.65	61.10	4.33	33.6	1.4

Concerning relevant diagrams confer Appendix.

4.5.2 Calculated HRT and comparison with measured HRT

The results of HRT calculated based on daily influent volume and pore volume range from 2.3 (PE) to 5.5 (MX 75) (cf. Table 4.5-2). Because of interaction of KCl solution and BE, MX 50, MX 75, and FE the results of measured HRT are falsified strongly and not reliable. Hence, a comparison does not make sense. It is noticeable that for all materials except TS the calculated HRT is higher than the measured one (cf. Figure 4.5-1) A shorter measured HRT than the calculated indicates the development of short circuit flow within the filter material. The problem

of development of pathways along the contact area between the stiff PVC-pipe of columns and the filter material, described in chapter 4.3, could occur in column experiments, too. This would lead to an intensified flow along the contact area and to a lower HRT. A longer measured HRT than the calculated indicates compaction respectively clogging within the column. Another reason for differences could be that for permeability not the pore volume is determining but the pore size distribution. The values concerning HRT of TS match roughly. This is an indication for a uniform flow through the column.

Table 4.5-2: Results of calculated HRT

	Loading Volume [ml/load]	Influent Volume [m³/d]	Filter Diameter [m]	Filter Surface [m²]	Filter Height [m]	Filter Volume [m³]	Porosity Average [-]	Pore Volume [m³]	HRT [d]
SL	520	0.00208	0.20	0.0314	0.50	0.0157	0.5087	0.0080	3.8
PE	520	0.00208	0.20	0.0314	0.50	0.0157	0.3052	0.0048	2.3
PU	519	0.00208	0.20	0.0314	0.50	0.0157	0.3449	0.0054	2.6
TS	550	0.00220	0.20	0.0314	0.50	0.0157	0.3614	0.0057	2.6
TZ	530	0.00212	0.20	0.0314	0.50	0.0157	0.5243	0.0082	3.9
BE	530	0.00212	0.20	0.0314	0.50	0.0157	0.4730	0.0074	3.5
FE	530	0.00212	0.20	0.0314	0.50	0.0157	0.7149	0.0112	5.3
AZ1	546	0.00218	0.20	0.0314	0.50	0.0157	0.5626	0.0088	4.0
AZ2	520	0.00208	0.20	0.0314	0.50	0.0157	0.5123	0.0080	3.9
AS	520	0.00208	0.20	0.0314	0.50	0.0157	0.3067	0.0048	2.3
FE+TZ	520	0.00208	0.20	0.0314	0.50	0.0157	0.6977	0.0110	5.3
MX 30	490	0.00196	0.20	0.0314	0.30	0.0094	0.4892	0.0046	2.4
MX 50	530	0.00212	0.20	0.0314	0.50	0.0157	0.4892	0.0077	3.6
MX 75	520	0.00208	0.20	0.0314	0.75	0.0236	0.4892	0.0115	5.5

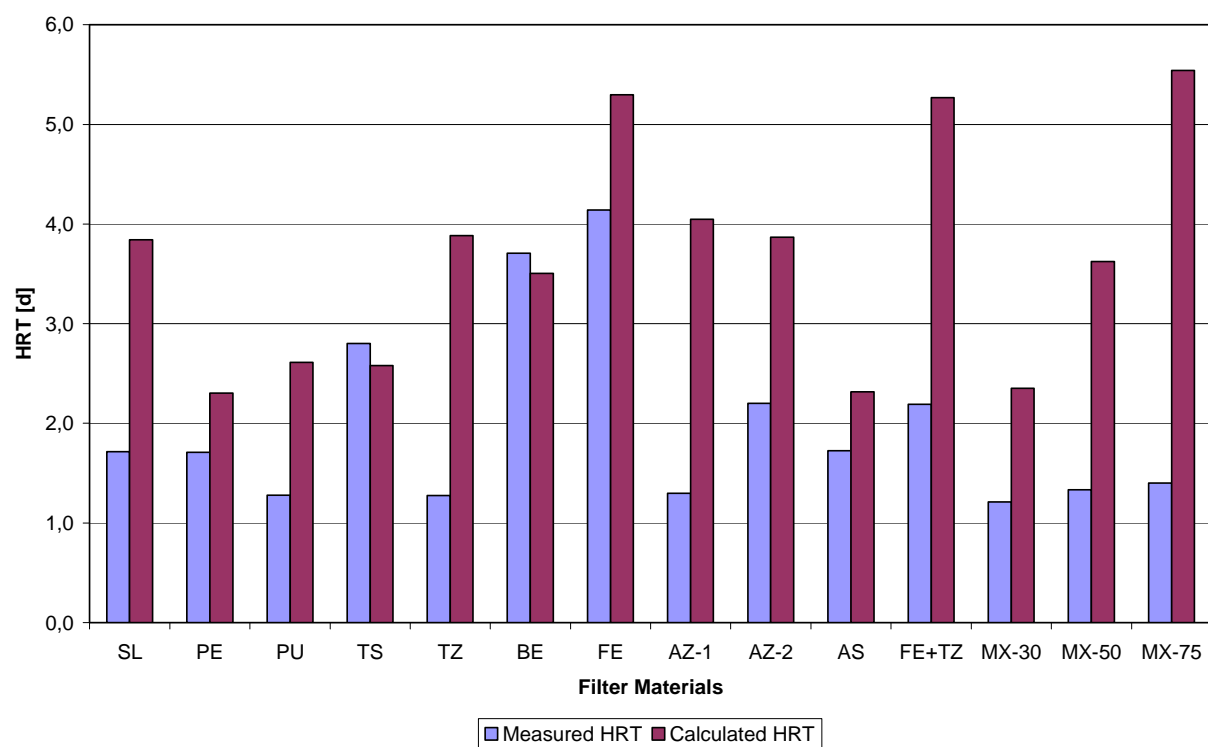


Figure 4.5-1: Measured vs. calculated HRT

5 Discussion

5.1 Used methods

The methods are reviewed in following order:

- Sieve analysis
- Pycnometer experiments
- K – value measurement
- Column experiment

5.1.1 Sieve analysis

Sieve analysis were not conducted as wet sieving. This could lead to residuals of smallest particles and dust which are not taken in account at analysis but they could affect permeability. Wet sieving is recommended.

Sieve analysis with different sample sizes to see if sample size has an influence on results is not necessary. On the one hand, the differences were very small and on the other hand, at DIN 18123 (1996), to insure comparability of results, a minimum sample size according to maximum grain size is defined.

5.1.2 Pycnometer experiments

For particle density measurement, shaking of pycnometers, filled with filter material and water, was necessary to deaerate the pores. If air remains within the pores of the filter material, it is not saturated with water and the results of weighting are falsified. This could be the reason for the high standard deviation of the results of particle density measurement. The results of bulk density have a very low standard deviation. In bulk density pores are included. Because porosity is calculated based on bulk- and particle density, the standard deviation of porosity mainly results from particle density measurement.

A possibility to prevent falsification of particle density could be dwell times between repeated shakings of pycnometer to deaerate the material more effectively.

5.1.3 k-value measurement

At materials where a comparison between measured and calculated k-values was possible it was attracting attention that at any single filter material the measured values were higher than the calculated ones. The reason was that at the contact area between the stiff PVC-pipe of the measurement device and the filter material the porosity was enhanced. This led to an intensified flow along the contact area and to a higher measured permeability with a high standard deviation. This effect would not occur if the filter material within the pipe would be welted by an elastic membrane and supported by external pressure. Additionally, the filter material became loosened by ubstreaming water, which led to a higher measured k-value, too. Thus, it seems reasonable to substitute measurements by calculation based on d_{10} as it is suggested at DWA A 262 (2006).

5.1.4 Column experiments

During the column experiment, due to particles in the municipal wastewater influent and insufficient sedimentation and particle separation by sieving, clogging of the used silicon pipes occurred. This effect was intensified by MO growth. The diaphanous silicon pipes in combination with a high nutrient amount provided very good living conditions for them. Therefore, concerning loading volume, it was difficult to keep up steady experiment condition. Thus, an advanced particle separation is necessary and the use of lightproof silicon pipes would be better.

The fact that at the contact area between the stiff PVC-pipe and the filter material, the porosity is enhanced could lead to an intensified flow along the contact area and to falsification of infiltration conditions. This effect would not occur if the filter material within the pipe is welted by an elastic membrane and supported by external pressure.

5.2 Filter materials

For assessment of filter materials in terms of later use in CWs the results of evaluations are weighted differently. Basically, in comparison to the results of physical analysis (pycnometer experiments, sieve analysis), the results of hydrological and hydraulic analysis (k-value measurement, column experiments) are up rated. For instance, if a filter material fulfils the requirements of ATV A 262 (1997) and DWA A 262 (2006) and the recommendations of PLATZER (1997) concerning grain size distribution but at column experiments the same material shows insufficient infiltration characteristics the material has to be classified as unsuitable. In particular, for evaluation if compacting respectively clogging or short circuit flow developed the changes of hydrographs during the seven months between first and second measurement are important. Additionally, the comparison between measured HRT and calculated HRT provides an indication of change of infiltration conditions.

5.2.1 Criteria

- Conformance to requirements of ATV A 262 (1997) and DWA A 262 (2006) and PLATZER (1997) concerning grain size distribution and classification
- Difference between expectable porosity due to classification and measured porosity
- Conformance to requirements of ÖNORM B 2505 (1997) and DWA A 262 (1997) concerning k-value and comparison of measured k-values and calculated based on d_{10} . Calculation of k-value based on d_{10} is suggested by DWA A 262 (2006).
- Fulfilment of the ideal range of infiltration time and diffusion time
- Change of ratio of infiltration time and diffusion time
- Development of fingers respectively clogging
- Accumulation of water between two loadings
- Difference between measured and calculated HRT

5.2.1.1 Digression concerning BE

Even though the chemical composition of filter materials was not topic of this thesis it is important that BE can contain pollutants, which are harmful to health and environment and can be washed out by water. Pollutants can be such as chromate, arsenic, lead, cadmium, copper, nickel, mercury, zinc, and PAH (cf. chapter 3.1.2.1).

Therefore, from chemical point of view, BE and MIXTURE cannot be recommended as substrate for VF CWs.

5.2.2 Slag

Slag meets all requirements and recommendations concerning grain size distribution. It is classified as poorly graded pebbly sand. Therefore, porosity in a range of 0.28 and 0.35 can be expected. The measured porosity of SL is 46 % above this range. The measured k-value is 584 % higher than the calculated one and has a high standard deviation. This leads to a low reliability of results. Thus, for evaluation only the calculated k-value, which meets the requirements of ÖNORM B 2505 (1997) and DWA A 262 (2006) is considered (cf. Table 5.2-1).

When operated with tap water the column filled with SL had a low hydraulic capacity. With a uniform pore size distribution. The ratio of infiltration time and oxygen diffusion time of 1:1.3 means a high contact time and a low oxygen diffusion time. When operated with wastewater the hydraulic capacity increased notably. During seven month, particle displacement occurred and coarse pores developed. The ratio of infiltration time and diffusion time changed to 1:4. That means a fast dewatering of coarse pores. The oxygen diffusion time is four times higher than the contact time. Water was accumulated within the fine pores (cf. Figure 4.4-1).

The calculated HRT of SL amounts to 3.8 days. This is 55 % higher than the measured HRT.

Table 5.2-1: Results SL

Bulk density		Particle density		Porosity		Grading curves (ava. values)					k-value		HRT
Average	Standard deviation	Average	Standard deviation	Average	Standard deviation	d ₁₀	d ₃₀	d ₆₀	C _u	C _c	Average	Standard deviation	
[g/cm ³]	[-]	[g/cm ³]	[-]	[g/cm ³]	[-]	[mm]	[mm]	[mm]	[-]	[-]	[m/s]	[-]	[d]
1.0671	0.0233	2.1718	0.1468	0.5087	0.0301	0.48	0.95	1.54	3.19	1.21	0.0146	0.0033	1.7
Classification								fgrCSaMSa					

From physical and hydrological point of view, SL can be recommended as substrate for VF CWs

5.2.3 Perlite

PE meets all requirements and recommendations concerning grain size distribution. It is classified as poorly graded pebbly sand. Therefore, porosity in a range of 0.28 and 0.35 can be expected. The measured porosity is within this range. The measured k-value is 2125 % higher than the calculated one and has a high standard deviation. This leads to a low reliability of results. Thus, for evaluation only the calculated k-value, which meets the requirements of ÖNORM B 2505 (1997) and DWA A 262 (2006), is considered (cf. Table 5.2-2).

When operated with tap water the column filled with PE had a low hydraulic capacity. With a uniform pore size distribution. The ratio of infiltration time and oxygen diffusion time of 1:1.2 means a high contact time and a low oxygen diffusion time. When operated with wastewater the hydraulic capacity was almost the same. During seven month, almost no change in pore size distribution occurred. The ratio of infiltration time and diffusion time changed slightly to 1:1.7. The infiltration conditions did almost not change (cf. Figure 4.4-2).

The calculated HRT of PE amounts to 2.3 days. This is 26 % higher than the measured HRT.

Table 5.2-2: Results PE

Bulk density		Particle density		Porosity		Grading curves (ava. values)					k-value		HRT
Average	Standard deviation	Average	Standard deviation	Average	Standard deviation	d ₁₀	d ₃₀	d ₆₀	C _u	C _c	Average	Standard deviation	
[g/cm ³]	[-]	[g/cm ³]	[-]	[g/cm ³]	[-]	[mm]	[mm]	[mm]	[-]	[-]	[m/s]	[-]	[d]
1.5237	0.0044	2.1930	0.0138	0.3052	0.0058	0.23	0.54	1.02	4.47	1.25	0.0085	0.0017	1.7
Classification								fgrCSaMSa					

From physical and hydrological point of view, PE can be recommended as substrate for VF CWs.

5.2.4 Pumice

PU meets all requirements and recommendations concerning grain size distribution. It is classified as poorly graded pebbly sand. Therefore, porosity in a range of 0.28 and 0.35 can be expected. The measured porosity is within this range. The measured k-value is 1375 % higher than the calculated one and has a high standard deviation. This leads to a low reliability of results. Thus, for evaluation only the calculated k-value, which meets the requirements of ÖNORM B 2505 (1997) and DWA A 262 (2006), is considered (cf. Table 5.2-3).

When operated with tap water the column filled with PU had a hydraulic capacity, which met the ideal compromise between infiltration time and diffusion time. The pore size distribution was not uniform. The ratio of infiltration time and oxygen diffusion time was 1:2.4. When operated with wastewater the hydraulic capacity did not change. During seven month, particle displacement occurred and pore size distribution became more regular (cf. Figure 4.4-3).

The calculated HRT of PU amounts to 2.6 days. This is 50 % higher than the measured HRT.

Table 5.2-3: Results PU

Bulk density		Particle density		Porosity		Grading curves (ava. values)					k-value		HRT
Average	Standard deviation	Average	Standard deviation	Average	Standard deviation	d ₁₀	d ₃₀	d ₆₀	C _u	C _c	Average	Standard deviation	
[g/cm ³]	[-]	[g/cm ³]	[-]	[g/cm ³]	[-]	[mm]	[mm]	[mm]	[-]	[-]	[m/s]	[-]	[d]
1.3837	0.0222	2.1123	0.0206	0.3449	0.0121	0.17	0.33	0.69	3.93	0.90	0.0055	0.0006	1.3
Classification								fgrMSaCSa					

From physical and hydrological point of view, PU can be recommended as substrate for VF CWs.

5.2.5 Turkish Sand

TS is classified as pebbly sand and meets all recommendations of PLATZER (1997). Concerning d_{10} TS meets the requirements of DWA A 262 (2006) and ATV A 262 (1997). Concerning C_u the value is above the required range. Concerning C_c the requirements are met, thus TS can be classified as poorly graded. Due to classification a porosity in arrange of 0.28 and 0.35 can be expected. The measured porosity of TS is 3 % above this range. The measured k-value is 1525 % higher than the calculated one and has a high standard deviation. This leads to a low reliability of results. Thus, for evaluation only the calculated k-value, which meets the requirements of ÖNORM B 2505 (1997) and DWA A 262 (2006), is considered (cf. Table 5.2-4).

When operated with tap water the column filled with TS had a hydraulic capacity, which almost met the ideal compromise between infiltration time and diffusion time. The pore size distribution was not uniform. The ratio of infiltration time and oxygen diffusion time was 1:1.9. When operated with wastewater the hydraulic capacity increased slightly. During seven month, particle displacement occurred and more coarse pores developed. The ratio of infiltration time and diffusion time changed to 1:2.1. Diffusion time is more than two times longer than infiltration time (cf. Figure 4.4-4).

The calculated HRT of TS amounts to 2.6 days. This is 8 % lower than the measured HRT.

Table 5.2-4: Results TS

Bulk density		Particle density		Porosity		Grading curves (ava. values)					k-value		HRT
Average	Standard deviation	Average	Standard deviation	Average	Standard deviation	d_{10}	d_{30}	d_{60}	C_u	C_c	Average	Standard deviation	
[g/cm ³]	[-]	[g/cm ³]	[-]	[g/cm ³]	[-]	[mm]	[mm]	[mm]	[-]	[-]	[m/s]	[-]	
1.7179	0.0275	2.6903	0.0351	0.3614	0.0055	0.23	0.58	1.38	6.08	1.07	0.0066	0.0013	2.8
						Classification		fgrMSaCSa					

From physical and hydrological point of view, TS can be recommended as substrate for VF CWs.

5.2.6 Turkish Zeolite

TZ is classified as poorly graded pebbly sand and meets all requirements of ATV A 262 (1997). Concerning d_{10} neither the recommendations of PLATZER (1997) nor the requirements of DWA A 262 (2006) are met. The value of d_{10} is approximately twice as high. Due to classification porosity in a range of 0.28 and 0.35 can be expected. The measured porosity of TZ is 49 % higher. The measured k-value is 250 % higher than the calculated one and has a high standard deviation. This leads to a low reliability of results. Thus, for evaluation only the calculated k-value, which meets the requirements of ÖNORM B 2505 (1997) and DWA A 262 (2006), is considered (cf. Table 5.2-5).

When operated with tap water the column filled with TZ had hydraulic capacity, which met the ideal compromise between infiltration time and diffusion time. The pore size distribution was not uniform. The ratio of infiltration time and oxygen diffusion time was 1:2.8. The coarse pores are dewatered quickly. When operated with wastewater the hydraulic capacity increased notably. During seven month, particle displacement occurred and fingers were developed. The ratio of infiltration time and diffusion time changed to 1:9.3. Diffusion time is more than nine times longer than infiltration time and contact time is very short (cf. Figure 4.4-5).

The calculated HRT of TZ amounts to 3.9 days. This is 67 % higher than the measured HRT.

Table 5.2-5: Results TZ

Bulk density		Particle density		Porosity		Grading curves (ava. values)					k-value		HRT
Average	Standard deviation	Average	Standard deviation	Average	Standard deviation	d_{10}	d_{30}	d_{60}	C_u	C_c	Average	Standard deviation	
[g/cm ³]	[-]	[g/cm ³]	[-]	[g/cm ³]	[-]	[mm]	[mm]	[mm]	[-]	[-]	[m/s]	[-]	[d]
0.8907	0.0028	1.8723	0.0846	0.5243	0.0203	0.80	1.31	2.22	2.78	0.97	0.0162	0.0024	1.3
						Classification		CSaFGr					

The high effective grain diameter corresponds with the development of short circuit flow, TZ cannot be recommended as substrate for VF CWs.

5.2.7 Crushed concrete

BE is classified as pebbly sand and meets all recommendations of PLATZER (1997). Concerning d_{10} BE meets the requirements of DWA A 262 (2006) and ATV A 262 (1997). Concerning C_u the value is above the required range. Concerning C_c the requirements are met, thus BE can be classified as poorly graded. Due to classification porosity in a range of 0.28 and 0.35 can be expected. The measured porosity of BE is 34 % higher. The measured k-value is 2300 % higher than the calculated one and has a high standard deviation. This leads to a low reliability of results. Thus, for evaluation only the calculated k-value, which meets the requirements of ÖNORM B 2505 (1997) and DWA A 262 (2006), is considered (cf. Table 5.2-6).

When operated with tap water the column filled with BE had a hydraulic capacity, which met the ideal compromise between infiltration time and diffusion time. The pore size distribution was not uniform. The ratio of infiltration time and oxygen diffusion time was 1:2.1. The coarse pores are dewatered quickly. When operated with wastewater the hydraulic capacity decreased notably. During seven month, particle displacement occurred. The infiltration was uniform. This indicates a uniform pore size distribution. The ratio of infiltration time and diffusion time changed to 1:1.2. Diffusion time equals almost infiltration time (cf. Figure 4.4-6).

The calculated HRT of BE amounts to 3.8 days. This is 6 % lower than the measured HRT. The result of HRT measurement is extremely falsified by solution processes.

Table 5.2-6: Results BE

Bulk density		Particle density		Porosity		Grading curves (ava. values)					k-value		HRT
Average	Standard deviation	Average	Standard deviation	Average	Standard deviation	d_{10}	d_{30}	d_{60}	C_u	C_c	Average	Standard deviation	
[g/cm ³]	[-]	[g/cm ³]	[-]	[g/cm ³]	[-]	[mm]	[mm]	[mm]	[-]	[-]	[m/s]	[-]	
1.5605	0.0223	2.9614	0.8147	0.4730	0.1377	0.18	0.42	1.35	7.38	0.70	0.0093	0.0008	3.7
Classification								fgrMSaCSa					

Due to the notably decrease of hydraulic capacity within seven month of operating, which leads to clogging, in the case of continuous development, BE cannot be recommended as substrate for VF CWs. Additionally, the chemical composition of BE indicates a high risk of recontamination of water.

5.2.8 Ferro-Sorp©

FE fulfils all requirements and recommendations concerning grain size distribution. It is classified as poorly graded pebbly sand. Therefore, porosity in a range of 0.28 and 0.35 can be expected. The measured porosity of FE is 106 % higher. The measured k-value is 1580 % higher than the calculated one and has a high standard deviation. This leads to a low reliability of results. Thus, for evaluation only the calculated k-value, which meets the requirements of ÖNORM B 2505 (1997) and DWA A 262 (2006), is considered (cf. Table 5.2-7).

When operated with tap water the column filled with FE had a low hydraulic capacity. The pore size distribution was uniform. The ratio of infiltration time and oxygen diffusion time was 1:1.1. When operated with wastewater the hydraulic capacity decreased notably. During seven month, particle displacement occurred led to clogging (cf. Figure 4.4-7).

The calculated HRT of FE amounts to 5.3 days. This is 23 % higher than the measured HRT. The result of measured HRT is falsified by sorption processes.

Table 5.2-7: Results FE

Bulk density		Particle density		Porosity		Grading curves (ava. values)					k-value		HRT
Average	Standard deviation	Average	Standard deviation	Average	Standard deviation	d ₁₀	d ₃₀	d ₆₀	C _u	C _c	Average	Standard deviation	
[g/cm ³]	[-]	[g/cm ³]	[-]	[g/cm ³]	[-]	[mm]	[mm]	[mm]	[-]	[-]	[m/s]	[-]	
0.6856	0.0120	2.4044	0.4842	0.7149	0.0548	0.25	0.40	0.67	2.70	0.37	0.0063	0.0006	4.1
						Classification		fgrMSaFSa					

Although, FE fulfils the physical requirements, due to clogging, FE cannot be recommended as substrate for VF CWs.

5.2.9 Austrian Zeolite 1 (1.5-2.0 mm)

Because no more material was available, no sieve analysis was conducted. The porosity amounts to 0.56. Because of no material, k-value measurement was not possible (cf. Table 5.2-8).

When operated with tap water the column filled with AZ1 had a hydraulic capacity, which was slightly above the ideal compromise between infiltration time and diffusion time. The pore size distribution was not uniform. The ratio of infiltration time and oxygen diffusion time was 1:3.8. The coarse pores were dewatered quickly. When operated with wastewater the hydraulic capacity increased notably. During seven month, particle displacement occurred and fingers developed. The ratio of infiltration time and diffusion time changed to 1:5.6. Diffusion time is more than five times higher than infiltration time (cf. Figure 4.4-8).

The calculated HRT of AZ1 amounts to 4.0 days. This is 68 % higher than the measured HRT.

Table 5.2-8: Results AZ1

Bulk density		Particle density		Porosity		Grading curves (ava. values)					k-value		HRT
Average	Standard deviation	Average	Standard deviation	Average	Standard deviation	d ₁₀	d ₃₀	d ₆₀	C _u	C _c	Average	Standard deviation	
[g/cm ³]	[-]	[g/cm ³]	[-]	[g/cm ³]	[-]	[mm]	[mm]	[mm]	[-]	[-]	[m/s]	[-]	[d]
1.0419	0.0168	2.3821	0.4256	0.5626	0.0669	nsa	nsa	nsa	nsa	nsa	-	-	1.3
						Classification		nsa					

- No k-value

nsa No sieve analysis

Although AZ1 fulfils the physical requirements, however, due to the development of short circuit flow, AZ1 cannot be recommended as substrate for VF CWs.

5.2.10 Austrian Zeolite 2 (2.0-2.5 mm)

Because no more material was available, no sieve analysis was carried out. The porosity amounts to 0.51. The k-value of AZ2 amounts to 0.0464 m/s. A comparison is not possible because of no sieve analysis (cf. Table 5.2-9).

When operated with tap water the column filled with AZ2 had a hydraulic capacity, which was notably above the ideal compromise between infiltration time and diffusion time. The pore size distribution was not uniform. The ratio of infiltration time and oxygen diffusion time was 1:9.3. The coarse pores were dewatered quickly. When operated with wastewater the hydraulic capacity increased notably. During seven month, particle displacement occurred and fingers developed. The ratio of infiltration time and diffusion time changed to 1:23. Diffusion time is more than 23 times higher than infiltration time (cf. Figure 4.4-9).

The calculated HRT of AZ2 amounts to 3.9 days. This is 44 % higher than the measured HRT.

Table 5.2-9: Results AZ2

Bulk density		Particle density		Porosity		Grading curves (ava. values)					k-value		HRT
Average	Standard deviation	Average	Standard deviation	Average	Standard deviation	d ₁₀	d ₃₀	d ₆₀	C _u	C _c	Average	Standard deviation	
[g/cm ³]	[-]	[g/cm ³]	[-]	[g/cm ³]	[-]	[mm]	[mm]	[mm]	[-]	[-]	[m/s]	[-]	[d]
1.0119	0.0160	2.0751	0.0349	0.5123	0.0069	nsa	nsa	nsa	nsa	nsa	0.0464	0.0143	2.2
						Classification		nsa					

nsa No sieve analysis

Due to the development of short circuit flow, AZ2 cannot be recommended as substrate for VF CWs.

5.2.11 Austrian Sand

AS meets all requirements and recommendations concerning grain size distribution. It is classified as poorly graded pebbly sand. Therefore, porosity in a range of 0.28 and 0.35 can be expected. The measured porosity is within this range. The measured k-value is 337 % higher than the calculated one and has a high standard deviation. This leads to a low reliability of results. Thus, for evaluation only the calculated k-value, which meets the requirements of ÖNORM B 2505 (1997) and DWA A 262 (2006), is considered (cf. Table 5.2-10).

When operated with tap water the column filled with AS had hydraulic capacity, which is lower than the ideal compromise between infiltration time and diffusion time. The pore size distribution was not uniform. The ratio of infiltration time and oxygen diffusion time was 1:1.5. When operated with wastewater after decrease of effluent the curve shows a second peak which is an indication of reopening of preliminary clogged pores and the hydraulic capacity increased slightly. During seven month, particle displacement occurred and more coarse pores developed. The ratio of infiltration time and diffusion time changed to 1:1.9. Diffusion time is almost two times longer than infiltration time (cf. Figure 4.4-10).

The calculated HRT of AS amounts to 2.3 days. This is 26 % higher than the measured HRT.

Table 5.2-10: Results AS

Bulk density		Particle density		Porosity		Grading curves (ava. values)					k-value		HRT
Average	Standard deviation	Average	Standard deviation	Average	Standard deviation	d ₁₀	d ₃₀	d ₆₀	C _u	C _c	Average	Standard deviation	
[g/cm ³]	[-]	[g/cm ³]	[-]	[g/cm ³]	[-]	[mm]	[mm]	[mm]	[-]	[-]	[m/s]	[-]	[d]
1.7860	0.0172	2.5762	0.0597	0.3067	0.0212	0.26	0.59	1.11	4.22	1.18	0.0030	0.0002	1.7
Classification								fgrCSaMSa					

From physical and hydrological point of view AS can be recommended as substrate for VF CWs.

5.2.12 Ferro-Sorp© + Turkish Zeolite

Because no more material was available, no sieve analysis was carried out. The porosity amounts to 0.70. The k-value of FE+TZ amounts to 0.0156 m/s. A comparison is not possible because of any sieve analysis (cf. Table 5.2-11).

When operated with tap water the column filled with FE+TZ had a low hydraulic capacity. Infiltration time almost equals diffusion time. The pore size distribution was not uniform. The ratio of infiltration time and oxygen diffusion time was 1:1.1. When operated with wastewater the hydraulic capacity increased. During seven month, particle displacement occurred and more coarse pores developed. The ratio of infiltration time and diffusion time changed to 1:2.1. Diffusion time is more than two times longer than infiltration time (cf. Figure 4.4-11).

The calculated HRT of FE+TZ amounts to 5.3 days. This is 58 % higher than the measured HRT.

Table 5.2-11: Results FE+TZ

Bulk density		Particle density		Porosity		Grading curves (ava. values)					k-value		HRT
Average	Standard deviation	Average	Standard deviation	Average	Standard deviation	d ₁₀	d ₃₀	d ₆₀	C _u	C _c	Average	Standard deviation	
[g/cm ³]	[-]	[g/cm ³]	[-]	[g/cm ³]	[-]	[mm]	[mm]	[mm]	[-]	[-]	[m/s]	[-]	[d]
0.8116	0.0041	2.6848	0.0785	0.6977	0.0075	nsa	nsa	nsa	nsa	nsa	0.0156	0.0027	2.2
						Classification		Nsa					

nsa No sieve analysis

From physical and hydrological point of view, FE+TZ can be recommended as substrate for VF CWs.

5.2.13 Mixtures

Because no more material was available, no sieve analysis was carried out. Porosity amounts to 0.50. The k-value of FE+TZ amounts to 0.0126 m/s. A comparison is not possible because of no sieve analysis (cf. Table 5.2-12).

When operated with tap water the column filled with MX and a height of filter of 30 cm, had a low hydraulic capacity with a uniform pore size distribution. The ratio of infiltration time and oxygen diffusion time of 1:1.9 means a low contact time and a high oxygen diffusion time. When operated with wastewater the hydraulic capacity increased notably. During seven month, particle displacement occurred fingers developed. The ratio of infiltration time and diffusion time changed to 1:5.6. That means a fast dewatering of coarse pores. The oxygen diffusion time is more than five times higher than the contact time. The uniformity of pore size distribution and effluent of mixtures increased with increasing filter height. Similarly, the hydraulic capacity decreased (cf. Figure 4.4-12, Figure 4.4-13, and Figure 4.4-14)

The calculated HRT of MX 30 amounts to 2.4 days. This is 50 % higher than the measured HRT. The calculated HRT increased with increasing height of the filter as well as the difference between measured HRT and calculated HRT did.

Table 5.2-12: Results MX 30, MX 50, MX 75

Bulk density		Particle density		Porosity		Grading curves (ava. value)					k-value		HRT		
Average	Standard deviation	Average	Standard deviation	Average	Standard deviation	d ₁₀	d ₃₀	d ₆₀	C _u	C _c	Average	Standard deviation	MX 30	MX 50	MX 75
[g/cm ³]	[-]	[g/cm ³]	[-]	[g/cm ³]	[-]	[mm]	[mm]	[mm]	[-]	[-]	[m/s]	[-]	[d]	[d]	[d]
1.2649	0.0222	2.4762	0.0186	0.4892	0.0124	nsa	Nsa	nsa	nsa	nsa	0.0126	0.0006	1.2	1.3	1.4
						Classification		nsa							

nsa No sieve analysis

Due to the fact, that mixtures include BE, from the chemical point of view mixtures cannot be recommended as substrate for VF CWs.

6 Summary

VSSF CWs are used for removal of organic matter, total suspended solids, nutrients and microbiological contaminations. Although, VSSF CWs with intermittent loading are state-of-the art in Europe it is sometimes impossible to apply them in small to medium communities (<2000 PE), where land is valuable, because of their extensive surface requirement from 3 to 10 m² /PE (KORKUSUZ and LANGERGRABER, 2006). To enhance the capabilities of VSSF CWs concerning surface requirement and nutrient removal the project called ONUREM was developed.

ONUREM was funded by the European Commission by a “Marie Curie Intra European Individual Fellowship” (Project No. 515515). In the framework of ONUREM, different natural and artificial materials, commercially available in Turkey and Austria, with potential application as substrates in VSSF CWs, were tested. The materials were provided from Turkey (slag, perlite, pumice, sand and zeolite) and Austria (crushed concrete, Ferro-Sorp®, zeolite in two grain sizes and sand). Moreover a mixture of all materials in equal parts and one of Ferro-Sorp® and Turkish zeolite half-and-half was composed.

The main objectives of the ONUREM project were:

- Quantification of the effect of different materials mentioned above on the removal performance of organic matter and nutrients in a lab-scale VSSF CWs.
- Development of a catalogue of materials suitable as filter materials including a database of their hydraulic, physical, and chemical characteristics and their transport parameters.

Within the framework of ONUREM, the diploma thesis was carried out. The objectives of the diploma thesis were the analysis and evaluation of physical and hydrological characteristics of the single materials and the compositions mentioned above in terms of application in VSSF CWs.

Analysed physical characteristics:

- Grading curve
- Particle density
- Bulk density

Analysed hydrological characteristics:

- Hydraulic conductivity
- Hydraulic retention time (HRT)
- Hydraulic load rate (HLR)
- Hydrograph and cumulative effluent

For the determination of these characteristics, the following experiments were conducted:

- Sieve analysis (grading curves)
- Pycnometer experiment (particle density, bulk density)
- Determination of permeability (k-value)
- Lab-scale column experiment (HLR, hydrographs, summation curves)
- Tracer experiments at the lab-scale column experiment (HRT)

Comments on used methods where problems occurred:

Sieve analysis

Sieve analysis were not conducted as wet sieving. This could lead to residuals of smallest particles and dust which are not taken in account at analysis but they could affect permeability. Wet sieving is recommended.

To see, if sample size has an influence on results, sieve analysis were conducted with different sample sizes of 450 g and 1000 g. It has been shown that this is not necessary. On the one hand, the differences were very small and on the other hand, at DIN 18123 (1996), a minimum sample size, based on the maximum grain size, is defined to insure comparability of results.

Pycnometer experiments

Particle density measurements leaded to results with a high standard deviation. If air remains within the pores during weighing, the filter material is not saturated with water and the results are falsified. This had an influence on the results of calculated porosities. A possibility to prevent falsification of the results of particle density measurements could be the introduction of a settling time between repeated shakings of Pycnometer to deaerate the material more effectively.

k-value measurement

At materials where a comparison between measured and calculated k-values was possible it was attracting attention that at any single filter material the measured values were higher than the calculated ones. The reason was that at the contact area between the stiff PVC-pipe of the measurement device and the filter material the porosity was enhanced. This led to an intensified flow along the contact area and to a higher measured permeability with a high standard deviation. This effect would not occur if the filter material within the pipe would be welted by an elastic membrane and supported by external pressure. Additionally, the filter material became loosened by ubstreaming water, which leaded to a higher measured k-value, too. Thus, it seems reasonable to substitute measurements by calculation based on d_{10} as it is suggested at DWA A 262 (2006).

Column experiments

During the column experiment, due to particle content of municipal wastewater and insufficient sedimentation and particle separation by sieving, clogging within the used silicon pipes occurred. This effect was intensified by MO growth. The diaphanous silicon pipes in combination with a high nutrient amount provided very good living conditions for them. Therefore, concerning loading volume, it was difficult to keep up steady experiment condition. Thus, an advanced particle separation is necessary and the use of lightproof silicon pipes would be better. The fact that at the contact area between the stiff PVC-pipe and the filter material, the porosity is enhanced could lead to an intensified flow along the contact area and to falsification of infiltration conditions. This effect would not occur if the filter material within the pipe is welted by an elastic membrane and supported by external pressure.

Summary of investigations of filter materials

With AZ1 and AZ2, no sieve analysis was done because of the uniformity of grain sizes. The grain size of AZ1 ranged from 1.5 to 2.0 mm. The grain size of AZ2 ranged from 2.0 to 2.5 mm. The grading curve of MX equals the average of its components and no significant change due to the mix of single materials was expected. Thus, no sieve analysis was carried out with mixtures. With AZ1, no k-value measurement was conducted because no material was left (cf. Table 6-1).

Table 6-1: Summary of the measurements for all filter materials

	Pycnometer experiments			Sieve analysis					k-value	HRT	Column experiments		Special explanatory Notes	Rating
	Bulk density	Particle density	Porosity	d ₁₀	d ₃₀	d ₆₀	C _u	C _c			Ratio Inf.time Diff.time tap water.	Ratio Inf.time Diff.time Wastewater.		
	[g/cm ³]	[g/cm ³]	[-]	[mm]	[mm]	[mm]	[-]	[-]			[-]	[-]		
SL	1.0671	2.1718	0.5087	0.48	0.95	1.54	3.19	1.21	0.0146	1.7	1:1.3	1:4		+
PE	1.5237	2.1930	0.3052	0.23	0.54	1.02	4.47	1.25	0.0085	1.7	1:1.2	1:1.7		+
PU	1.3837	2.1123	0.3449	0.17	0.33	0.69	3.93	0.90	0.0055	1.3	1:2.4	1:2.4		+
TS	1.7179	2.6903	0.3614	0.23	0.58	1.38	6.08	1.07	0.0066	2.8	1:1.9	1:2.1		+
TZ	0.8907	1.8723	0.5243	0.80	1.31	2.22	2.78	0.97	0.0162	1.3	1:2.8	1:9.2	Short circuit flow	-
BE	1.5605	2.9614	0.4730	0.18	0.42	1.35	7.38	0.70	0.0093	3.7	1:2.1	1:1.2	Clogging	-*
FE	0.6856	2.4044	0.7149	0.25	0.40	0.67	2.70	0.37	0.0063	4.1	1:1.1	**	Clogging	-
AZ1	1.0419	2.3821	0.5626	n.m.	n.m.	n.m.	n.m.	n.m.	n.m.	1.3	1:3.8	1:5.6	Short circuit flow	-
AZ2	1.0119	2.0751	0.5123	n.m.	n.m.	n.m.	n.m.	n.m.	0.0464	2.2	1:9.3	1:23	Short circuit flow	-
AS	1.7860	2.5762	0.3067	0.26	0.59	1.11	4.22	1.18	0.0030	1.7	1:1.5	1:1.9		+
FE+TZ	0.8116	2.6848	0.6977	n.m.	n.m.	n.m.	n.m.	n.m.	0.0156	2.2	1:1.1	1:2.1		+
MX 30	1.2649	2.4762	0.4892	n.m.	n.m.	n.m.	n.m.	n.m.	0.0126	1.2	1:1.9	1:5.6	Short circuit flow	-*
MX 50	1.2649	2.4762	0.4892	n.m.	n.m.	n.m.	n.m.	n.m.	0.0126	1.3	1:1.2	1:1.2	Clogging	-*
MX 75	1.2649	2.4762	0.4892	n.m.	n.m.	n.m.	n.m.	n.m.	0.0126	1.4	1:1.1	1:0.6	Clogging	-*

n.m. No measurement

- Not recommendable due to hydrological characteristics

+ Recommendable

-* Not recommendable due to hydrological and chemical characteristics

** Not even minimum effluent was reached

From the physical and the hydrological point of view usable as filter material for the main layer of VF CWs are:

- Slag
- Perlite
- Pumice
- Turkish sand
- Austrian sand
- Ferro-Sorp©+Turkish zeolite

Not usable due to clogging are:

- Crushed concrete
- Ferro-Sorp©
- Mixtures with a filter height of 50 cm and 75 cm

Not usable due to development of short circuit flow are:

- Turkish zeolite
- Austrian zeolite 1 (1.5-2.0 mm)
- Austrian zeolite 2 (2.0-2.5 mm)
- Mixture with filter height of 30 cm

7 Indexes

7.1 References

- AKTIENGESELLSCHAFT FÜR STEININDUSTRIE, Companies website, Online on the Internet:
URL: http://www.agstein.de/bims_55.html [last visit 30.10.2010]
- ATV A 262 (1997): Grundsätze für Bemessung, Bau und Betrieb von Pflanzenbeeten für kommunales Abwasser bei Ausbaugrößen bis 1000 Einwohnerwerte, Deutschland
- BIEHL, R. (2009): Erd- und Grundbautechnische Aspekte beim Bau von Logistikhallen, Ingenieurgesellschaft Prof. Czurda und Partner mbH.
- BÖRNER, T. (1992): Einflussfaktoren für die Leistungsfähigkeit von Pflanzenkläranlagen, Schriftenreihe 58, Verein zur Förderung des Institutes für Wasserversorgung, Abwasserbeseitigung und Raumplanung der TH Darmstadt, 1992
- CEN ISO/TS 17892 – 4 (2004): Geotechnische Erkundung und Untersuchung – Laborversuche an Bodenproben – Teil 4: Bestimmung der Korngrößenverteilung, DIN Deutsches Institut für Normung e.V., Berlin
- CEN ISO/TS 17892-11 (2004): Geotechnische Erkundung und Untersuchung – Laborversuche an Bodenproben – Teil 11: Bestimmung der Durchlässigkeit mit konstanter und fallender Druckhöhe, DIN Deutsches Institut für Normung e.V., Berlin
- DIN 18123 (1996): Baugrund, Untersuchung von Bodenproben, Bestimmung der Korngrößenverteilung, DIN Deutsches Institut für Normung e.V., Berlin
- DIN 18124 (1997): Baugrund, Untersuchung von Bodenproben, Bestimmung der Korndichte, Kapillarpiknometer – Weithalspyknometer, DIN Deutsches Institut für Normung e.V., Berlin
- DWA A 262 (2006): Grundsätze für Bemessung, Bau und Betrieb von Pflanzenkläranlagen mit bepflanzten Bodenfiltern zur biologischen Reinigung kommunalen Abwassers, Deutsche Vereinigung für Wasserwirtschaft, Abwasser und Abfall e. V, Hennef
- ENLI MINING CORPORATION, Companies Website, Online on the Internet:
URL: <http://www.enli.com.tr/index.php?page=zeolite> [last visit 30.10.2010]
URL: <http://www.enli.com.tr/index.php?page=clinoptilolite> [last visit 30.10.2010]
- GELLER, G., HÖNER, G. (2003): Anwenderhandbuch Pflanzenkläranlagen, Praktisches Qualitätsmanagement bei Planung, Bau und Betrieb, Springer Verlag, Berlin Heidelberg
- GRÜBL, P., WEIGLER, H., KARL, S. (2001): Beton Arten, Herstellung und Eigenschaften, 2. Auflage, Verlag Ernst & Sohn, Berlin
- HEGO BIOTEC GMBH, Companies Website, Online on the Internet:
URL: <http://www.ferrosorp.de/deutsch/produkte/ferrosorpplus/index.html>
[last visit 30.11.2010]
- HÖTZEL, H., WERNER, A. (1992): Tracer Hydrology, A.A. Balkema, P.O. 1675 3000 BR Rotterdam, Netherlands
- KADLEC, R., H., KNIGHT, R., L. (1996): Treatment Wetlands, CRC Press, Inc., 2000 Corporate Blvd., N.W., Boca Raton, Florida 33431
- KÄSS, W., et al. (1992): Lehrbuch der Hydrogeologie, Band 9: Geohydrologische Markierungstechnik, Gebrüder Borntraeger, Berlin, Stuttgart

- KELLER, Th., HÅKANSON, I. (2010): Estimation of reference bulk density from soil particle size distribution and soil organic matter content. *Geoderma* Vol 154 Issues 3-4 pp 398-406
- KNAUF PERLITE GMBH, Companies Website, Online on the Internet:
URL: <http://www.knauf-perlite.de/industrie/rohperlit.html> [last visit 29.10.2010]
URL: <http://www.knauf-perlite.de/industrie/perlit.html> [last visit 29.10.2010]
- KOLYMBAS, D. (2007): *Geotechnik, Bodenmechanik, Grundbau und Tunnelbau*, 2. korrigierte und ergänzte Auflage, Springer Verlag, Berlin
- KORKUSUZ, E., A. (2004): Domestic wastewater treatment in pilot-scale constructed wetlands implemented in the Middle East Technical University, Department of Biotechnology, M
- KORKUSUZ, E., A., LANGERGRABER, G. (2006): ONUREM Project description paper, Investigation of special substrates to optimize nutrient removal in constructed wetlands, Institute of Sanitary Engineering and Water Pollution Control, BOKU – University of Natural Resources and Applied Life Sciences, Vienna, Muthgasse 18, A -1190 Vienna
- LABER, J. (2001): *Bepflanzte Bodenfilter zur weitergehenden Reinigung von Oberflächenwasser und Kläranlagenabläufe*, Wiener Mitteilungen, Band 167
- LECHER, K., et al. (2001): *Taschenbuch der Wasserwirtschaft*, 8. völlig neubearbeitete Auflage, Parey Buchverlag, Berlin
- MANIAK, U. (1997): *Hydrologie und Wasserwirtschaft, Eine Einführung für Ingenieure*, 4. überarbeitete und erweiterte Auflage, Springer Verlag, Berlin
- MÜLLER, I. (2010): Oral Information
- ÖNORM EN ISO 14688-1 (2002): *Geotechnische Untersuchung und Erkundung – Benennung, Beschreibung und Klassifizierung von Böden – Teil 1: Benennung und Beschreibung*, Österreichisches Normungsinstitut, Wien
- ÖNORM B 2505 (1997): *Vornorm: Bepflanzte Bodenfilter (Pflanzenkläranlagen) Anwendung, Bemessung, Bau und Betrieb*, Österreichisches Normungsinstitut, Wien
- PLATZER, C. (1997): *Entwicklung eines Bemessungsansatzes zur Stickstoffelimination in Pflanzenkläranlagen*, Dissertation TU Berlin, Eigenverlag, Eigenverlag
- POMZA EXPORT Ltd. co, Companies Website, Online on the Internet:
URL: <http://www.pomzaexport.com/en/> [last visit 30.10.2010]
- RÖSKE, I., UHLMANN, D. (2005): *Biologie der Wasser- und Abwasserbehandlung*, Verlag Eugen Ulmer, Stuttgart
- SCHUMANN, W. (2009): *Der große BLV Steine- und Mineralienführer*, BLV Buchverlag GmbH & Co. KG, München
- SMOLTCZYK, U., et al. (2001): *Grundbau – Taschenbuch, Teil 1: Geotechnische Grundlagen*, 6. Auflage, Verlag Ernst & Sohn, Berlin
- TAUSENDSCHÖN, M. (1998): *Evaluation of Subsurface Flow Hydraulic Characteristics of Constructed Wetlands for Treatment of Winery Effluent*, diploma thesis, Institute of Sanitary Engineering and Water Pollution Control, BOKU Vienna.
- TECHNISCHE HOCHSCHULE DARMSTADT, Project Website Baustoffkreislauf im Massivbau, Bericht zum Statusseminar Juni 1997 Teilprojekt A 03, Online on the Internet:
URL: <http://www.b-i-m.de/Berichte/A03/A03z0697.htm> [last visit 25.11.2010]

UNIVERSITÄT BREMEN, Institut für Umweltverfahrenstechnik, Online on the Internet:

URL: <http://www.wasser-wissen.de/abwasserlexikon/n/nitrifikation.htm>

[last visit 10.08.2011]

URL: <http://www.wasser-wissen.de/abwasserlexikon/d/denitrifikation.htm>

[last visit 10.08.2011]

ZEOLITH UMWELTTECHNIK GMBH, Companies Website, Online on the Internet:

URL: <http://www.deutsche-zeolith.de/images/FERROSORPGW.pdf>

[last visit 30.11.2010]

7.2 List of figures

Figure 2-1: Mechanisms of action of CWs	4
Figure 3.1-1: Slag	7
Figure 3.1-2: Perlite	8
Figure 3.1-3: Pumice	9
Figure 3.1-4: Turkish sand	10
Figure 3.1-5: Turkish zeolite	11
Figure 3.1-6: Crushed concrete	12
Figure 3.1-7: Ferro-Sorp©	13
Figure 3.1-8: Austrian zeolite 1	14
Figure 3.1-9: Austrian zeolite 2	14
Figure 3.1-10: Austrian sand	15
Figure 3.1-11: Ferro-Sorp© + Turkish zeolite	15
Figure 3.1-12: Mixture	16
Figure 3.2-1: Experimental set-up	17
Figure 3.2-2: Scheme of experimental set up	18
Figure 3.2-3: Peristaltic pump	19
Figure 3.2-4: Top view (inlet)	19
Figure 3.2-5: Interior view of a column	21
Figure 3.2-6: Bottom view (outlet)	21
Figure 3.3-1: Sieving machine	23
Figure 3.3-2: Recommended grain size distribution	26
Figure 3.3-3: Pycnometers	27
Figure 3.3-4: Desiccator	27
Figure 3.3-5: Scale, type Sartorius	27
Figure 3.3-6: Scheme of Darcy's experiment	31
Figure 3.3-7: Scheme of experimental set up	32
Figure 3.3-8: Device for k-value measurement	33
Figure 3.3-9: Columns; cups for effluent collection	36
Figure 3.3-10: Columns, silicon pipes and peristaltic pump	36
Figure 3.3-11: Collection of inflow	37
Figure 3.3-12: Impulse input and output function	39
Figure 3.3-13: Continuous input and output function	39
Figure 3.3-14: Conductivity meter WTW LF-196	40
Figure 3.3-15: Standard diagram conductivity	41

Figure 3.3-16: Application of tracer.....	41
Figure 3.3-17: Effluent measurement	42
Figure 3.3-18: Scheme of conductivity measurement of effluent.....	43
Figure 3.3-19: Data logger.....	43
Figure 3.3-20: Tracer raw data	44
Figure 3.3-21: Tracer median-data	45
Figure 3.3-22: Tracer mean-data.....	45
Figure 3.3-23: Correction of tracer median-data	46
Figure: 3.3-24: Corrected tracer mean-data.....	46
Figure 3.3-25: Cumulative conductivity.....	47
Figure 4.1-1: Grading curve SL vs. Platzer.....	49
Figure 4.1-2: Grading curve PE vs. Platzer.....	51
Figure 4.1-3: Grading curve PU vs. Platzer	53
Figure 4.1-4: Grading curve TS vs. Platzer.....	55
Figure 4.1-5: Grading curve TZ vs. Platzer.....	57
Figure 4.1-6: Grading curve BE vs. Platzer.....	59
Figure 4.1-7: Grading curve FE vs. Platzer.....	61
Figure 4.1-8: Grading curve AS vs. Platzer.....	63
Figure 4.1-9: Grading curves of all analysed materials	65
Figure 4.2-1: Particle density all materials	67
Figure 4.2-2: Bulk density all materials	69
Figure 4.2-3: Porosity all materials	71
Figure 4.3-1: k-values all materials.....	73
Figure 4.4-1: Hydrographs and cumulative effluent SL	76
Figure 4.4-2: Hydrographs and cumulative effluent PE.....	77
Figure 4.4-3: Hydrographs and cumulative effluent PU.....	78
Figure 4.4-4: Hydrographs and cumulative effluent TS.....	79
Figure 4.4-5: Hydrographs and cumulative effluent TZ	80
Figure 4.4-6: Hydrographs and cumulative effluent BE.....	81
Figure 4.4-7: Hydrographs and cumulative effluent FE	82
Figure 4.4-8: Hydrographs and cumulative effluent AZ1	83
Figure 4.4-9: Hydrographs and cumulative effluent AZ2.....	84
Figure 4.4-10: Hydrographs and cumulative effluent AS.....	85
Figure 4.4-11: Hydrographs and cumulative effluent FE+TZ.....	86
Figure 4.4-12: Hydrographs and cumulative effluent MX 30	87
Figure 4.4-13: Hydrographs and cumulative effluent MX 50	88

Figure 4.4-14: Hydrographs and cumulative effluent MX 75	89
Figure 4.5-1: Measured vs. calculated HRT.....	92
Figure 8-1: Determination of the HRT for the SL column	120
Figure 8-2: Determination of the HRT for the PU column.....	120
Figure 8-3: Determination of the HRT for the PU column.....	121
Figure 8-4: Determination of the HRT for the TS column	121
Figure 8-5: Determination of the HRT for the TZ columns	122
Figure 8-6: Determination of the HRT for the BE column.....	122
Figure 8-7: Determination of the HRT for the FE column.....	123
Figure 8-8: Determination of the HRT for the AZ1 column	123
Figure 8-9: Determination of the HRT for the AZ2 column	124
Figure 8-10: Determination of the HRT for the AS column.....	124
Figure 8-11: Determination of the HRT for the FE+TZ column.....	125
Figure 8-12: Determination of the HRT for the MX 30 column	125
Figure 8-13: Determination of the HRT for the MX 50 column	126
Figure 8-14: Determination of the HRT for the MX 75 column	126

7.3 List of tables

Table 3.1-1: Composition of SL	7
Table 3.1-2: Composition of PE	8
Table 3.1-3: Composition of PU	9
Table 3.1-4: Composition of TZ	11
Table 3.2-1: Characteristics of the columns	20
Table 3.3-1: Operating schedule	22
Table 3.3-2: Soil classification	26
Table 3.3-3: Pairs of value of the standard diagram	40
Table 4.1-1: Classification SL	49
Table 4.1-2: Measured parameters SL	50
Table 4.1-3: Comparison of SL parameters with recommendations and standards	50
Table 4.1-4: Classification PE	51
Table 4.1-5: Measured parameters PE	52
Table 4.1-6: Comparison of PE parameters with recommendations and standards	52
Table 4.1-7: Classification PU	53
Table 4.1-8: Measured parameters PU	54
Table 4.1-9: Comparison of PU parameters with recommendations and standards	54
Table 4.1-10: Classification TS	55
Table 4.1-11: Measured parameters TS	56
Table 4.1-12: Comparison of TS parameters with recommendations and standards	56
Table 4.1-13: Classification TZ	57
Table 4.1-14: Measured parameters TZ	58
Table 4.1-15: Comparison of TZ parameters with recommendations and standards	58
Table 4.1-16: Classification BE	59
Table 4.1-17: Measured parameters BE	60
Table 4.1-18: Comparison of BE parameters with recommendations and standards	60
Table 4.1-19: Classification FE	61
Table 4.1-20: Measured parameters FE	62
Table 4.1-21: Comparison of FE parameters with recommendations and standards	62
Table 4.1-22: Classification AS	63
Table 4.1-23: Measured parameters AS	64
Table 4.1-24: Comparison of AS parameters with recommendations and standards	64
Table 4.2-1: Results Pycnometer experiments all materials	66
Table 4.2-2: Expected porosity	66

Table 4.2-3: Particle density of all filter materials.....	67
Table 4.2-4: Bulk density of all filter materials.....	69
Table 4.2-5: Measured porosity of all filter materials.....	71
Table 4.2-6: Comparison of measured and expected porosity	72
Table 4.3-1: k-values of all filter materials.....	73
Table 4.3-2: Comparison of measured and calculated k-values.....	74
Table 4.4-1: Summary hydrographs and cumulative effluent SL.....	76
Table 4.4-2: Summary hydrographs and cumulative effluent PE	77
Table 4.4-3: Summary hydrographs and cumulative effluent PU	78
Table 4.4-4: Summary hydrographs and cumulative effluent TS.....	79
Table 4.4-5: Summary hydrographs and cumulative effluent TZ.....	80
Table 4.4-6: Summary hydrographs and cumulative effluent BE	81
Table 4.4-7: Summary hydrographs and cumulative effluent FE.....	82
Table 4.4-8: Summary hydrographs and cumulative effluent AZ1	83
Table 4.4-9: Summary hydrographs and cumulative effluent AZ2.....	84
Table 4.4-10: Summary hydrographs and cumulative effluent AS	85
Table 4.4-11: Summary hydrographs and cumulative effluent FE+TZ	86
Table 4.4-12: Summary hydrographs and cumulative effluent MX 30.....	87
Table 4.4-13: Summary hydrographs and cumulative effluent MX 50.....	88
Table 4.4-14: Summary hydrographs and cumulative effluent MX 75.....	89
Table 4.5-1: Measured HRT	90
Table 4.5-2: Results of calculated HRT	91
Table 5.2-1: Results SL.....	96
Table 5.2-2: Results PE.....	97
Table 5.2-3: Results PU	98
Table 5.2-4: Results TS.....	99
Table 5.2-5: Results TZ.....	100
Table 5.2-6: Results BE.....	101
Table 5.2-7: Results FE.....	102
Table 5.2-8: Results AZ1	103
Table 5.2-9: Results AZ2.....	104
Table 5.2-10: Results AS.....	105
Table 5.2-11: Results FE+TZ	106
Table 5.2-12: Results MX 30, MX 50, MX 75.....	107
Table 6-1: Summary of the measurements for all filter materials	110

8 Appendix

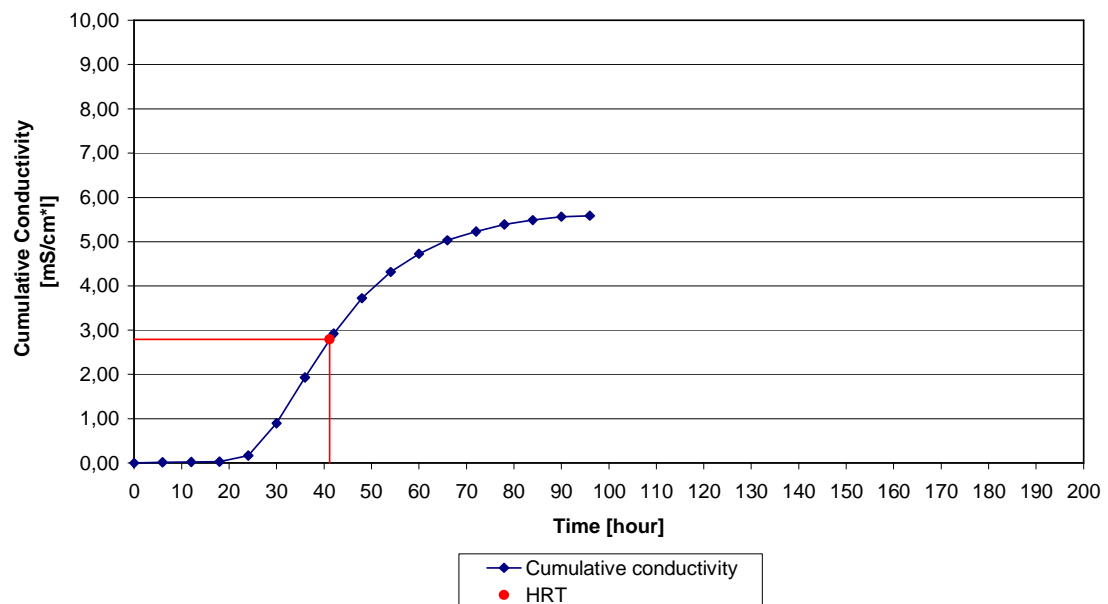


Figure 8-1: Determination of the HRT for the SL column

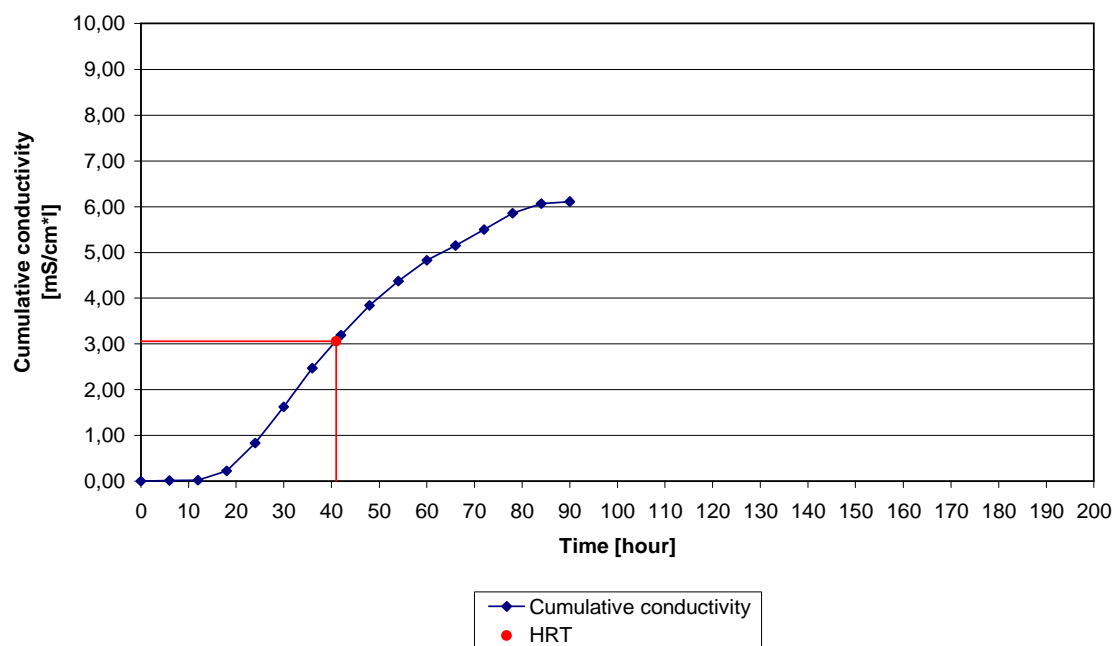


Figure 8-2: Determination of the HRT for the PU column

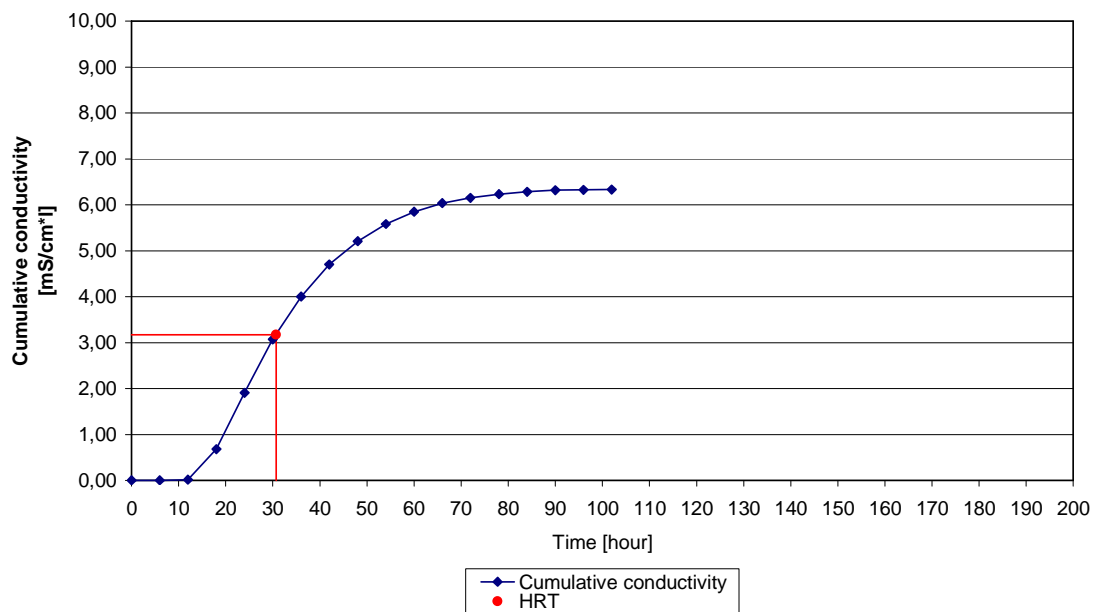


Figure 8-3: Determination of the HRT for the PU column

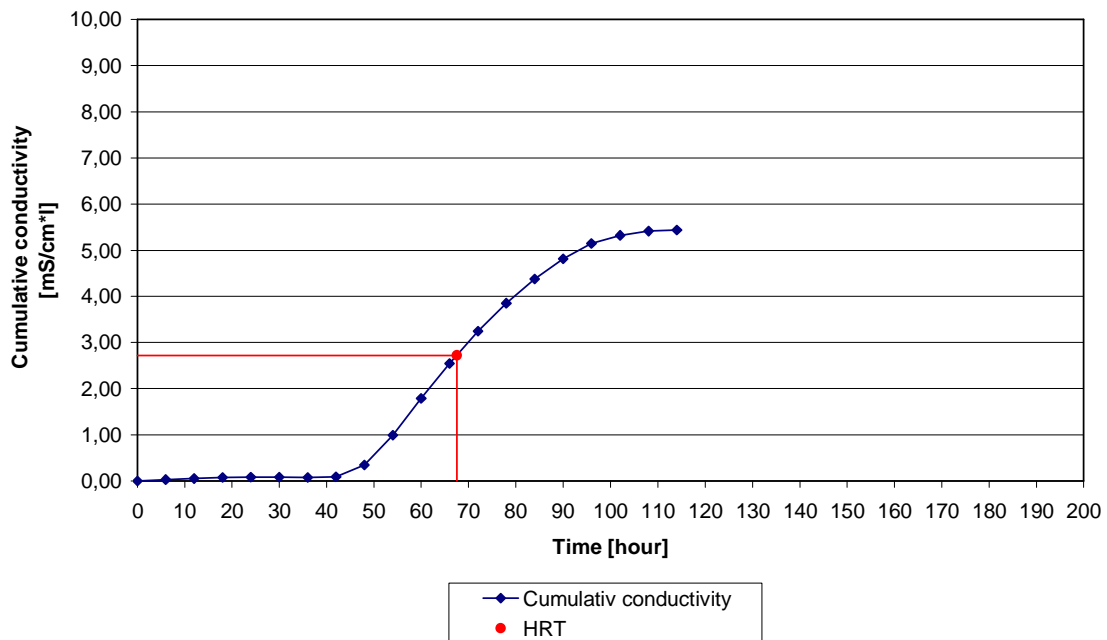


Figure 8-4: Determination of the HRT for the TS column

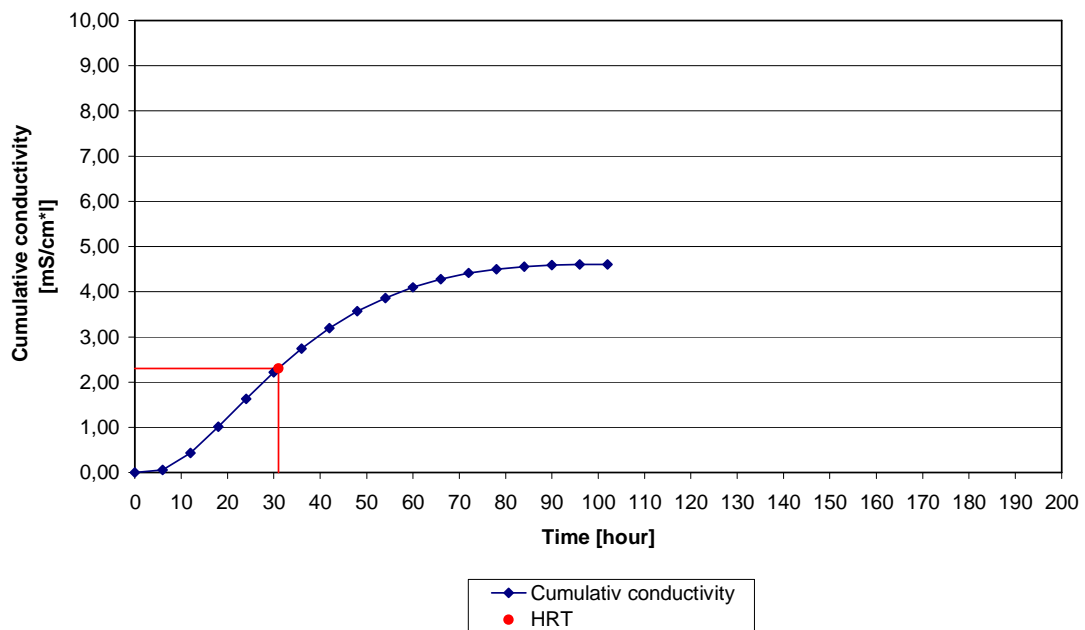


Figure 8-5: Determination of the HRT for the TZ columns

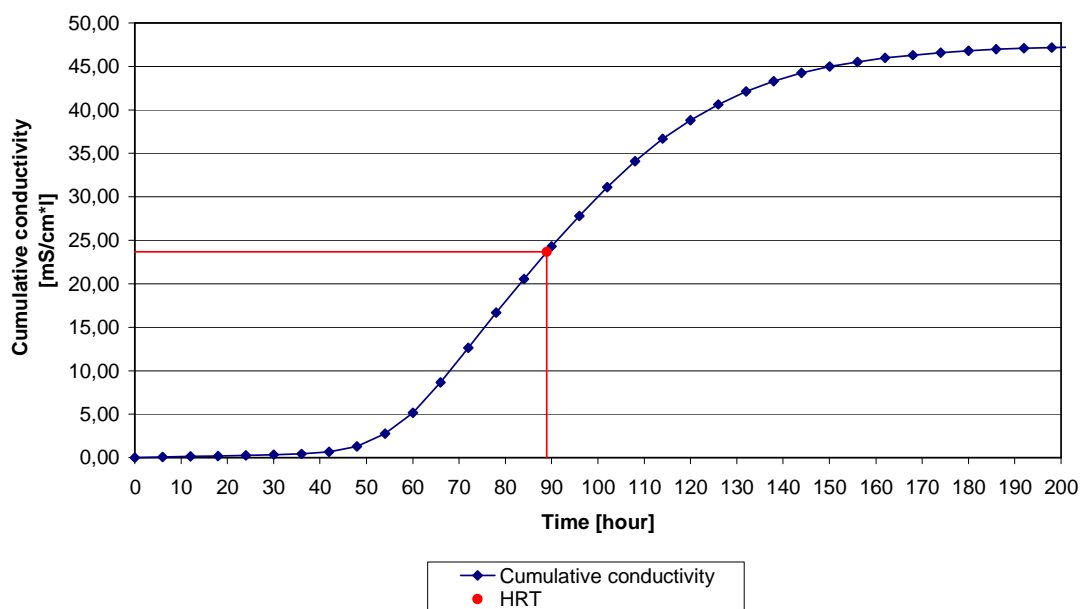


Figure 8-6: Determination of the HRT for the BE column

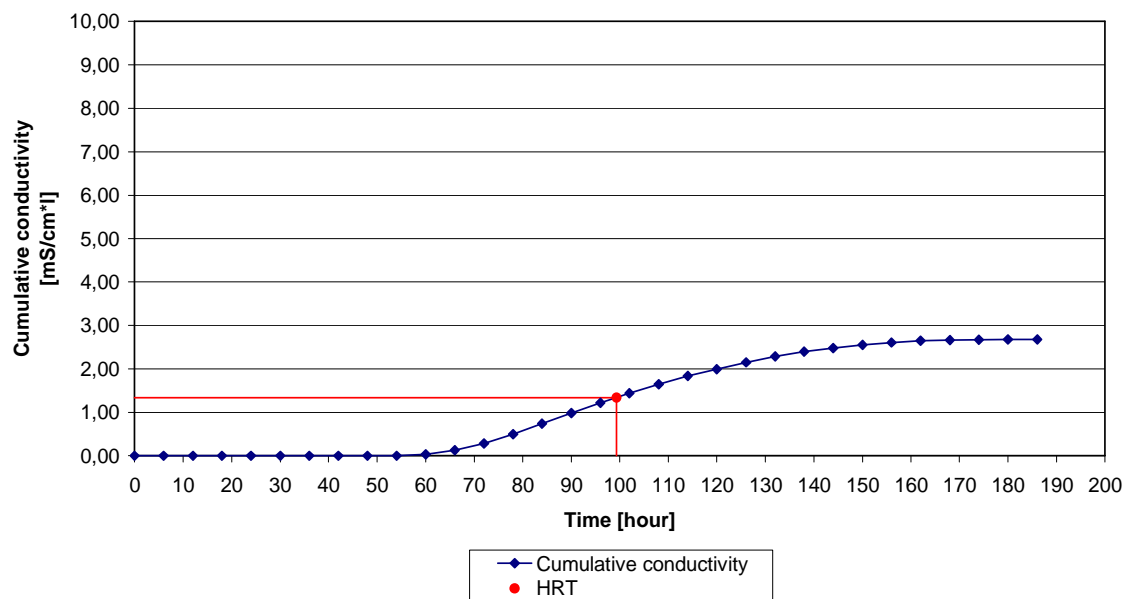


Figure 8-7: Determination of the HRT for the FE column

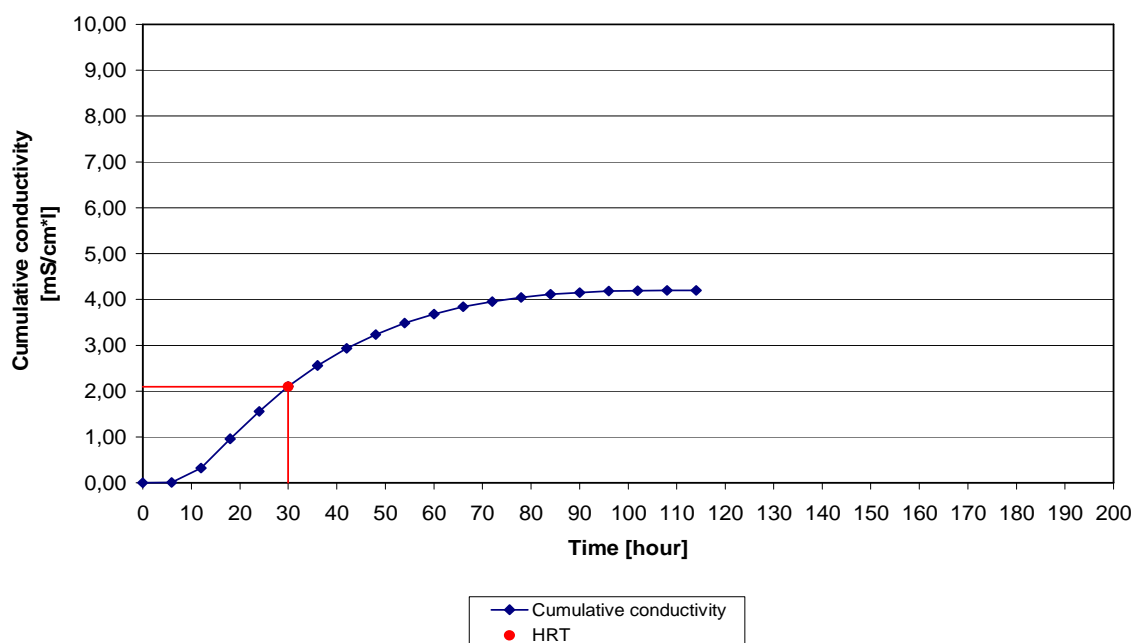


Figure 8-8: Determination of the HRT for the AZ1 column

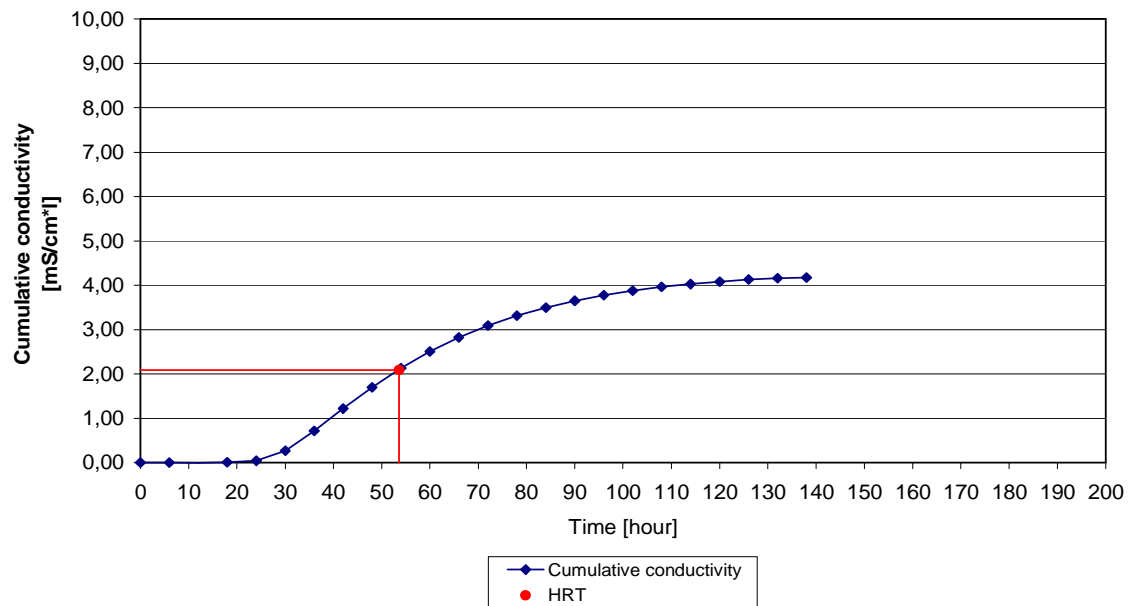


Figure 8-9: Determination of the HRT for the AZ2 column

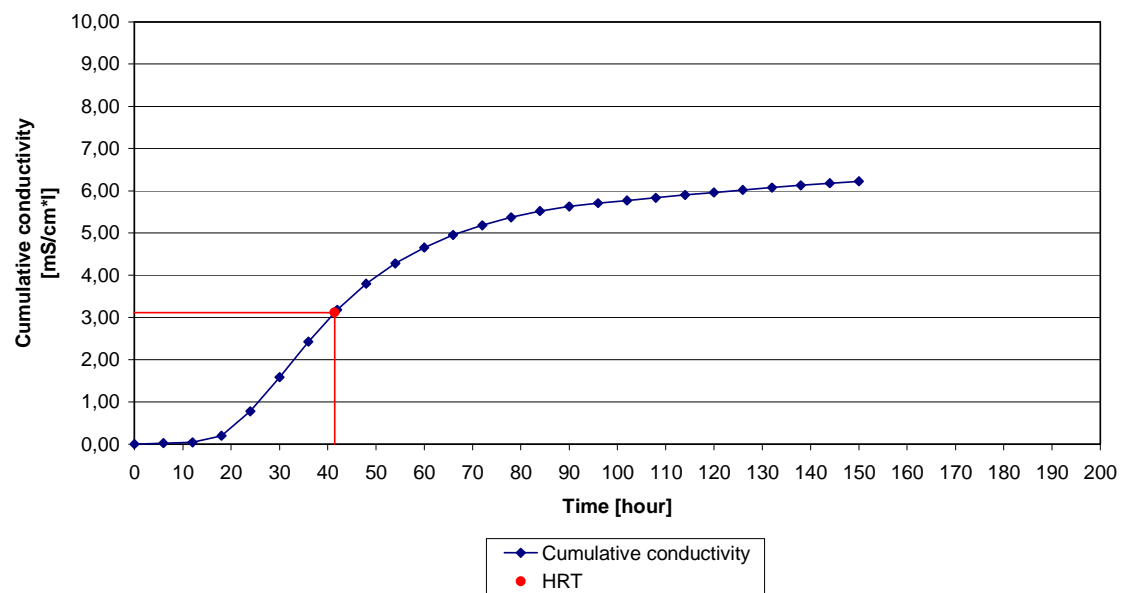


Figure 8-10: Determination of the HRT for the AS column

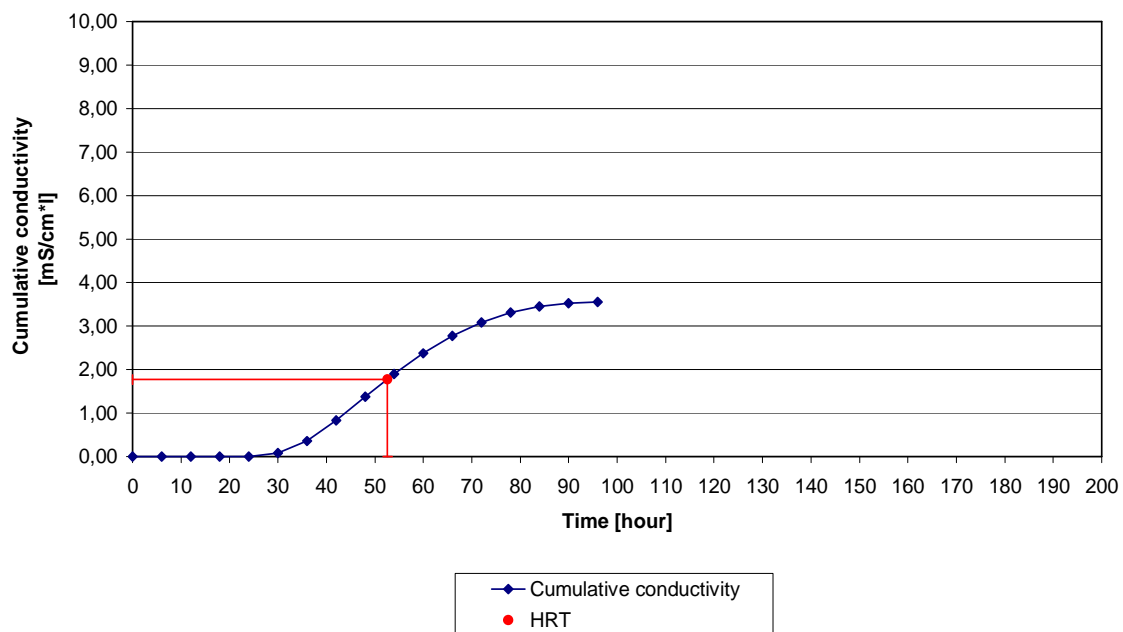


Figure 8-11: Determination of the HRT for the FE+TZ column

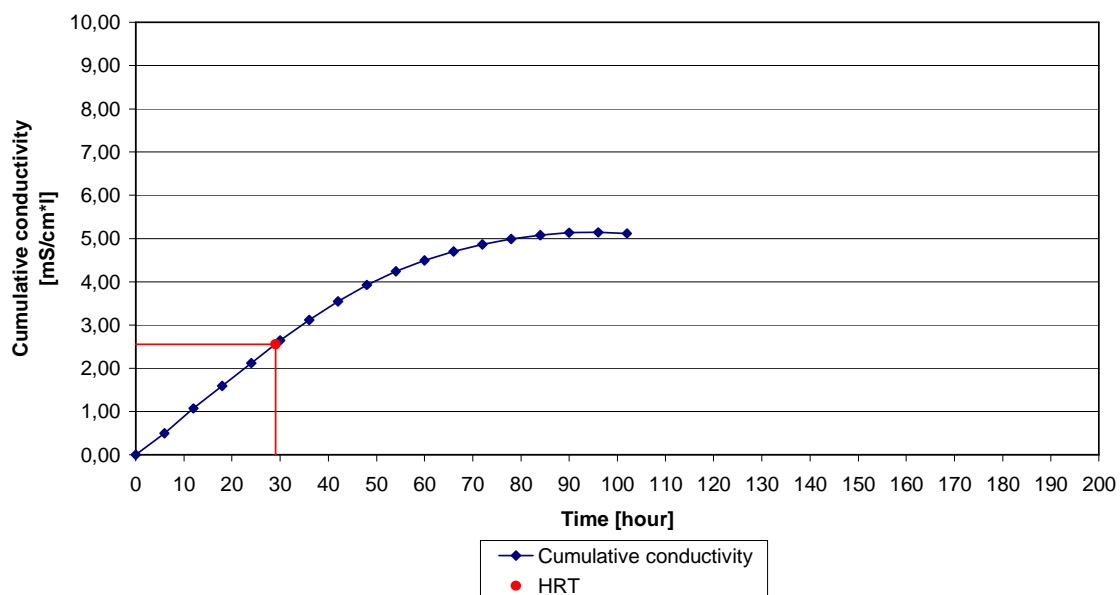


Figure 8-12: Determination of the HRT for the MX 30 column

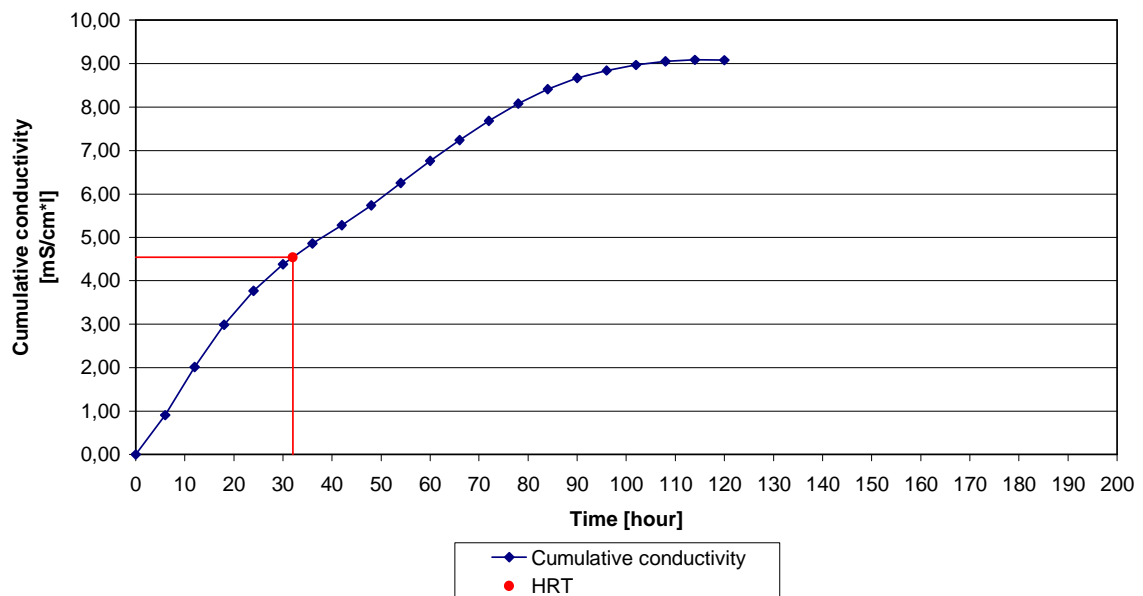


Figure 8-13: Determination of the HRT for the MX 50 column

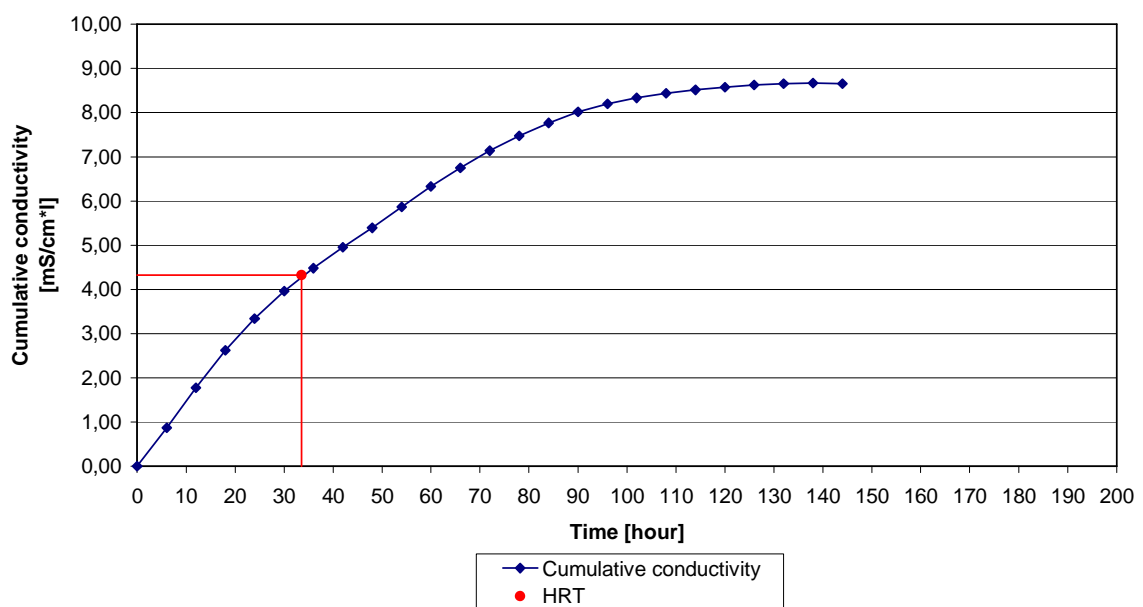


Figure 8-14: Determination of the HRT for the MX 75 column

9 Curriculum vitae

Personal data

Date of birth: 14.10.1970
Birthplace: Bruck an der Mur
Family status: Unmarried



History

Since 1992: **Study at the University of Life Sciences, Vienna**
Subject: KTWW

Occasionally: Work at Greece (Tourism)
Work at RHI

09.1997 – 05.1998: Basic military service (Wireless service for Austrian – UN – Contingent)

1992 – 1997: Real estate development (Including pulling down of a plant)

1991 – 1992: **Study at University of Vienna**
Subject: Genetics

1986 – 1991: Gymnasium Kindberg (Matura)
1981 – 1986: Gymnasium Leoben

Additional qualifications

- CAD two – dimensional (advanced)
- English
- French (Matura)
- Czech (rudimental)